Theoretical and FEM Free Vibration Analysis of Cylindrical Honeycomb Sandwich Laminate with Random Material Properties

By

V. MARIMUTHU

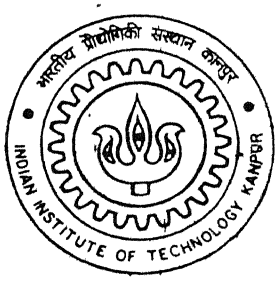

DEPARTMENT OF AEROSPACE ENGINEERING

Indian Institute of Technology Kanpur

NOVEMBER, 2001

Theoretical and FEM Free Vibration Analysis of Cylindrical Honeycomb Sandwich Laminate with Random Material Properties

A Thesis Submitted

In Partial Fulfillment of the Requirements

For the Degree of

Master of Technology

By

V. MARIMUTHU

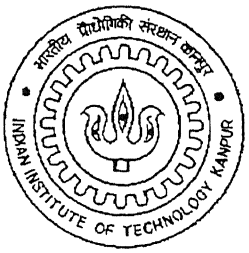

to the

Department of Aerospace Engineering
Indian Institute of Technology, Kanpur
India

November 2001

Dedicated to

God Ayyanar

And

My Parents, Uncle and Sister

CERTIFICATE

It is certified that work contained in the thesis entitled **THEORETICAL AND FEM FREE VIBRATION ANALYSIS OF CYLINDRICAL HONEYCOMB SANDWICH LAMINATE WITH RANDOM MATERIAL PROPERTIES,** by V. Marimuthu, has been carried out under my supervision and that this work has not been submitted elsewhere for a degree.

D. Yadav
Professor
Dept. of Aerospace Engineering
I.I.T.Kanpur.

November, 2001

Abstract

The cylindrical honeycomb sandwich laminate has been analyzied for natural frequency theoretically and by finite element method. The basic material properties $E_{11}, E_{22}, G_{12}, G_{23}, G_{31}, \nu_{12}, E_s, G_s$ are considered to be random variables with known statistics. The randomness in the material properties is handled by using a perturbation technique and the mean and the standared deviation of the natural frequency has been obtained for the cylindrical laminate. The boundary conditions are assummed to be simply supported at the panel ends. The results are validated by comparision with cylindrical composite panel.

Numerical results for mean and variance of the honeycomb cylinder are also obtained using FEM with Monte Carlo simulation. However the small size sample is not found to yield representative results.

ACKNOWLEDGMENTS

I record my deep sense of gratitude to Prof. D. Yadav for his exemplary supervision, complete support, unlimited freedom, constant encouragement, immense patience, and benevolence. It was a privildge to be associated with him, which was a rich, memorable and cherishing experience.

The room lectures of Prof. N.G.R. Iyengar were the source of inspiration for the present work and I am indebted to him in all ways.

I must acknowledge with lot of gratitude, the spontaneous assistance and co-operation extended by Prof. E. Rathakrishnan.

I thank my Uncle, Mr. P. Shanmugam Teacher and sister, Mrs. S. Kothai for the encouragement to do my higher studies. I am greatly indebted to my brother Mr. V. Periyasamy family and my sister Mrs. V. Latha family.

I thank my friends Mr. G. Saravanakumar, Mr. M. Sivakumar, Mr. K. Arun and Mr. Sharad Chauhan for their continued support doing my thesis work. I am also grateful to all my other friends whose name list goes beyond this page.

Finally thank Indian Institute of Technology-Kanpur for the opportunity to do Master Degree Programme.

V. Marimuthu

Contents

1 Introduction **1**
- 1.1 Sandwich Construction . . . 1
- 1.2 Literature survey . . . 3
  - 1.2.1 Theoretical and Experiment Studies . . . 3
  - 1.2.2 Imperfection in System Parameters . . . 8
- 1.3 Present Work . . . 9

2 Theory **11**
- 2.1 The In-Plane Properties of Honeycomb . . . 11
  - 2.1.1 Uniaxial Loading . . . 11
  - 2.1.2 Biaxial Loading . . . 16
- 2.2 Out-of-plane properties of Honeycombs . . . 17
- 2.3 Stress-Strain relation for honeycomb . . . 20
- 2.4 Shear Deformable Curved Sandwich Panel . . . 25
  - 2.4.1 Displacement Field . . . 26
  - 2.4.2 Stress-Strain Relation . . . 28
- 2.5 System Equation For Sandwich Panel . . . 30
- 2.6 Composite Material . . . 35

3 Solution Approach **38**
- 3.1 Eigen Value Problem . . . 38
- 3.2 Perturbation Approach . . . 39
- 3.3 FEM Approach . . . 42
  - 3.3.1 Generating Random Number . . . 42
  - 3.3.2 Modelling . . . 42

4 Results And Discussion **46**
- 4.1 Validation . . . 47
- 4.2 Natural frequency statistics . . . 47
  - 4.2.1 Mean frequency . . . 47
- 4.3 Natural Frequency Variance . . . 48
  - 4.3.1 Only E_{11} Changing . . . 48
  - 4.3.2 Only E_{22} Changing . . . 49
  - 4.3.3 Only G_{12} Changing . . . 49
  - 4.3.4 Only G_{23} Changing . . . 49
  - 4.3.5 Only G_{31} Changing . . . 50
  - 4.3.6 Only E_s Changing . . . 50

4.3.7 Only G_s Changing 50
4.3.8 Only ν_{12} Changing 50
4.3.9 All Material Properties Simultaneously Random 51
4.4 FEM Result 51

5 Conclusion **92**
5.1 Suggestion for future work 93

6 References **94**

A Appendix A **97**
A.1 Stiffness Matrix Coefficent 97
A.2 Mass Matrix Coefficent 121

B Appendix B **124**
B.1 Coefficent of characterstic Equation 124

List of Figures

2.1 Unit cell of hexagonal honeycomb 12
2.2 Cell deformation by cell wall bending and rotation due to shear . . . 15
2.3 Honeycomb loading face to the normal 18
2.4 Sandwich Panel Element 27
2.5 Honeycomb structure 37

3.1 Honeycomb structure 44
3.2 FEM Model of Honeycomb structure 45

4.1 Variance of Natural Frequencies Vs SD of Input Random Variable E_{11} 64
4.2 Variance of Natural Frequencies Vs SD of Input Random Variable E_{11} 65
4.3 Variance of Natural Frequencies Vs SD of Input Random Variable E_{11} 66
4.4 Variance of Natural Frequencies Vs SD of Input Random Variable E_{22} 67
4.5 Variance of Natural Frequencies Vs SD of Input Random Variable E_{22} 68
4.6 Variance of Natural Frequencies Vs SD of Input Random Variable E_{22} 69
4.7 Variance of Natural Frequencies Vs SD of Input Random Variable G_{12} 70
4.8 Variance of Natural Frequencies Vs SD of Input Random Variable G_{12} 71
4.9 Variance of Natural Frequencies Vs SD of Input Random Variable G_{12} 72
4.10 Variance of Natural Frequencies Vs SD of Input Random Variable G_{23} 73
4.11 Variance of Natural Frequencies Vs SD of Input Random Variable G_{23} 74
4.12 Variance of Natural Frequencies Vs SD of Input Random Variable G_{23} 75
4.13 Variance of Natural Frequencies Vs SD of Input Random Variable G_{31} 76
4.14 Variance of Natural Frequencies Vs SD of Input Random Variable G_{31} 77
4.15 Variance of Natural Frequencies Vs SD of Input Random Variable G_{31} 78
4.16 Variance of Natural Frequencies Vs SD of Input Random Variable E_s 79
4.17 Variance of Natural Frequencies Vs SD of Input Random Variable E_s 80
4.18 Variance of Natural Frequencies Vs SD of Input Random Variable E_s 81
4.19 Variance of Natural Frequencies Vs SD of Input Random Variable G_s 82
4.20 Variance of Natural Frequencies Vs SD of Input Random Variable G_s 83
4.21 Variance of Natural Frequencies Vs SD of Input Random Variable G_s 84
4.22 Variance of Natural Frequencies Vs SD of Input Random Variable ν_{12} 85
4.23 Variance of Natural Frequencies Vs SD of Input Random Variable ν_{12} 86
4.24 Variance of Natural Frequencies Vs SD of Input Random Variable ν_{12} 87
4.25 Variance of Natural Frequencies Vs SD all material properties 88
4.26 Variance of Natural Frequencies Vs SD all material properties 89
4.27 Variance of Natural Frequencies Vs SD all material properties 90
4.28 Natural Frequencies Vs Input Random Variable FEM Result 91

List of Tables

4.1 Comparison of mean $\bar{\omega}$ 51
4.2 Mean natural frequency for different L/R, lay up sequence(1) 52
4.3 Mean natural frequency for different L/R, lay up sequence(2) 54
4.4 Mean natural frequency for different L/R, lay up sequence(3) 56
4.5 Mean natural frequency for different Web Thickness, lay up sequence(1) 58
4.6 Mean natural frequency for different Web Thickness, lay up sequence(2) 60
4.7 Mean natural frequency for different Web Thickness, lay up sequence(3) 62

Chapter 1

Introduction

1.1 Sandwich Construction

Sandwich with aluminium honeycomb cores or flex cores are used extensively in aerospace, land and water transportation and sports industries because of their high specific strength and stiffness. Some examples of structures composed of sandwich panels are launch vehicles, satellites, helicopter rotor blades, aircraft control surfaces, ship hulls, jet engine nacelles and skin, high-speed trains, etc.

This type of construction consists of two thin facing layers separated by a core material. Several types of core shapes and core material have been applied to the construction of sandwich structures. The core layer is made of low specific weight material like balsa, porous rubber, corrugated metal sheet, metallic and non-metallic honeycomb, etc., which may be much less stiff and strong than the face sheets.

In addition to the possibility of achieving high flexural-stiffness providing a smoother aerodynamic surface in a high-speed range, sandwich-type constructions also exhibit many properties of exceptional importance for aerospace and civil constructions. Among these are: (a) excellent thermal and sound insulation; (b) a longer time of exploitation as compared to stiffened-reinforced structures; (c) possibility of being designed as to meet very close thermal distortion tolerances such as those required for communication satellite antennas and reflectors.

The most popular core is the honeycomb construction that consists of very thin foils in the form of hexagonal cells perpendicular to the facings. Face sheets usually

consist of aluminium or fiber-reinforced composite laminates. Face sheets are stiff and strong because they carry most of the loads, while lightweight core separates face sheets so that a higher bending stiffness of the composite plate can be achieved.

Regardless of the face sheet and core materials, the sandwich panel is considered to be a composite structure because of its inherent in homogeneous and anisotropic nature. Sandwich construction is frequently used instead of increasing material thickness. A sandwich construction provides excellent structural efficiency, for example high ratio of strength to weight. Other advantages offered by sandwich construction are elimination of welding, superior insulating qualities and design versatility. Even though the concept of sandwich construction is not very new, it has only been adopted for primary part of structures very recently. This is because there are a variety of problem areas to be investigated and overcome when the sandwich construction is applied to design of dynamically loaded structures. To enhance the attractiveness of sandwich construction, it is thus essential to have a understanding of the local strength and dynamic characteristics of individual sandwich panel/beam members.

Advanced sandwich-type constructions imply the presence of thick orthotropic core with bonded anisotropic face sheets that are treated as composite laminates. this arrangement presents an opportunity to tailor both the physical and mechanical properties of the faces by proper selection of laminate materials, their stacking sequence and fiber orientation. Suitable selection of fiber orientation and stacking sequence can result in substantial improvements of the buckling strength and the non-linear response behavior to a variety of load conditions. The transverse shear elastic module of the core layer can also be optimized so as to enhance the overall response behavior of the sandwich constructions.

As expected, analytical modelling of sandwich-type panels is much more intricate than that of the usual laminated composite structure. In contrast to the case of the regular laminated composite structure for which the assumptions are postulated for the structure as a whole, in the case of sandwich-type constructions the assumptions involving the core layer are different from those associated with the face sheets. More over, the analysis of sandwich panels featuring laminated face sheets is much more complicated than that with single layered faces. The complexity is due to the presence

of three types of asymmetries resulting from the lay-up sequences in the face sheets namely: (1) asymmetry with respect to the mid-surface of the face sheets, referred to as face asymmetry, inducing face bending-stretching coupling (2) asymmetry with respect to the mid-surface of the core, refer to as global asymmetry, which induces global bending-stretching coupling, and (3) presence of ply-angles between the principle axis of orthotropy of the face sheets materials and the geometric axes of the panel, inducing a structural coupling between stretching and shearing.

1.2 Literature survey

1.2.1 Theoretical and Experiment Studies

Many investigators have carried out noteworthy theoretical and experimental studies on linear elastic and nonlinear behavior of aluminium sandwich panels. Paik et al. [1] have studied the strength characteristic of aluminium sandwich panels with aluminium honeycomb core theoretically and experimentally. A series of strength tests have been carried out on aluminium honeycomb-core sandwich panels specimen in three point bending, axial compression and lateral crushing. Simplified theories have been applied to analyze bending deformation, buckling/ultimate strength and crushing strength of honeycomb sandwich panels subjected to the corresponding load component. The structural failure characteristics of aluminium sandwich panels have been discussed.

Becker [2] has performed closed-form analysis of the thickness effect of regular honeycomb core material. In sandwich structure in many cases the effect of a honeycomb core in not only to maintain the distance between the face skins, but it also contributes to the overall in-plane stiffness. Due to the coupling of the core displacements with those of the face sheets the stiffness contribution is not simply proportional to its total thickness but is a nonlinear function of the core thickness which is the so-called *core thickness effect.* The closed-from analysis is given for the effective in-plane core stiffnesses including the thickness effect. Based on an approximate representation for the displacement field within the core cell walls, the effective core stiffness have been derived by energy considerations. The results have been validated by comparing with

finite element analysis [FEM].

Fatt and Park. [3] have studied experimentally a three stage, progressive damage model for the perforation of a honeycomb sandwich plate subjected to normal impact by blunt and spherical projectiles. The residual velocities in three stages have been found from energy balances between each stage. The plastic work dissipated in deformation and fracture at each stage have been approximated from the solution of the previous stage. Shear forces have been transmitted in the bond between face sheets and honeycomb core. The predicted ballistic limits have been found to be within 5% of the measured ballistic limits for sandwich plates perforated by the blunt and spherical projectiles. The lateral extent and deformation of the damaged face sheets have been also found to be with 34 and 51% of limited test results. They have found that most of the work is dissipated in perforation of the bottom face sheet during impact. Li [4] has obtained stress concentration and local behavior of prestressed composite laminates/sandwich shells with overhangs in cylindrical bending. The laminates have been considered as cross-ply/angle-ply multilayer shells with overhangs in cylindrical bending caused by transversely concentrated line-load and in-plane uniform load. The high stress gradient, wich could not be measured by experimentally, Li has determined theoretically around the load area and sharply support regions. The experimental results have been compared with FEM. Li has used FEM package operating system MARC.

Glass et al. [5] have analysed Graphite/epoxy honeycomb core sandwich permeability under mechanical loads. The core material for the test specimens were either Hexcel HRP-3/16-8.0 or DuPont Korex-1/8-4.5 and had nominally 1.27 cm thickness. The facesheets were made of Hercules' AS4/8552 graphite/epoxy composite with nominally 0.15 cm thickness. The sandwich specimens were studied during both static and dynamic shear loads. The permeability was measured as the rate of air flow through the core from a 2.54 cm diameter circular area of the core exposed to an air pressure of 68.9 kPa. During both static and dynamic testing, the Korex core experienced sudden increase in core permeability corresponding to the core catastrophic failure while the HRP core generally experienced a gradual increase in the permeability prior to a bond line failure.

Petras and Sutcliffe. [6] have presented failure mode maps for honeycomb sandwich panels. Theoretical models using honeycomb mechanics and classical beam theory are described. A failure mode map for loading under 3-point bending have been constructed. The dependence of failure mode and load on the ratio of skin thickness to span length and honeycomb relative density has been obtained. Beam specimens are tested in 3-point bending. The experimental data agree satisfactorily with the theoretical predication. Muc and Zuchara. [7] have performed the analysis of a thin-walled sandwich laminate composite faces subject to axial compression. The analytical results have been compared with FEM NISA II package.

Cho and Averill. [8] have studied the sandwich construction with three-dimensional finite element based on first-order zig-zag sublaminate approximations. The in-plane displacement fields in each sublaminate are assumed to be piecewise linear function and vary in a zig-zag fashion through the thickness of the sublaminate. the zig-zag function have been evaluated by enforcing the continuity of transverse shear stresses at layer interfaces. The in-plane displacement fields have been assumed to vary linearly through the thickness. The transverse normal strain predication have improved by assuming a constant variation of transverse normal stress in each sublaminate. In the computational model, each finite element represents one sublaminate. The finite element has been developed with the topology of an eight-noded brick, allowing the thickness of the shell to be discretized into several elements, or sublaminates, where each sublaminate can contain more than one physical layer. Each node has five engineering degrees of freedom, three translation and two rotation. Shafizadeh and Seferis. [9] have performed scaling of honeycomb compressive yield stresses. A honeycomb-scaling factor and geometric end constraint have been found to relate the rings and core through the relative yield stresses and the physical dimensions and properties of the honeycomb materials. The compressive properties of the Nomex rings have been also investigated using both a model and a commercial phenolic honeycomb dip resin. The Nomex rings manufactured from the model resin were found to have higher compressive properties. These properties were attributed to the higher fracture toughness of the resin, and both resins were found to accurately scale from rings to core with the honeycomb-scaling factor.

Guo and Gibson. [10] have analysed the behaviour of intact and damaged honeycombs using finite elements. The Young's moduli, the elastic buckling strength and the plastic collapse strength of regular honeycomb with defects consisting of missing cells in the structure have been analyzed using the finite element method. The behavior of intact honeycombs have been found to be consistent with those of previous analyses. The effect of single isolated defects of varying sizes and the effect of the separation distance between two defects on the elastic and plastic behaviors has been studied. Single isolated defects reduce the modulus and strength. The elastic strength of honeycomb with a defect normalized by the intact strength decrease directly with the ratio of the minimum net cross-sectional area normalized by the intact cross-sectional area. The plastic collapse strength of honeycomb with a defect normalized by the intact strength decreases less rapidly than the ratio of the minimum net cross-sectional area normalized by the intact cross-sectional area. Burton and Noor. [11] have obtained the assessment of continuum models for sandwich panel honeycomb cores. Finite element models have been used for predicting the free-vibration response of infinitely long and rectangular sandwich panels. The panels considered have square-cell honeycomb core and simply supported edges. The sandwich core and face sheets have been modelled as three-dimensional solid elements and two-dimensional plate elements. The predications of the finite element models have been compared with those obtained by using higher-order sandwich theory for panels with the core replaced by an effective continuum.

Palazotto et al. [12] has analysed the response of composite sanwich plate to low-velocity impact predicted by a displacement-based, plate bending, finite element algorithm. Fifth order Hermitian interpolation allows three-dimensional equilibrium integration for transverse stress calculation to be carried out symbolically on the interpolation function so that transverse stress within the elements are expressed directly in terms of nodal quantities. Nomex honeycomb sandwich cores have been modeled using an elastic-plastic foundation and contact loading have been simulated by Hertzian pressure distribution for which the contact radius have been determined iteratively. Damage predication by failure criteria and damage progression via stiffness reduction have been employed. Vaidya et al. [13] have studied the impact

response of integrated hollow core sandwich composite panels. In comparison with traditional foam and honeycomb cores, the integrated space core provides a means to route wires/rods, embed electronic assemblies, and store fuel and fireretardant foam, among other conceivable benefits. The low velocity impact response of innovative integrated sandwich core composite have been investigated. Three thickness of integrated and functionality-embedded E-glass/epoxy sandwich core have been considered. The low-velocity impact results indicated that the hallow and functionality-embedded integrated core suffered a localized damage state limited to a system of core members in the vicinity of the impact. Results have been compared with experimental findings. The specimens were loaded in compression at a loading rate of 1.27 mm/min and taken to failure. The low velocity-impact test have been conducted in a Dynatup 8120 impact-testing machine equipped with a load cell capacity of 7700 kg. The samples were clamped using pneumatic assit, such that a circular opening of 76.2 mm diameter have exposed to the impactor. The impactor had 12.5 mm hemispherical tup. The force-time, energy-time and load-deflection response of the samples have been measured using the instrumented feature of the Dynatup machine.

Meraghni et al. [14] have studied the mechanical behaviour of sandwich panel analytically performed a finite element analysis , an and experimentally. The efficiency of a new analytical method for sandwich panels core has been presented. The separation of the skins by the core increase the inertia of the sandwich panel, the flexure and shear stiffness. Improved mechanical behaviour has been obtained with a little increase in weight, producing an efficient structure to resist bending and buckling loads. The approaches (theoretical and experimental) have been used to determine elastic properties and ultimate stress. Daniel and Abot [15] have studied the flexural behaviour of composite sandwich beams and compared the results with predications of theoretical models. Sandwich beams have been fabricated by bonding unidirectional carbon/epoxy laminate face sheets to aluminium honeycomb cores with an adhesive film. All constituent materials (composite laminates, adhesive and core) have been characterized independently. Special techniques have been developed to pervent premature failure under the loading pins and to ensure failure in the test section. Sandwich beams have been tested under four-point and three-point bending.

Strain to failure in the face sheets have been recorded with strain gauges, and beam deflection and strain in the honeycomb core have been recorded by using moire techniques. The beam face sheets exhibited a softening non-linearity on the compression side and a stiffening non-linearity on the tension side.

Thomsen [16] has presented high-order theory for the analysis of multi-layer sandwich panels. Multi-layer composte assemblies are characterized by having interchanging layers of high density and high stiffness separated by complaint interface layers. A characteristic feature of these assemblies is that severe and highly localized stress concentrations appear under certain conditions. The quantitative understanding of these phenomena involves a detailed description of the complicated mechanical interaction of the stiff layers through the compliant interface layers. A high-order plate theory formulation, which includes the through-thickness flexibilty, and which inherently includes a description of the global response as well as the local responses of the individual layers of an arbitrary, multi-layer structural plate assembly. Wang and Yang [17] have performed experimental investigation of the damping behaviour of laminated honeycomb cantilever beams with fine solder balls enclosed in the cells as dampers. Attenuation have been achieved through the exchange of momentum between the balls and the beam. The effect of the mass ratio (the number of balls to be enclosed in each honeycomb cell) have been studied by varying the number of balls used. The damping variation have been found to be effective in reducing the amplitude without significantly shifting the natural frequency of the cantilever.

1.2.2 Imperfection in System Parameters

As is well known, many uncertainties exist during the process of fabrication measurement and manufacture of structures. A composite laminate is a stack of layers of fiber-reinforced laminae. The fiber-reinforced laminae are made of fibers and matrix that are of two different materials. The way in which the fiber and matrix materials are assembled to make a lamina, as well as lay-up and curing of laminae, are complicated processes and may involve a lot of uncertain factors. Therefore, the material properties and geometry of composite laminate are random in nature.

In many engineering applications, the structures may be subjected to different ran-

dom loads and the corresponding failure modes may be different as well. If the loads are not applied simultaneously, there may be some stochastic correlation between the different loadings. This leads to the necessity to take account of the uncertainties of loads and some other design parameters in the reliability analysis. More effort is need in developing analysis techniques to obtain the combined effect of uncertainties in applied loads, material properties, fiber orientations and plate thickness on the reliability of composite laminates. This attaines special significance if highly reliable composite structures are to be designed.

It's well known that discrepancies between analytical and experimental predictions of response of sandwich panels and shells are mainly due to the presence of unavoidable geometric and material imperfections. For this reason, in recent years the study of the implications of the imperfection on the load carrying capacity of sandwich structures and its influence upon the structural design has been very important.

Chen et al. [18] have performed a finite element study of the effect of holes and rigid inclusion on the elastic modulus and yield strength of regular honeycombs under biaxial loading. The focus honeycomb were weakened by a small degree of geometrical imperfection, such as a random distribution of fractured cell walls. It has been found that the strength of an imperfect honeycomb is relatively insensitive to the presence of holes and inclusions, consistent with recent experimental observations on commercial aluminium alloy foams.

A problem of considerable practical importance towards accurate analysis and enhancement of load carrying capacity of sandwich curved panels consists of a better understanding of the possible implication of material imperfections, and implementation of the yielding mechanism and the attenuation of imperfection sensitivity to unavoidable geometric and material imperfections. However, in spite of the evident importance of the problem, to the author's knowledge, no results related with these issues have been reported in the specialized literature.

1.3 Present Work

Uncertainity in structural dynamics mainly arise from the uncertainity in the structural properties. The problem is statistical in nature and is due, for example, to the stiffness or damping fluctuation caused by random variations in material properties, randomness in boundary conditions, and variations caused by manufacturing and assembly techniques.

The aim of the present study is to investigate the dynamic characteristics of the honeycomb-cored sandwich cylinders under material imperfection. The material properties are modeled as random in nature. The system equations involve partial differential equations whose coefficients are random function of space.

This modelling of the material properties as random variables results in random eigenvalues, eigenvectors, and response of system in question. In general, it is possible to obtain close from expression for the response statistical characteristics for only specific simple cases of geometry, boundary conditions and loadings. Cases for which analytical solutions are not available, some numerical approach has to be used. The numerical methods include the Monte Carlo simulation and finite element method. These, through computational intensive and time consuming, can be applied to any problem in this area. The present study has used the two in combination to generate the second order statistics of the response of the sandwich cylinder. The simply supported edge conditions have been considered for the cylinder. The effect of shear deformation has been incorporated in the study.

Chapter 2

Theory

The behaviour of the sandwich panel may be studied by considering the behaviour of the honeycomb core and the facing lamina separately. The performance of the complete sandwich is obtained by combining the two portion together.

2.1 The In-Plane Properties of Honeycomb

The honeycomb portion is not a homogeneous section. The behaviour of the thin walled cells under loading is not similar to a solid lamina. The thin walls under load acts as slender beams. The performance of the honeycomb is being examined under inplane loading of uniaxial and biaxial types.

2.1.1 Uniaxial Loading

The in-plane stiffness and strength,that is, (Figure 2.1) those in the $X_1 - X_2$ plane of hexagonal honeycomb panel are the lowest because stresses in this plane make the cell walls bend. The out-of-plane stiffness and strength those in X_3 direction are much larger because they require the axial extension or compression of the cell walls. The out-of-plane analysis is carried out separately as it gives the additional stiffnesses which are needed for the design of honeycomb cores in sandwich panels and for the complete description of the behaviour of natural honeycomb. Figure 2.1 shows a unit cell of the hexagonal core. The figure shows the undeformed cell with dimensions. h is the cell wall length in X_2 direction, l is the length of the inclined wall, t is the wall

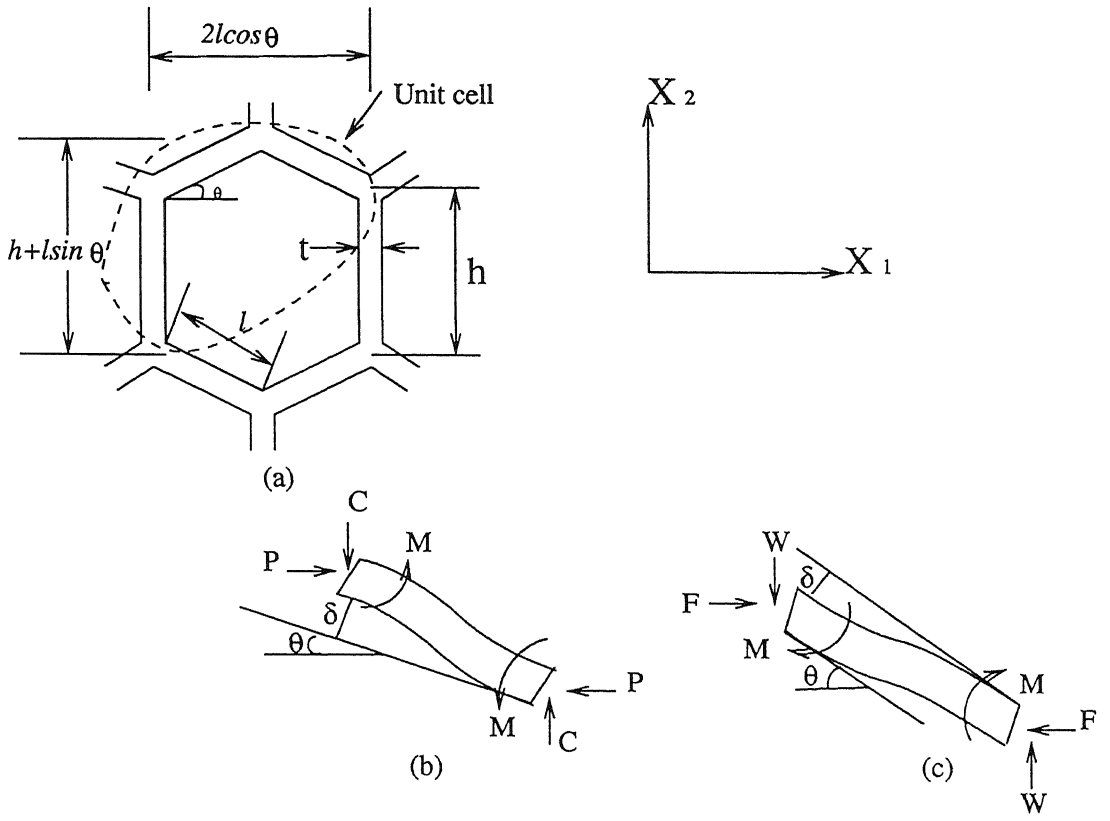

Figure 2.1: Unit cell of hexagonal honeycomb

(a) undeformed honeycomb, (b) and (c) bending due to loads in the X_1 and X_2 directions

thickness and θ gives the angle of inclination. It is assumed that the general cell may have different thickness for different walls. We wish to analyse its response to load applied in the $X_1 - X_2$ plane. if the hexagonal is regular, that is, the side are equal and the angle are all 120^o and the cell walls are of the same thickness, then the in-plane properties are isotropic: they do not depend on direction. Such a structure has two independent equivalent elastic moduli a Young's modulus E and a shear modulus G, for instance. But when the hexagon is irregular or the cell walls in one direction are thicker than those in the others, the properties are anisotropic and a complete description of the in-plane properties requires five modulii, say $E_1, E_2, G_{12}, \nu_{12}$ and ν_{21}. When a honeycomb, loaded in the X_1 or the X_2 direction, deforms in linear-elastic way, the cell walls bend. The response is conveniently described by the above five moduli, but the five are not independent. The reciprocal relation reduces the number of independent moduli to four. They are the same in tension as in compression.

Consider a unit cell, as shown in figure 2.1a, to include two inclined walls and one wall parallel to X_2 axis. A force component P giving rise to stress σ_1 parallel to X_1 causes one set of cell walls-those of length l-to bend as shown in Figure(2.1 b). Equilibrium requires that the component of forces C parallel to X_2 be zero. The moment M acting to bend the cell wall,which we treat as a beam of length l, thickness t, depth b, and Young's modulus E_s, is from moment equilibrium

$$M = \frac{Plsin\theta}{2} \tag{2.1}$$

where, from force equilibrium in X_1 direction with b as the height of the cell

$$P = \sigma_1 \left(h + lsin\theta\right) b \tag{2.2}$$

From standard beam theory, modelling the wall as a cantilever beam, the wall deflects by:

$$\delta = \frac{Pl^3 sin\theta}{12E_s I} \tag{2.3}$$

where I is the second moment of inertia of the cell wall ($I = bt^3/12$ for a wall of uniform thickness t). A component of the deflection $\delta sin\theta$ is parallel to the X_1 axis, giving a strain:

$$\epsilon_1 = \frac{\delta sin\theta}{lcos\theta} \tag{2.4}$$

Using eq (2.3)

$$\epsilon_1 = \frac{Pl^2 sin^2\theta}{12E_s I cos\theta} \tag{2.5}$$

Substitute eq (2.2) in eq (2.5)

$$\epsilon_1 = \frac{\sigma_1 \left(h + lsin\theta\right) bl^2 sin^2\theta}{12E_s I cos\theta} \tag{2.6}$$

The Young's modulus parallel to X_1 is just $E_1 = \sigma_1/\epsilon_1$, giving the equivalent modulus

$$E_1 = \frac{\sigma_1 12E_s I cos\theta}{\sigma_1 (h + lsin\theta) bl^2 sin^2\theta}$$

For a cell with uniform wall thickness t

$$E_1 = \left(\frac{t}{l}\right)^3 \frac{E_s cos\theta}{\left(\frac{h}{l} + sin\theta\right) sin^2\theta} \tag{2.7}$$

Proceeding as above for the X_2 direction, the force acting on the cell wall of length, l and depth, b is given by

$$W = \sigma_2 lbcos\theta$$

When σ_2 is the stress parallel to X_2. The bending moment acting on the wall is

$$M = \frac{Wlcos\theta}{2} \tag{2.8}$$

The wall taken as cantilever beam, deflects by:

$$\delta = \frac{Wl^3cos\theta}{12E_sI} \tag{2.9}$$

Of this, a component $\delta cos\theta$ is parallel to X_2 axis, giving a strain:

$$\epsilon_2 = \frac{\delta cos\theta}{h + lsin\theta} \tag{2.10}$$

Substituting for δ from eq (2.9) and for W in-terms of δ_2 gives

$$\epsilon_2 = \frac{\sigma_2 lbcos\theta l^3 cos^3\theta}{12E_sI(h + lsin\theta)}$$

After simplify

$$\epsilon_2 = \frac{\sigma_2 bl^4 cos^3\theta}{12E_sI(h + lsin\theta)}. \tag{2.11}$$

The Young's modulus parallel to X_2 is simply $E_2 = \sigma_2/\epsilon_2$, giving:

$$E_2 = \frac{\sigma_2 12E_sI(h + lsin\theta)}{\sigma_2 bl^4 cos^3\theta}$$

For a beam of constant thickness, thesis becomes

$$E_2 = \left(\frac{t}{l}\right)^3 \frac{E_s\left(\frac{h}{l} + sin\theta\right)}{cos^3\theta} \tag{2.12}$$

The poisson's ratios are calculated by taking the negative ratio of the strains normal to, and parallel to, the loading direction. We find for loading in X_1 direction:

$$\nu_{12} = -\frac{\epsilon_2}{\epsilon_1} = \frac{cos^2\theta}{\left(\frac{h}{l} + sin\theta\right) sin\theta} \tag{2.13}$$

and for loading in X_2 direction:

$$\nu_{21} = -\frac{\epsilon_1}{\epsilon_2} = \frac{\left(\frac{h}{l} + sin\theta\right) sin\theta}{cos^2\theta} \tag{2.14}$$

The shear modulus, G_{12} can be calculated using Figure 2.2. Because of symmetry there is no relative motion of the points A, B and C when the honeycomb is sheared; the shear deflection u_s is entirely due to the bending of beam BD and its rotation

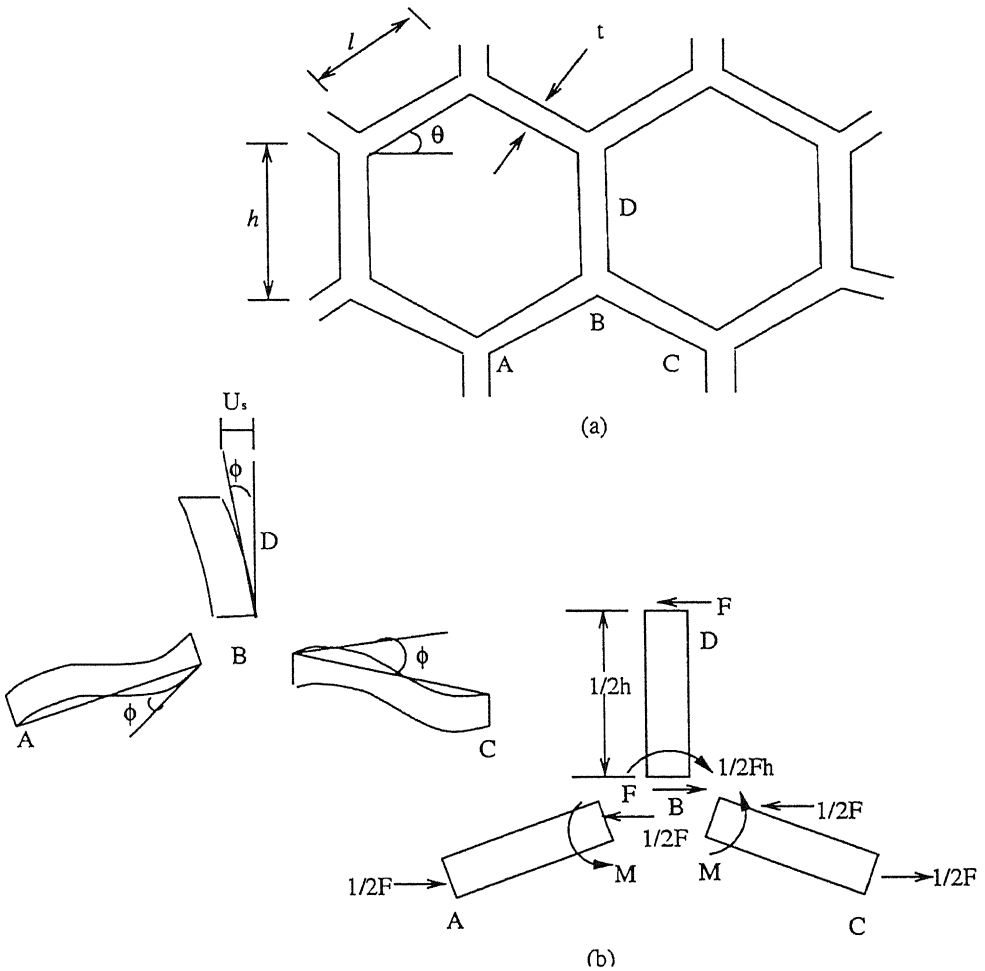

Figure 2.2: Cell deformation by cell wall bending and rotation due to shear

(a) the undeformed honeycomb (b) loads, moments, displacements and rotations due to shear.

(through the angle ϕ) about the point B. The force are shown in the figure. Summing moments at B gives the bending moment applied to the members AB and BC:

$$M = \frac{Fh}{4} \tag{2.15}$$

Then, using the standard result for cantilever beam

$$\delta = Ml^2/6E_sI$$

The angle of rotation is:

$$\phi = \frac{Fhl}{24E_sI}$$

The shearing deflection u_s of the point D with respect to B is:

$$u_s = \frac{1}{2}\phi h + \frac{F}{3E_sI}\left(\frac{h}{2}\right)^3 = \frac{Fh^2}{48E_sI}(l+2h)$$

The shear strain γ is given by:

$$\gamma = \frac{2u_s}{(h+lsin\theta)} = \frac{Fh^2}{24E_sI}\frac{(l+2h)}{(h+lsin\theta)} \tag{2.16}$$

The shear stress is $\tau = F/2lbcos\theta$. The shear modulus can be obtained as $G_{12} = \tau/\gamma$,

$$G_{12} = \frac{12E_sI\,(h+lsin\theta)}{lbh^2cos\theta\,(l+2h)}$$

For a cell with uniform wall thickness

$$G_{12} = \left(\frac{t}{l}\right)^3 \frac{E_s(\frac{h}{l}+sin\theta)}{\left(\frac{h}{l}\right)^2\left(1+\frac{2h}{l}\right)cos\theta} \tag{2.17}$$

2.1.2 Biaxial Loading

The biaxial in-plane loading of the honeycomb can be visualised with the help of Figure 2.1. The principal stresses are assumed to be σ_1 and σ_2 and P and W are the forces in X_1 and X_2 directions. The low in-plane stiffness of honeycomb is due to cell-wall bending. In uniaxial loading the bending displacements are so much larger than the axial stretching or compression of the walls that these can be neglected. For the biaxial loading the effects of the axial strains are incorporated below.

Consider the strains due to bending first. Referring to Figure 2.1, the force components P in the X_1 direction causes the cell walls of length l to bend in one direction.

In the biaxial loading a force W in the X_2 direction in superimposed. The net displacement is calculated by the method of section 2.1.1 and from this the strain ϵ_1 and ϵ_2 are obtained.

$$\begin{aligned} \epsilon_1 &= \tfrac{1}{E_1}(\sigma_1 - \nu_{12}\sigma_2) \\ \epsilon_2 &= \tfrac{1}{E_2}(\sigma_2 - \nu_{21}\sigma_1) \end{aligned} \tag{2.18}$$

The stresses σ_1 and σ_2 introduce an axial force F_1 on the walls of length l, and an axial force F_2 on the walls of length h.

$$F_1 = Pcos\theta + Wsin\theta \qquad\qquad F_2 = 2W$$

The additional strain in X_1 direction is:

$$\epsilon_1 = \frac{Pcos\theta + Wsin\theta}{btE_s} \tag{2.18a}$$

In the X_2 direction the additional strain is:

$$\epsilon_2 = \frac{1}{btE_s}\left\{\frac{(Pcos\theta + Wsin\theta)lsin\theta + 2Wh}{(h + lsin\theta)}\right\} \tag{2.18b}$$

substituting for P and W from the equations in section 2.1.1 gives the additional strains in terms of t, l, h and θ. Adding these to the contribution from bending gives the full elastic consecutive equation for in-plane deformation:

$$\begin{aligned} \epsilon_1 &= \tfrac{1}{E_1}(\sigma_1 - \nu_{12}\sigma_2) + \tfrac{1}{E_s(\frac{t}{l})}\left\{\sigma_1\left(\tfrac{h}{l} + sin\theta\right)cos\theta + \sigma_2 sin\theta cos\theta\right\} \\ \epsilon_2 &= \tfrac{1}{E_2}(\sigma_2 - \nu_{21}\sigma_1) + \tfrac{1}{E_s(\frac{t}{l})}\left\{\sigma_1 sin\theta cos\theta + \sigma_2 \tfrac{cos\theta(2h/l + sin^2\theta)}{(h/l + sin\theta)}\right\} \end{aligned} \tag{2.19}$$

2.2 Out-of-plane properties of Honeycombs

Here we note that the function of the honeycomb core is to carry normal and shear loads in planes containing the axis of the hexagonal prisms in the X_3 direction. When loaded in this direction the cell walls are extended or compressed rather than bent and the moduli can be expressed as Ref[22]

$$E_3 = E_s\frac{t}{l}\left\{\frac{h/l + 2}{2(h/l + sin\theta)cos\theta}\right\} \tag{2.20}$$

The strain energy can be calculated using Figure (2.3) . A set of displacements are assumed which satisfy the external boundary conditions. Consider the uniform

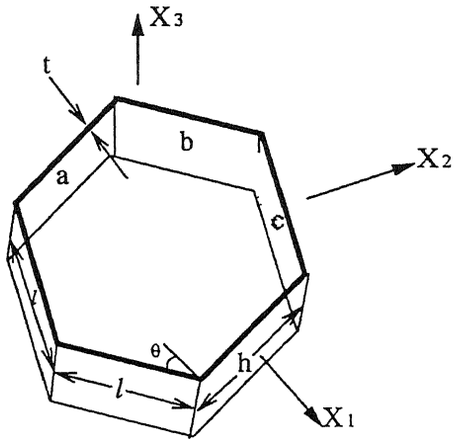

Figure 2.3: Honeycomb loading face to the normal

shear strain γ_{13} and associated shear stress τ_{13} acting on the normal face to X_3 in the X_1 direction. The elastic strain energy is stored in the shear displacements in the cell walls. The bending stiffnesses and the energies associated with bending are much smaller. The shear strains in wall a, b and c are

$$\begin{aligned} \gamma_a &= 0 \\ \gamma_b &= \gamma_{13} cos\theta \\ \gamma_c &= \gamma_{13} cos\theta \end{aligned}$$

A lower bound for moduli is Ref[22]

$$G_{13} \leq \frac{G_s cos\theta}{(h/l + sin\theta)} \left(\frac{t}{l}\right) \tag{2.21}$$

The stress distributions satisfy equilibrium at each point and are in equilibrium with the external loads. Consider first loading in the X_1 direction. An external stress τ_{13} induces the set of shear stresses τ_a, τ_b and τ_c in the three cell walls. By symmetry and as the wall a is loaded in simple bending it does not carry significant load are

$$\tau_a = 0$$

And

$$\tau_b = \tau_c$$

$$2\tau_{13}(h + lsin\theta)cos\theta = 2\tau_b tlcos\theta \tag{2.21a}$$

The equilibrium equation, gives a lower bound

$$G_{13} \geq \frac{G_s cos\theta}{(h/l + sin\theta)} \left(\frac{t}{l}\right) \tag{2.21b}$$

For regular hexagons it reduces to

$$G_{13} = 0.577 G_s \left(\frac{t}{l}\right) \tag{2.21c}$$

Due to an external shear strain γ_{23} in the X_2 direction the strains in the cell walls are

$$\begin{aligned} \gamma_a &= \gamma_{23} \\ \gamma_b &= \gamma_{23} sin\theta \\ \gamma_c &= \gamma_{23} sin\theta \end{aligned}$$

And a lower bound the moduli is

$$G_{23} \leq \frac{1}{2} \frac{G_s(h/l + 2sin^2\theta)}{(h/l + sin\theta)cos\theta} \left(\frac{t}{l}\right) \tag{2.22}$$

Consider loading in the X_2 direction an external stress τ_{23} induces the set of shear stresses τ_a, τ_b and τ_c in the three cell walls.

$$\tau_b = \tau_c$$

Equilibrium in the X_3 direction

$$\tau_a = \tau_b + \tau_c = 2\tau_b$$

and equilibrium with the external stress gives

$$2\tau_{23} l(h + lsin\theta)cos\theta = 2\tau_b tlsin\theta + \tau_a th \tag{2.22a}$$

$$\tau_b = \tau_{23} cos\theta \frac{l}{l}$$

$$G_{23} \geq \frac{G_s(h/l + sin\theta)}{(2h/l + 1)cos\theta} \left(\frac{t}{l}\right) \tag{2.22b}$$

In this case the two bound do not coincide for a general, anisotropic honeycomb, even though they are close. But for regular hexagons it reduces to

$$G_{23} = 0.577 G_s \left(\frac{t}{l}\right) \tag{2.22c}$$

The two Poisson's ratios ν_{31} and ν_{32} are simply equal to those for the solid

$$\nu_{31} = \nu_{32} = \nu_s \tag{2.22d}$$

The Possion's ratio's ν_{13} and ν_{23} are found from the reciprocal relation

$$\nu_{13} = \frac{E_1}{E_3}\nu_s \approx 0, \qquad \nu_{23} = \frac{E_2}{E_3}\nu_s \approx 0. \tag{2.22e}$$

2.3 Stress-Strain relation for honeycomb

The three-dimensional consititutive relations for stress and strain for the honeycomb panel can be expressed as

$$\epsilon_{11} = \frac{1}{E_1}(\sigma_{11} - \nu_{12}\sigma_{22}) + \sigma_{11}a_1 + \sigma_{22}a_2 - \frac{\nu_{13}\sigma_{33}}{E_1} \tag{2.23}$$

$$\epsilon_{22} = \frac{1}{E_2}(-\nu_{21}\sigma_{11} + \sigma_{22}) + \sigma_{11}a_2 + \sigma_{22}a_3 - \frac{\nu_{23}\sigma_{33}}{E_2} \tag{2.24}$$

$$\epsilon_{33} = \frac{1}{E_3}(-\nu_{31}\sigma_{11} - \nu_{32}\sigma_{22} + \sigma_{33}) \tag{2.25}$$

$$\frac{1}{\gamma_{12}} = \frac{G_{12}}{\tau_{12}} \tag{2.26}$$

$$\frac{1}{\gamma_{23}} = \frac{G_{23}}{\tau_{23}} \tag{2.27}$$

$$\frac{1}{\gamma_{31}} = \frac{G_{31}}{\tau_{31}} \tag{2.28}$$

where

$$a_1 = \frac{(h/l+sin\theta)cos\theta}{E_s(t/l)}$$

$$a_2 = \frac{sin\theta cos\theta}{E_s(t/l)}$$

$$a_3 = \frac{cos\theta(2h/l+sin^2\theta)}{E_s(t/l)(h/l+sin\theta)}$$

In matrix notation eq (2.23) to (2.28) can be expressed as

$$\begin{Bmatrix} \epsilon_{11} \\ \epsilon_{22} \\ \epsilon_{33} \\ \gamma_{23} \\ \gamma_{31} \\ \gamma_{12} \end{Bmatrix} = \begin{bmatrix} \frac{1}{E_1}+a_1 & -\frac{\nu_{21}}{E_2}+a_2 & -\frac{\nu_{31}}{E_3} & 0 & 0 & 0 \\ -\frac{\nu_{12}}{E_1}+a_2 & \frac{1}{E_2}+a_3 & -\frac{\nu_{32}}{E_3} & 0 & 0 & 0 \\ -\frac{\nu_{13}}{E_1} & -\frac{\nu_{23}}{E_2} & \frac{1}{E_3} & 0 & 0 & 0 \\ 0 & 0 & 0 & \frac{1}{G_{23}} & 0 & 0 \\ 0 & 0 & 0 & 0 & \frac{1}{G_{31}} & 0 \\ 0 & 0 & 0 & 0 & 0 & \frac{1}{G_{12}} \end{bmatrix} \begin{Bmatrix} \sigma_{11} \\ \sigma_{22} \\ \sigma_{33} \\ \tau_{23} \\ \tau_{31} \\ \tau_{12} \end{Bmatrix} \tag{2.29}$$

or

$$\{\epsilon\} = [S]\{\sigma\}$$

Inverting the above relation

$$\begin{Bmatrix} \sigma_{11} \\ \sigma_{22} \\ \sigma_{33} \\ \tau_{23} \\ \tau_{31} \\ \tau_{12} \end{Bmatrix} = \begin{bmatrix} \frac{b_1}{\beta} & \frac{b_2}{\beta} & \frac{b_3}{\beta} & 0 & 0 & 0 \\ \frac{b_4}{\beta} & \frac{b_5}{\beta} & \frac{b_6}{\beta} & 0 & 0 & 0 \\ \frac{b_7}{\beta} & \frac{b_8}{\beta} & \frac{b_9}{\beta} & 0 & 0 & 0 \\ 0 & 0 & 0 & G_{23} & 0 & 0 \\ 0 & 0 & 0 & 0 & G_{31} & 0 \\ 0 & 0 & 0 & 0 & 0 & G_{12} \end{bmatrix} \begin{Bmatrix} \epsilon_{11} \\ \epsilon_{22} \\ \epsilon_{33} \\ \gamma_{23} \\ \gamma_{32} \\ \gamma_{12} \end{Bmatrix} \tag{2.30}$$

where for the sake of compactness β denotes $|\beta|$

$$\begin{aligned}
|\beta| = \; & \tfrac{1}{E_1E_2E_3} + \tfrac{a_3}{E_1E_3} + \tfrac{a_1}{E_2E_3} + \tfrac{a_3a_1}{E_3} - \tfrac{\nu_{32}\nu_{23}}{E_1E_2E_3} - \tfrac{a_1\nu_{32}\nu_{23}}{E_2E_3} \\
& - \tfrac{a_2^2}{E_3} + \tfrac{a_2\nu_{12}}{E_1E_3} + \tfrac{a_2\nu_{21}}{E_2E_3} - \tfrac{\nu_{21}\nu_{12}}{E_1E_2E_3} + \tfrac{a_2\nu_{13}\nu_{32}}{E_1E_3} - \tfrac{\nu_{21}\nu_{13}\nu_{32}}{E_1E_2E_3} \\
& + \tfrac{a_2\nu_{31}\nu_{12}}{E_1E_2E_3} - \tfrac{\nu_{12}\nu_{23}\nu_{31}}{E_1E_2E_3} - \tfrac{\nu_{13}\nu_{31}}{E_1E_2E_3} - \tfrac{\nu_{31}\nu_{13}a_3}{E_1E_3} \\
b_1 = \; & \tfrac{1}{E_2E_3} + \tfrac{a_3}{E_3} - \tfrac{\nu_{32}\nu_{23}}{E_2E_3} \\
b_2 = \; & -\tfrac{a_2}{E_3} + \tfrac{\nu_{21}}{E_2E_3} + \tfrac{\nu_{23}\nu_{31}}{E_2E_3} \\
b_3 = \; & -\tfrac{a_2\nu_{32}}{E_3} + \tfrac{\nu_{21}\nu_{32}}{E_2E_3} + \tfrac{\nu_{31}}{E_3E_2} + \tfrac{a_3\nu_{31}}{E_3} \\
b_4 = \; & -\tfrac{a_2}{E_3} + \tfrac{\nu_{12}}{E_1E_3} + \tfrac{\nu_{13}\nu_{32}}{E_1E_3} \\
b_5 = \; & \tfrac{1}{E_1E_3} + \tfrac{a_1}{E_3} - \tfrac{\nu_{31}\nu_{13}}{E_1E_3} \\
b_6 = \; & \tfrac{\nu_{32}}{E_1E_3} + \tfrac{\nu_{32}a_1}{E_3} - \tfrac{\nu_{31}a_2}{E_3} + \tfrac{\nu_{12}\nu_{31}}{E_1E_3} \\
b_7 = \; & -\tfrac{a_2\nu_{23}}{E_2} + \tfrac{\nu_{12}\nu_{23}}{E_1E_2} + \tfrac{\nu_{13}}{E_1E_2} + \tfrac{a_3\nu_{13}}{E_1} \\
b_8 = \; & \tfrac{\nu_{23}}{E_1E_2} + \tfrac{\nu_{23}a_1}{E_2} - \tfrac{\nu_{13}a_2}{E_1} + \tfrac{\nu_{21}\nu_{13}}{E_1E_2} \\
b_9 = \; & \tfrac{1}{E_1E_2} + \tfrac{a_3}{E_1} + \tfrac{a_1}{E_2} + a_1a_3 - a_2^2 + \tfrac{a_2\nu_{12}}{E_1} + \tfrac{\nu_{21}a_2}{E_2} - \tfrac{\nu_{21}\nu_{12}}{E_1E_2}
\end{aligned}$$

$$\textit{These} \qquad \{\sigma\} = [Q]\{\epsilon\}$$

where $S^{-1} = Q$

$$[Q_{ij}] = \begin{bmatrix} \frac{b_1}{\beta} & \frac{b_2}{\beta} & \frac{b_3}{\beta} & 0 & 0 & 0 \\ \frac{b_4}{\beta} & \frac{b_5}{\beta} & \frac{b_6}{\beta} & 0 & 0 & 0 \\ \frac{b_7}{\beta} & \frac{b_8}{\beta} & \frac{b_9}{\beta} & 0 & 0 & 0 \\ 0 & 0 & 0 & G_{23} & 0 & 0 \\ 0 & 0 & 0 & 0 & G_{31} & 0 \\ 0 & 0 & 0 & 0 & 0 & G_{12} \end{bmatrix} \tag{2.31}$$

or

$$[Q_{ij}] = \begin{bmatrix} A_1 & A_2 & A_3 & 0 & 0 & 0 \\ A_4 & A_5 & A_6 & 0 & 0 & 0 \\ A_7 & A_8 & A_9 & 0 & 0 & 0 \\ 0 & 0 & 0 & G_{23} & 0 & 0 \\ 0 & 0 & 0 & 0 & G_{31} & 0 \\ 0 & 0 & 0 & 0 & 0 & G_{12} \end{bmatrix}$$

where

$$A_1 = \frac{b_1}{|\beta|}, \quad A_2 = \frac{b_2}{|\beta|}, \quad A_3 = \frac{b_3}{|\beta|}, \quad A_4 = \frac{b_4}{|\beta|}, \quad A_5 = \frac{b_5}{|\beta|}$$

$$A_6 = \frac{b_6}{|\beta|}, \quad A_7 = \frac{b_7}{|\beta|}, \quad A_8 = \frac{b_8}{|\beta|}, \quad A_9 = \frac{b_9}{|\beta|}$$

The laminate theory is valid for composite materials which are laminated in thin layers. Core materials constituting the sandwich panel have a high thickness. Hence sandwich panel can't be studied by using the laminate theory. In this theory it is possible to determine the equivalent rigidities. Laminate theory can be modified to take into account the transverse shear. Laminate approach also can be used for sandwich panel. A regular unit cell is consider with cell parameters l and h. X_3 axis is directed vertically upwards. The honeycomb walls is considered to be one solid layer of laminate. The wall thickness in the three inclined directions of the hexagonal shape are used to evaluate the equivalent geometric and material parameters of this lamina. The transformation matrix around X_3-axis is defined by:

$$[T] = \begin{bmatrix} cos^2\theta & sin^2\theta & 0 & 0 & 0 & 2cos\theta sin\theta \\ sin^2\theta & cos^2\theta & 0 & 0 & 0 & -2cos\theta sin\theta \\ 0 & 0 & 1 & 0 & 0 & 0 \\ 0 & 0 & 0 & cos\theta & -sin\theta & 0 \\ 0 & 0 & 0 & sin\theta & cos\theta & 0 \\ -cos\theta sin\theta & cos\theta sin\theta & 0 & 0 & 0 & cos^2\theta - sin^2\theta \end{bmatrix} \tag{2.32}$$

and

$$[T]^{-1} = \begin{bmatrix} cos^2\theta & sin^2\theta & 0 & 0 & 0 & -2cos\theta sin\theta \\ sin^2\theta & cos^2\theta & 0 & 0 & 0 & 2cos\theta sin\theta \\ 0 & 0 & 1 & 0 & 0 & 0 \\ 0 & 0 & 0 & cos\theta & sin\theta & 0 \\ 0 & 0 & 0 & -sin\theta & cos\theta & 0 \\ cos\theta sin\theta & -cos\theta sin\theta & 0 & 0 & 0 & cos^2\theta - sin^2\theta \end{bmatrix} \tag{2.33}$$

Where [R] is the Router matrix defined by:

$$[R] = \begin{bmatrix} 1 & 0 & 0 & 0 & 0 & 0 \\ 0 & 1 & 0 & 0 & 0 & 0 \\ 0 & 0 & 1 & 0 & 0 & 0 \\ 0 & 0 & 0 & 2 & 0 & 0 \\ 0 & 0 & 0 & 0 & 2 & 0 \\ 0 & 0 & 0 & 0 & 0 & 2 \end{bmatrix} \tag{2.34}$$

and

$$[R]^{-1} = \begin{bmatrix} 1 & 0 & 0 & 0 & 0 & 0 \\ 0 & 1 & 0 & 0 & 0 & 0 \\ 0 & 0 & 1 & 0 & 0 & 0 \\ 0 & 0 & 0 & 1/2 & 0 & 0 \\ 0 & 0 & 0 & 0 & 1/2 & 0 \\ 0 & 0 & 0 & 0 & 0 & 1/2 \end{bmatrix} \tag{2.35}$$

The relationship between $[Q_{ij}]$ and $[\bar{Q_{ij}}]$ is:

$[\bar{Q_{ij}}] = [T]^{-1}[Q_{ij}][R][T][R]^{-1}$ where i,j=1 to 6

$$[\bar{Q_{ij}}] = \begin{bmatrix} \bar{Q_{11}} & \bar{Q_{12}} & \bar{Q_{13}} & \bar{Q_{14}} & \bar{Q_{15}} & \bar{Q_{16}} \\ \bar{Q_{21}} & \bar{Q_{22}} & \bar{Q_{23}} & \bar{Q_{24}} & \bar{Q_{25}} & \bar{Q_{26}} \\ \bar{Q_{31}} & \bar{Q_{32}} & \bar{Q_{33}} & \bar{Q_{34}} & \bar{Q_{35}} & \bar{Q_{36}} \\ \bar{Q_{41}} & \bar{Q_{42}} & \bar{Q_{43}} & \bar{Q_{44}} & \bar{Q_{45}} & \bar{Q_{46}} \\ \bar{Q_{51}} & \bar{Q_{52}} & \bar{Q_{53}} & \bar{Q_{54}} & \bar{Q_{55}} & \bar{Q_{56}} \\ \bar{Q_{61}} & \bar{Q_{62}} & \bar{Q_{63}} & \bar{Q_{64}} & \bar{Q_{65}} & \bar{Q_{66}} \end{bmatrix}$$

where the elements are expressed as

$$
\begin{aligned}
\bar{Q_{11}} &= A_1 cos^4\theta + A_4 cos^2\theta sin^2\theta + A_2 cos^2\theta sin^2\theta + A_5 sin^4\theta + 4G_{12} cos^2\theta sin^2\theta \\
\bar{Q_{12}} &= A_1 sin^2\theta cos^2\theta + A_4 sin^4\theta + A_2 cos^4\theta + A_5 sin^2\theta cos^2\theta - 4G_{12} cos^2\theta sin^2\theta \\
\bar{Q_{13}} &= A_3 cos^2\theta + A_6 sin^2\theta \\
\bar{Q_{14}} &= 0 \\
\bar{Q_{15}} &= 0 \\
\bar{Q_{16}} &= A_1 cos^3\theta sin\theta + A_4 cos\theta sin^3\theta - A_2 cos^3\theta sin\theta - A_5 cos\theta sin^3\theta \\
&\quad -2G_{12} cos^3\theta sin\theta + 2G_{12} cos\theta sin^3\theta \\
\bar{Q_{21}} &= A_1 cos^2\theta sin^2\theta + A_4 cos^4\theta + A_2 sin^4\theta + A_5 cos^2\theta sin^2\theta - 4G_{12} cos^2\theta sin^2\theta \\
\bar{Q_{22}} &= A_1 sin^4\theta + A_4 cos^2\theta sin^2\theta + A_2 sin^2\theta cos^2\theta + A_5 cos^4\theta + 4G_{12} cos^2\theta sin^2\theta \\
\bar{Q_{23}} &= A_3 sin^2\theta + A_6 cos^2\theta \\
\bar{Q_{24}} &= 0 \\
\bar{Q_{25}} &= 0 \\
\bar{Q_{26}} &= A_1 cos\theta sin^3\theta + A_4 cos^3\theta sin\theta - A_2 sin^3\theta cos\theta - A_5 cos^3\theta sin\theta \\
&\quad +2G_{12} cos^3\theta sin\theta - 2G_{12} cos\theta sin^3\theta \\
\bar{Q_{31}} &= A_7 cos^2\theta + A_8 sin^2\theta \\
\bar{Q_{32}} &= A_7 sin^2\theta + A_8 cos^2\theta \\
\bar{Q_{33}} &= A_9 \\
\bar{Q_{34}} &= 0 \\
\bar{Q_{35}} &= 0 \\
\bar{Q_{36}} &= A_7 cos\theta sin\theta - A_8 cos\theta sin\theta \\
\bar{Q_{41}} &= 0 \\
\bar{Q_{42}} &= 0 \\
\bar{Q_{43}} &= 0 \\
\bar{Q_{44}} &= G_{23} cos^2\theta + G_{31} sin^2\theta \\
\bar{Q_{45}} &= -G_{23} cos\theta sin\theta + G_{31} cos\theta sin\theta \\
\bar{Q_{46}} &= 0 \\
\bar{Q_{51}} &= 0 \\
\bar{Q_{52}} &= 0 \\
\bar{Q_{53}} &= 0 \\
\bar{Q_{54}} &= -G_{23} cos\theta sin\theta + G_{31} cos\theta sin\theta
\end{aligned}
$$

$$
\begin{aligned}
\bar{Q_{55}} &= G_{23}sin^2\theta + G_{31}cos^2\theta \\
\bar{Q_{56}} &= 0 \\
\bar{Q_{61}} &= A_1cos^3\theta sin\theta - A_4cos^3\theta sin\theta + A_2cos\theta sin^3\theta - A_5cos\theta sin^3\theta \\
&\quad -2G_{12}cos^3\theta sin\theta + 2G_{12}cos\theta sin^3\theta \\
\bar{Q_{62}} &= A_1cos\theta sin^3\theta - A_4cos\theta sin^3\theta + A_2cos^3\theta sin\theta - A_5cos^3\theta sin\theta \\
&\quad +2G_{12}cos^3\theta sin\theta - 2G_{12}sin^3\theta cos\theta \\
\bar{Q_{63}} &= A_3cos\theta sin\theta - A_6cos\theta sin\theta \\
\bar{Q_{64}} &= 0 \\
\bar{Q_{65}} &= 0 \\
\bar{Q_{66}} &= A_1cos^2\theta sin^2\theta - A_4cos^2\theta sin^2\theta - A_2cos^2\theta sin^2\theta + A_5cos^2\theta sin^2\theta \\
&\quad +G_{12}cos^4\theta - 2G_{12}cos^2\theta sin^2\theta + G_{12}sin^4\theta
\end{aligned}
$$

The stress-strain relation may be put as

$$
\begin{Bmatrix} \sigma_{11} \\ \sigma_{22} \\ \sigma_{33} \\ \tau_{23} \\ \tau_{31} \\ \tau_{12} \end{Bmatrix} = \begin{bmatrix} \bar{Q_{11}} & \bar{Q_{12}} & \bar{Q_{13}} & 0 & 0 & \bar{Q_{16}} \\ \bar{Q_{21}} & \bar{Q_{22}} & \bar{Q_{23}} & 0 & 0 & \bar{Q_{26}} \\ \bar{Q_{31}} & \bar{Q_{32}} & \bar{Q_{33}} & 0 & 0 & \bar{Q_{36}} \\ 0 & 0 & 0 & \bar{Q_{44}} & \bar{Q_{45}} & 0 \\ 0 & 0 & 0 & \bar{Q_{54}} & \bar{Q_{55}} & 0 \\ \bar{Q_{61}} & \bar{Q_{62}} & \bar{Q_{63}} & 0 & 0 & \bar{Q_{66}} \end{bmatrix} \begin{Bmatrix} \epsilon_{11} \\ \epsilon_{22} \\ \epsilon_{33} \\ \gamma_{23} \\ \gamma_{31} \\ \gamma_{12} \end{Bmatrix}
$$

Substituting eq. (2.22d) and eq. (2.22e) in the above relation

$$
\bar{Q_{13}} = \bar{Q_{23}} = \bar{Q_{63}} = 0.
$$

$$
\begin{Bmatrix} \sigma_{11} \\ \sigma_{22} \\ \sigma_{33} \\ \tau_{23} \\ \tau_{31} \\ \tau_{12} \end{Bmatrix} = \begin{bmatrix} \bar{Q_{11}} & \bar{Q_{12}} & 0 & 0 & 0 & \bar{Q_{16}} \\ \bar{Q_{21}} & \bar{Q_{22}} & 0 & 0 & 0 & \bar{Q_{26}} \\ \bar{Q_{31}} & \bar{Q_{32}} & \bar{Q_{33}} & 0 & 0 & \bar{Q_{36}} \\ 0 & 0 & 0 & \bar{Q_{44}} & \bar{Q_{45}} & 0 \\ 0 & 0 & 0 & \bar{Q_{54}} & \bar{Q_{55}} & 0 \\ \bar{Q_{61}} & \bar{Q_{62}} & 0 & 0 & 0 & \bar{Q_{66}} \end{bmatrix} \begin{Bmatrix} \epsilon_{11} \\ \epsilon_{22} \\ \epsilon_{33} \\ \gamma_{23} \\ \gamma_{31} \\ \gamma_{12} \end{Bmatrix} \tag{2.36}
$$

2.4 Shear Deformable Curved Sandwich Panel

Figure 2.4 show the orthogonal curvilinear coordinates or shell coordinates for the sandwich curved panel. The axis carry dual naming of X_1, X_2, X_3 and X,Y,Z. These

are used interchangeably in the analysis. The X and Y axis are along the lines of curvature on the mid-surface z=0, and Z-curves are straight lines perpendicular to the surface z=0. For cylindrical and spherical shells the lines of principal curvature coincide with the coordinate lines. The values of the principal radii of curvature of the middle surface are denoted by R_1 and R_2.

The position vector of a point on the middle surface is denoted by r, and the position of a point at distance z from the middle surface is denoted by R. The distance ds between points (x,y,0) and (x+dx,y+dy,0) is determined by [19,20]

$$\begin{aligned}(ds)^2 &= dr.dr \\ &= {\alpha_1}^2(dx)^2 + {\alpha_2}^2(dy)^2\end{aligned} \tag{2.37}$$

where $dr = t_1 dx + t_2 dy$, the vector t_1 and t_2 ($t_i = \frac{\partial r}{\partial x}$), i=1,2 are tangent to the x_1 and x_2 coordinate lines, and α_1 and α_2 are the surface matrices

$$\alpha_1^2 = t_1.t_1, \qquad \alpha_2^2 = t_2.t_2 \tag{2.38}$$

The distance dS between points(x,y,z) and (x+dx, y+dy, z+dz) is giving by

$$\begin{aligned}(dS)^2 &= dR.dR \\ &= L_1^2(dx) + L_2^2(dy) + L_3^2(dz)\end{aligned} \tag{2.39}$$

where $dR = \frac{\partial R}{\partial x}dx + \frac{\partial R}{\partial y}dy + \frac{\partial R}{\partial z}dz$, and L_1, L_2 and L_3 are Lame coefficients

$$L_1 = \alpha_1(1 + \frac{z}{R_1}), \qquad L_2 = \alpha_2(1 + \frac{z}{R_2}), \quad L_3 = 1 \tag{2.40}$$

2.4.1 Displacement Field

By using the equivalent material properties, the sandwich panel may be modelled as a common laminated panel with the honeycomb replaced by an equivalent solid lamina. The geometry of the panel would be unchanged. The displacement field for the sandwich panel satisfying the higher order shear deformation theory is [19,20]

$$\begin{aligned}\bar{u}(x,y,z,t) &= u(1 + \tfrac{z}{R_1}) + z\psi_x + z^2\xi_x + z^3\zeta_x \\ \bar{v}(x,y,z,t) &= v(1 + \tfrac{z}{R_2}) + z\psi_y + z^2\xi_y + z^3\zeta_y \\ \bar{w}(x,y,z,t) &= w\end{aligned} \tag{2.41}$$

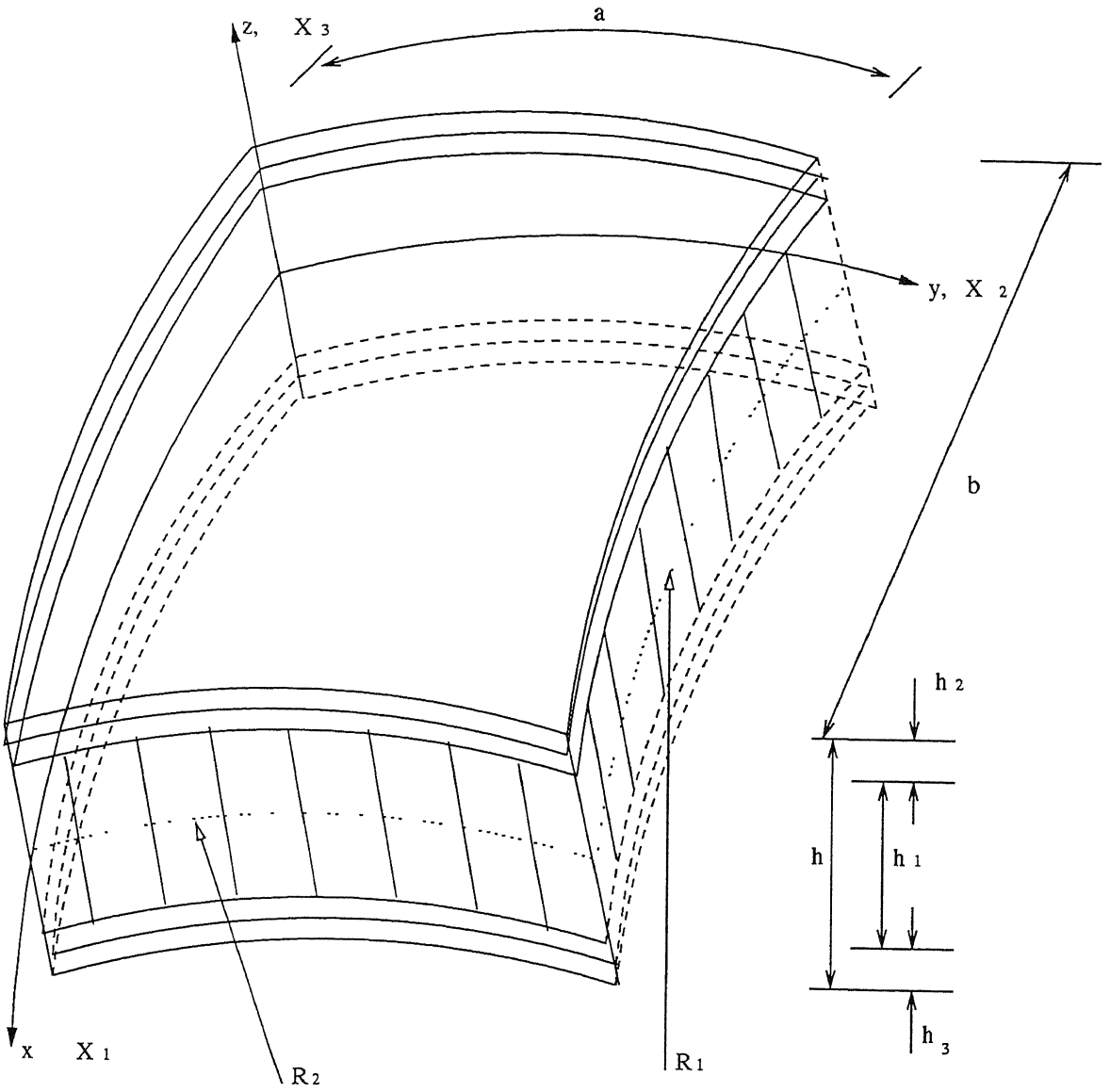

Figure 2.4: Sandwich Panel Element

where t is time, $(\bar{u}, \bar{v}, \bar{w})$ are the displacements along the (x,y,z) coordinates,(u,v,w) denotes the compounding displacements of the point (x,y,0) on the mid-plane and ψ_x and ψ_y are the rotations of normal to the mid-plane to x and y-axes respectively.

The functions ξ_x, ζ_x, ξ_y and ζ_y will be determined using the condition that transverse shear stresses τ_{xz} and τ_{yz} vanish on the top and bottom surfaces of the shell.

$$\tau_{xz}\left(x, y, \pm\frac{h}{2}, t\right) = 0, \qquad \tau_{yz}\left(x, y, \pm\frac{h}{2}, t\right) = 0 \tag{2.42}$$

These conditions are equivalent to the requirement that the corresponding strains be zero on these surfaces. The transverse shear strains of a shell with two principal radii of curvature are given by

$$\begin{aligned}
\epsilon_5 &= \frac{\partial \bar{u}}{\partial z} + \frac{\partial \bar{w}}{\partial x} \\
&= \frac{\partial \bar{u}}{\partial z} + \frac{1}{\alpha_1}\frac{\partial \bar{w}}{\partial x} - \frac{u}{R_1} \\
&= \frac{u}{R_1} + \psi_x + 2z\xi_x + 3z^2\zeta_x + \frac{1}{\alpha_1}\frac{\partial \bar{w}}{\partial x} - \frac{u}{R_1} \\
\epsilon_4 &= \frac{\partial \bar{v}}{\partial z} + \frac{\partial \bar{w}}{\partial y} \\
&= \frac{\partial \bar{v}}{\partial z} + \frac{1}{\alpha_1}\frac{\partial \bar{w}}{\partial y} - \frac{v}{R_2} \\
&= \frac{v}{R_2} + \psi_y + 2z\xi_y + 3z^2\zeta_y + \frac{1}{\alpha_1}\frac{\partial \bar{w}}{\partial y} - \frac{v}{R_2}
\end{aligned} \tag{2.43}$$

Setting $\epsilon_5\left(x, y, \pm\frac{h}{2}, t\right)$ and $\epsilon_4\left(x, y, \pm\frac{h}{2}, t\right)$ to zero,we obtain

$$\xi_x = \xi_y = 0$$

$$\begin{aligned}
\zeta_x &= -\frac{4}{3h^2}\left(\psi_x + \frac{1}{\alpha_1}\frac{\partial w}{\partial x}\right) \\
\zeta_y &= -\frac{4}{3h^2}\left(\psi_y + \frac{1}{\alpha_2}\frac{\partial w}{\partial y}\right)
\end{aligned} \tag{2.44}$$

Substituting eq (2.44) into eq (2.41), we obtain

$$\begin{aligned}
\bar{u}(x, y, z) &= \left(1 + \frac{z}{R_1}\right)u + z\psi_x - z^3\frac{4}{3h^2}\left[\psi_x + \frac{1}{\alpha_1}\frac{\partial w}{\partial x}\right] \\
\bar{v}(x, y, z) &= \left(1 + \frac{z}{R_2}\right)v + z\psi_y - z^3\frac{4}{3h^2}\left[\psi_y + \frac{1}{\alpha_2}\frac{\partial w}{\partial y}\right]
\end{aligned} \tag{2.45}$$

This displacement field is used to compute the strain and stress, and then in formulating the system equations

2.4.2 Stress-Strain Relation

Substituting eq (2.45) into the strain-displacement relation

$$
\begin{aligned}
\epsilon_{11} = \epsilon_1 &= \epsilon_1^0 + z(k_1^0 + z^2 k_1^2) \\
\epsilon_{22} = \epsilon_2 &= \epsilon_2^0 + z(k_2^0 + z^2 k_2^2) \\
\epsilon_{33} = \epsilon_3 &= 0 \\
\gamma_{23} = \epsilon_4 &= \epsilon_4^0 + z^2 k_4^2 \\
\gamma_{31} = \epsilon_5 &= \epsilon_5^0 + z^2 k_5^2 \\
\gamma_{12} = \epsilon_6 &= \epsilon_6^0 + z(k_6^0 + z^2 k_6^2)
\end{aligned}
\tag{2.46}
$$

where

$$
\begin{aligned}
&\epsilon_1^0 = \tfrac{\partial u}{\partial x} + \tfrac{w}{R_1}; \quad k_1^0 = \tfrac{\partial \psi_x}{\partial x}; && k_1^2 = -\tfrac{4}{3h^2}\left(\tfrac{\partial \psi_x}{\partial x} + \tfrac{\partial^2 w}{\partial x^2}\right) \\
&\epsilon_2^0 = \tfrac{\partial v}{\partial y} + \tfrac{w}{R_2}; \quad k_2^0 = \tfrac{\partial \psi_y}{\partial y}; && k_2^2 = -\tfrac{4}{3h^2}\left(\tfrac{\partial \psi_y}{\partial y} + \tfrac{\partial^2 w}{\partial y^2}\right) \\
&\epsilon_3^0 = 0 \\
&\epsilon_4^0 = \psi_y + \tfrac{\partial w}{\partial y}; \quad k_4^2 = -\tfrac{4}{h^2}\left(\psi_y + \tfrac{\partial w}{\partial y}\right) \\
&\epsilon_5^0 = \psi_x + \tfrac{\partial w}{\partial x}; \quad k_5^2 = -\tfrac{4}{h^2}\left(\psi_x + \tfrac{\partial w}{\partial x}\right) \\
&\epsilon_6^0 = \tfrac{\partial u}{\partial y} + \tfrac{\partial v}{\partial x}; \quad k_6^0 = \tfrac{\partial \psi_x}{\partial y} + \tfrac{\partial \psi_y}{\partial x}; && k_6^2 = -\tfrac{4}{3h^2}\left(\tfrac{\partial \psi_x}{\partial y} + \tfrac{\partial \psi_y}{\partial x} + 2\tfrac{\partial^2 w}{\partial x \partial y}\right)
\end{aligned}
\tag{2.47}
$$

Here x and y denote the Cartesian coordinates ($dx = \alpha_1 dz, dy = \alpha_2 dz$).

The transformed stress-strain relation for the k^{th} lamina with respect to the laminate coordinates are

$$
\begin{Bmatrix} \sigma_{11} \\ \sigma_{22} \\ \sigma_{33} \\ \tau_{23} \\ \tau_{31} \\ \tau_{12} \end{Bmatrix}_{(k)} =
\begin{bmatrix}
\bar{Q}_{11} & \bar{Q}_{12} & 0 & 0 & 0 & \bar{Q}_{16} \\
\bar{Q}_{21} & \bar{Q}_{22} & 0 & 0 & 0 & \bar{Q}_{26} \\
\bar{Q}_{31} & \bar{Q}_{32} & \bar{Q}_{33} & 0 & 0 & \bar{Q}_{36} \\
0 & 0 & 0 & \bar{Q}_{44} & \bar{Q}_{45} & 0 \\
0 & 0 & 0 & \bar{Q}_{54} & \bar{Q}_{55} & 0 \\
\bar{Q}_{61} & \bar{Q}_{62} & 0 & 0 & 0 & \bar{Q}_{66}
\end{bmatrix}_{(k)}
\begin{Bmatrix} \epsilon_{11} \\ \epsilon_{22} \\ \epsilon_{33} \\ \gamma_{23} \\ \gamma_{31} \\ \gamma_{12} \end{Bmatrix}_{(k)}
\tag{2.48}
$$

Rearrange eq (2.48)

$$
\begin{Bmatrix} \sigma_{11} \\ \sigma_{22} \\ \tau_{12} \end{Bmatrix}_{(k)} =
\begin{bmatrix}
\bar{Q}_{11} & \bar{Q}_{12} & \bar{Q}_{16} \\
\bar{Q}_{21} & \bar{Q}_{22} & \bar{Q}_{26} \\
\bar{Q}_{61} & \bar{Q}_{62} & \bar{Q}_{66}
\end{bmatrix}_{(k)}
\begin{Bmatrix} \epsilon_{11} \\ \epsilon_{22} \\ \gamma_{12} \end{Bmatrix}_{(k)}
\tag{2.49}
$$

$$
\begin{Bmatrix} \tau_{23} \\ \tau_{31} \end{Bmatrix}_{(k)} =
\begin{bmatrix}
\bar{Q}_{44} & \bar{Q}_{45} \\
\bar{Q}_{54} & \bar{Q}_{55}
\end{bmatrix}_{(k)}
\begin{Bmatrix} \gamma_{23} \\ \gamma_{31} \end{Bmatrix}_{(k)}
\tag{2.50}
$$

$$\sigma_{33} = \bar{Q_{31}}\epsilon_{11} + \bar{Q_{32}}\epsilon_{22} + \bar{Q_{33}}\epsilon_{33} + \bar{Q_{36}}\gamma_{12}$$

Here

$$\sigma_{11} = \sigma_{xx} \quad \sigma_{22} = \sigma_{yy} \quad \sigma_{33} = \sigma_{zz} \quad \tau_{12} = \tau_{xy} \quad \tau_{23} = \tau_{yz} \quad \tau_{31} = \tau_{zx}$$
$$\epsilon_{11} = \epsilon_{xx} \quad \epsilon_{22} = \epsilon_{yy} \quad \epsilon_{33} = \epsilon_{zz} \quad \gamma_{12} = \gamma_{xy} \quad \gamma_{23} = \gamma_{yz} \quad \gamma_{31} = \gamma_{zx}$$

2.5 System Equation For Sandwich Panel

The virtual variation in the total strain energy must be equal to zero. Hence

$$0 = \frac{1}{2}\int_0^t \left[\int_{-h/2}^{h/2} \left\{\int_0^a \int_0^b \left[\sigma_1\delta\epsilon_1 + \sigma_2\delta\epsilon_2 + \sigma_6\delta\epsilon_6 + \sigma_4\delta\epsilon_4 + \sigma_5\delta\epsilon_5\right] dxdy - q\delta w dxdy\right\} dz\right] dt$$
$$- \delta\int_0^t \left[\int_{-h/2}^{h/2} \left\{\int_0^a \int_0^b \rho\left[(\dot{\bar{u}})^2 + (\dot{\bar{v}})^2 + (\dot{\bar{w}})^2\right] dxdy\right\} dz\right] dt \qquad (2.51)$$

or

$$0 = \int_0^t \left\{\int_0^a \int_0^b \Big[\left[N_1\delta\epsilon_1^0 + M_1\delta K_1^0 + P_1\delta K_1^2 + N_2\delta\epsilon_2^0 + M_2\delta K_2^0 + P_2\delta K_2^2 + N_6\delta\epsilon_6^0\right.\right.$$
$$\left. + M_6\delta K_6^0 + P_6\delta K_6^2 + Q_2\delta\epsilon_4^0 + K_2\delta K_4^1 + Q_1\delta\epsilon_5^0 + K_1\delta K_5^1 - q\delta w\right]$$
$$+ \left(\bar{I}_1\ddot{u} + \bar{I}_2\ddot{\psi}_x - \bar{I}_3\frac{\partial\ddot{w}}{\partial x}\right)\delta u + \left(\bar{I}_1'\ddot{v} + \bar{I}_2'\ddot{\psi}_y - \bar{I}_3'\frac{\partial\ddot{w}}{\partial y}\right)\delta v$$
$$+ \left(\bar{I}_3\frac{\partial\ddot{u}}{\partial x} + \bar{I}_5\frac{\partial\ddot{\psi}_x}{\partial x} + \bar{I}_3'\frac{\partial\ddot{v}}{\partial y} + \bar{I}_5'\frac{\partial\ddot{\psi}_y}{\partial y} - \frac{16I_7}{9h^4}\left(\frac{\partial\ddot{w}}{\partial x^2} + \frac{\partial\ddot{w}}{\partial y^2}\right) + I_1\ddot{w}\right)\delta w$$
$$\left. + \left(\bar{I}_2\ddot{u} + \bar{I}_4\ddot{\psi}_x - \bar{I}_5\frac{\partial\ddot{w}}{\partial x}\right)\delta\psi_x + \left(\bar{I}_2'\ddot{v} + \bar{I}_4'\ddot{\psi}_y - \bar{I}_5'\frac{\partial\ddot{w}}{\partial y}\right)\delta\psi_y\Big] dxdy\right\} dt$$

Where δ indicates the virtual variation in the parameter.

Where q is the distributed transverse load, $N_i, M_i, P_i, Q_2, Q_1, K_2, K_1$ are the resultants,

$$(N_i, M_i, P_i) = \sum_{k=1}^{n}\int_{-h/2}^{h/2}\sigma_i^{(k)}\left(1, z, z^3\right)dz \qquad (i = 1, 2, 6)$$
$$(Q_1, K_1) = \sum_{k=1}^{n}\int_{-h/2}^{h/2}\sigma_5^{(k)}\left(1, z^2\right)dz$$
$$(Q_2, K_2) = \sum_{k=1}^{n}\int_{-h/2}^{h/2}\sigma_4^{(k)}\left(1, z^2\right)dz \qquad (2.52)$$

The inertias $\bar{I}_i$and$\bar{I}_i'$(i=1,2,3,4,5) are defined by the equations,

$$(I_1, I_2, I_3, I_4, I_5, I_7) = \sum_{k=1}^{n}\int_{-h/2}^{h/2}\rho^{(k)}\left(1, z, z^2, z^3, z^4, z^6\right)dz$$

$$
\begin{aligned}
\bar{I}_1 &= I_1 + \tfrac{2}{R_1} I_2 \\
\bar{I}_1{}' &= I_1 + \tfrac{2}{R_2} I_2 \\
\bar{I}_2 &= I_2 + \tfrac{1}{R_1} I_3 - \tfrac{4}{3h^2} I_4 - \tfrac{4}{3h^2 R_1} I_5 \\
\bar{I}_2{}' &= I_2 + \tfrac{1}{R_2} I_3 - \tfrac{4}{3h^2} I_4 - \tfrac{4}{3h^2 R_2} I_5 \\
\bar{I}_3 &= \tfrac{4}{3h^2} I_4 + \tfrac{4}{3h^2 R_1} I_5 \\
\bar{I}_3{}' &= \tfrac{4}{3h^2} I_4 + \tfrac{4}{3h^2 R_2} I_5 \\
\bar{I}_4 &= I_3 - \tfrac{8}{3h^2} I_5 + \tfrac{16}{9h^4} I_7 \\
\bar{I}_4{}' &= I_3 - \tfrac{8}{3h^2} I_5 + \tfrac{16}{9h^4} I_7 \\
\bar{I}_5 &= \tfrac{4}{3h^2} I_5 - \tfrac{16}{9h^4} I_7 \\
\bar{I}_5{}' &= \tfrac{4}{3h^2} I_5 - \tfrac{16}{9h^4} I_7
\end{aligned}
\tag{2.53}
$$

The governing equations of motion can be derived from eq (2.51) by integrating the displacement gradients by parts and setting the coefficients of $\delta u, \delta v, \delta w, \delta\psi_x$ *and* $\delta\psi_y$ to zero separately with the moment terms in the first two equations being omitted

$$
\delta u: \quad \frac{\partial N_1}{\partial x} + \frac{\partial N_6}{\partial y} = \bar{I}_1 \ddot{u} + \bar{I}_2 \ddot{\psi}_x - \bar{I}_3 \frac{\partial \ddot{w}}{\partial x}
$$

$$
\delta v: \quad \frac{\partial N_6}{\partial x} + \frac{\partial N_2}{\partial y} = \bar{I}_1{}' \ddot{v} + \bar{I}_2{}' \ddot{\psi}_y - \bar{I}_3{}' \frac{\partial \ddot{w}}{\partial y}
$$

$$
\begin{aligned}
\delta w: \quad & \frac{\partial Q_1}{\partial x} + \frac{\partial Q_2}{\partial y} - \frac{4}{h^2}\left(\frac{\partial K_1}{\partial x} + \frac{\partial K_2}{\partial y}\right) + \frac{4}{3h^2}\left(\frac{\partial^2 P_1}{\partial x^2} + \frac{\partial^2 P_2}{\partial y^2} + 2\frac{\partial^2 P_6}{\partial x \partial y}\right) - \frac{N_1}{R_1} - \frac{N_2}{R_2} \\
& = \bar{I}_3 \frac{\partial \ddot{u}}{\partial x} + \bar{I}_5 \frac{\partial \ddot{\psi}_x}{\partial x} + \bar{I}_3{}' \frac{\partial \ddot{v}}{\partial x} + \bar{I}_5{}' \frac{\partial \ddot{\psi}_y}{\partial y} + \bar{I}_1 \ddot{w} - \frac{16 I_7}{9h^4}\left(\frac{\partial^2 \ddot{w}}{\partial x^2} + \frac{\partial^2 \ddot{w}}{\partial y^2}\right) - q
\end{aligned}
\tag{2.54}
$$

$$
\delta\psi_x: \quad \frac{\partial M_1}{\partial x} + \frac{\partial M_6}{\partial y} - Q_1 + \frac{4}{h^2} K_1 - \frac{4}{3h^2}\left(\frac{\partial P_1}{\partial x} + \frac{\partial P_6}{\partial y}\right) = \bar{I}_2 \partial \ddot{u} + \bar{I}_4 \ddot{\psi}_x - \bar{I}_5 \frac{\partial \ddot{w}}{\partial x}
$$

$$
\delta\psi_y: \quad \frac{\partial M_6}{\partial x} + \frac{\partial M_2}{\partial y} - Q_2 + \frac{4}{h^2} K_2 - \frac{4}{3h^2}\left(\frac{\partial P_6}{\partial x} + \frac{\partial P_2}{\partial y}\right) = \bar{I}_2{}' \partial \ddot{v} + \bar{I}_4{}' \ddot{\psi}_y - \bar{I}_5{}' \frac{\partial \ddot{w}}{\partial y}
$$

The Resultants are expressed in terms of the strain components using eq(2.46) and eq(2.48)in eq(2.52) we get

$$
\begin{aligned}
N_i &= A_{ij}\epsilon_j^0 + B_{ij}K_j^0 + E_{ij}K_j^2 \\
M_i &= B_{ij}\epsilon_j^0 + D_{ij}K_j^0 + F_{ij}K_j^2 \qquad (i,j = 1,2,6) \\
P_i &= E_{ij}\epsilon_j^0 + F_{ij}K_j^0 + H_{ij}K_j^2 \\
Q_2 &= A_{4j}\epsilon_j^0 + D_{4j}K_j^1 \\
Q_1 &= A_{5j}\epsilon_j^0 + D_{5j}K_j^1 \\
K_2 &= D_{4j}\epsilon_j^0 + F_{4j}K_j^1 \qquad (j = 4,5) \\
K_1 &= D_{5j}\epsilon_j^0 + F_{5j}K_j^1
\end{aligned}
\tag{2.55}
$$

Where $A_{ij}, B_{ij}, D_{ij}, E_{ij}, F_{ij}, H_{ij}$ are the laminate stiffnesses

$$(A_{ij}, B_{ij}, D_{ij}, E_{ij}, F_{ij}, H_{ij}) = \sum_{k=1}^{n} \int_{-h/2}^{h/2} Q_{ij}^{k} \left(1, z, z^2, z^3, z^4, z^6\right) dz \tag{2.56}$$

for i,j=1,2,4,5,6.

$$\frac{\partial N_1}{\partial x} = A_{11}\frac{\partial \epsilon_1^0}{\partial x} + A_{12}\frac{\partial \epsilon_2^0}{\partial x} + A_{16}\frac{\partial \epsilon_6^0}{\partial x} + B_{11}\frac{\partial K_1^0}{\partial x} + B_{12}\frac{\partial K_2^0}{\partial x} + B_{16}\frac{\partial K_6^0}{\partial x}$$
$$+E_{11}\frac{\partial K_1^2}{\partial x} + E_{12}\frac{\partial K_2^2}{\partial x} + E_{16}\frac{\partial K_6^2}{\partial x}$$

$$\frac{\partial N_2}{\partial y} = A_{21}\frac{\partial \epsilon_1^0}{\partial y} + A_{22}\frac{\partial \epsilon_2^0}{\partial y} + A_{26}\frac{\partial \epsilon_6^0}{\partial y} + B_{21}\frac{\partial K_1^0}{\partial y} + B_{22}\frac{\partial K_2^0}{\partial y} + B_{26}\frac{\partial K_6^0}{\partial y}$$
$$+E_{21}\frac{\partial K_1^2}{\partial y} + E_{22}\frac{\partial K_2^2}{\partial y} + E_{26}\frac{\partial K_6^2}{\partial y}$$

$$\frac{\partial N_6}{\partial x} = A_{61}\frac{\partial \epsilon_1^0}{\partial x} + A_{62}\frac{\partial \epsilon_2^0}{\partial x} + A_{66}\frac{\partial \epsilon_6^0}{\partial x} + B_{61}\frac{\partial K_1^0}{\partial x} + B_{62}\frac{\partial K_2^0}{\partial x} + B_{66}\frac{\partial K_6^0}{\partial x}$$
$$+E_{61}\frac{\partial K_1^2}{\partial x} + E_{62}\frac{\partial K_2^2}{\partial x} + E_{66}\frac{\partial K_6^2}{\partial x}$$

$$\frac{\partial N_6}{\partial y} = A_{61}\frac{\partial \epsilon_1^0}{\partial y} + A_{62}\frac{\partial \epsilon_2^0}{\partial y} + A_{66}\frac{\partial \epsilon_6^0}{\partial y} + B_{61}\frac{\partial K_1^0}{\partial y} + B_{62}\frac{\partial K_2^0}{\partial y} + B_{66}\frac{\partial K_6^0}{\partial y}$$
$$+E_{61}\frac{\partial K_1^2}{\partial y} + E_{62}\frac{\partial K_2^2}{\partial y} + E_{66}\frac{\partial K_6^2}{\partial y}$$

$$\frac{\partial M_1}{\partial x} = B_{11}\frac{\partial \epsilon_1^0}{\partial x} + B_{12}\frac{\partial \epsilon_2^0}{\partial x} + B_{16}\frac{\partial \epsilon_6^0}{\partial x} + D_{11}\frac{\partial K_1^0}{\partial x} + D_{12}\frac{\partial K_2^0}{\partial x} + D_{16}\frac{\partial K_6^0}{\partial x}$$
$$+F_{11}\frac{\partial K_1^2}{\partial x} + F_{12}\frac{\partial K_2^2}{\partial x} + F_{16}\frac{\partial K_6^2}{\partial x}$$

$$\frac{\partial M_2}{\partial y} = B_{21}\frac{\partial \epsilon_1^0}{\partial y} + B_{22}\frac{\partial \epsilon_2^0}{\partial y} + B_{26}\frac{\partial \epsilon_6^0}{\partial y} + D_{21}\frac{\partial K_1^0}{\partial y} + D_{22}\frac{\partial K_2^0}{\partial y} + D_{26}\frac{\partial K_6^0}{\partial y}$$
$$+F_{21}\frac{\partial K_1^2}{\partial y} + F_{22}\frac{\partial K_2^2}{\partial y} + F_{26}\frac{\partial K_6^2}{\partial y}$$

$$\frac{\partial M_6}{\partial x} = B_{61}\frac{\partial \epsilon_1^0}{\partial x} + B_{62}\frac{\partial \epsilon_2^0}{\partial x} + B_{66}\frac{\partial \epsilon_6^0}{\partial x} + D_{61}\frac{\partial K_1^0}{\partial x} + D_{62}\frac{\partial K_2^0}{\partial x} + D_{66}\frac{\partial K_6^0}{\partial x}$$
$$+F_{61}\frac{\partial K_1^2}{\partial x} + F_{62}\frac{\partial K_2^2}{\partial x} + F_{66}\frac{\partial K_6^2}{\partial x}$$

$$\frac{\partial M_6}{\partial y} = B_{61}\frac{\partial \epsilon_1^0}{\partial y} + B_{62}\frac{\partial \epsilon_2^0}{\partial y} + B_{66}\frac{\partial \epsilon_6^0}{\partial y} + D_{61}\frac{\partial K_1^0}{\partial y} + D_{62}\frac{\partial K_2^0}{\partial y} + D_{66}\frac{\partial K_6^0}{\partial y}$$
$$+F_{61}\frac{\partial K_1^2}{\partial y} + F_{62}\frac{\partial K_2^2}{\partial y} + F_{66}\frac{\partial K_6^2}{\partial y}$$

$$\frac{\partial Q_1}{\partial x} = A_{54}\frac{\partial \epsilon_4^0}{\partial x} + A_{55}\frac{\partial \epsilon_5^0}{\partial x} + D_{54}\frac{\partial K_4^1}{\partial x} + D_{55}\frac{\partial K_5^1}{\partial x}$$

$$
\begin{aligned}
\frac{\partial Q_2}{\partial y} &= A_{44}\frac{\partial \epsilon_4^0}{\partial y} + A_{45}\frac{\partial \epsilon_5^0}{\partial y} + D_{44}\frac{\partial K_4^1}{\partial y} + D_{45}\frac{\partial K_5^1}{\partial y} \\
\frac{\partial K_1}{\partial x} &= D_{54}\frac{\partial \epsilon_4^0}{\partial x} + D_{55}\frac{\partial \epsilon_5^0}{\partial x} + F_{54}\frac{\partial K_4^1}{\partial x} + F_{55}\frac{\partial K_5^1}{\partial x} \\
\frac{\partial K_2}{\partial y} &= D_{44}\frac{\partial \epsilon_4^0}{\partial y} + D_{45}\frac{\partial \epsilon_5^0}{\partial y} + F_{44}\frac{\partial K_4^1}{\partial y} + F_{45}\frac{\partial K_5^1}{\partial y} \\
\frac{\partial P_1}{\partial x} &= E_{11}\frac{\partial \epsilon_1^0}{\partial x} + E_{12}\frac{\partial \epsilon_2^0}{\partial x} + E_{16}\frac{\partial \epsilon_6^0}{\partial x} + F_{11}\frac{\partial K_1^0}{\partial x} + F_{12}\frac{\partial K_2^0}{\partial x} + F_{16}\frac{\partial K_6^0}{\partial x} \\
&\quad + H_{11}\frac{\partial K_1^2}{\partial x} + H_{12}\frac{\partial K_2^2}{\partial x} + H_{16}\frac{\partial K_6^2}{\partial x} \\
\frac{\partial P_2}{\partial y} &= E_{21}\frac{\partial \epsilon_1^0}{\partial y} + E_{22}\frac{\partial \epsilon_2^0}{\partial y} + E_{26}\frac{\partial \epsilon_6^0}{\partial y} + F_{21}\frac{\partial K_1^0}{\partial y} + F_{22}\frac{\partial K_2^0}{\partial y} + F_{26}\frac{\partial K_6^0}{\partial y} \\
&\quad + H_{21}\frac{\partial K_1^2}{\partial y} + H_{22}\frac{\partial K_2^2}{\partial y} + H_{26}\frac{\partial K_6^2}{\partial y} \\
\frac{\partial P_6}{\partial x} &= E_{61}\frac{\partial \epsilon_1^0}{\partial x} + E_{62}\frac{\partial \epsilon_2^0}{\partial x} + E_{66}\frac{\partial \epsilon_6^0}{\partial x} + F_{61}\frac{\partial K_1^0}{\partial x} + F_{62}\frac{\partial K_2^0}{\partial x} + F_{66}\frac{\partial K_6^0}{\partial x} \\
&\quad + H_{61}\frac{\partial K_1^2}{\partial x} + H_{62}\frac{\partial K_2^2}{\partial x} + H_{66}\frac{\partial K_6^2}{\partial x} \\
\frac{\partial P_6}{\partial y} &= E_{61}\frac{\partial \epsilon_1^0}{\partial y} + E_{62}\frac{\partial \epsilon_2^0}{\partial y} + E_{66}\frac{\partial \epsilon_6^0}{\partial y} + F_{61}\frac{\partial K_1^0}{\partial y} + F_{62}\frac{\partial K_2^0}{\partial y} + F_{66}\frac{\partial K_6^0}{\partial y} \\
&\quad + H_{61}\frac{\partial K_1^2}{\partial y} + H_{62}\frac{\partial K_2^2}{\partial y} + H_{66}\frac{\partial K_6^2}{\partial y} \\
\frac{\partial^2 P_1}{\partial^2 x} &= E_{11}\frac{\partial^2 \epsilon_1^0}{\partial^2 x} + E_{12}\frac{\partial^2 \epsilon_2^0}{\partial^2 x} + E_{16}\frac{\partial^2 \epsilon_6^0}{\partial^2 x} + F_{11}\frac{\partial^2 K_1^0}{\partial^2 x} + F_{12}\frac{\partial^2 K_2^0}{\partial^2 x} + F_{16}\frac{\partial^2 K_6^0}{\partial^2 x} \\
&\quad + H_{11}\frac{\partial K_1^2}{\partial x} + H_{12}\frac{\partial K_2^2}{\partial x} + H_{16}\frac{\partial K_6^2}{\partial x} \\
\frac{\partial^2 P_2}{\partial^2 y} &= E_{21}\frac{\partial^2 \epsilon_1^0}{\partial^2 y} + E_{22}\frac{\partial^2 \epsilon_2^0}{\partial^2 y} + E_{26}\frac{\partial^2 \epsilon_6^0}{\partial^2 y} + F_{21}\frac{\partial^2 K_1^0}{\partial^2 y} + F_{22}\frac{\partial^2 K_2^0}{\partial^2 y} + F_{26}\frac{\partial^2 K_6^0}{\partial^2 y} \\
&\quad + H_{21}\frac{\partial^2 K_1^2}{\partial^2 y} + H_{22}\frac{\partial^2 K_2^2}{\partial^2 y} + H_{26}\frac{\partial^2 K_6^2}{\partial^2 y} \\
\frac{\partial^2 P_6}{\partial x \partial y} &= E_{61}\frac{\partial^2 \epsilon_1^0}{\partial x \partial y} + E_{62}\frac{\partial^2 \epsilon_2^0}{\partial x \partial y} + E_{66}\frac{\partial^2 \epsilon_6^0}{\partial x \partial y} + F_{61}\frac{\partial^2 K_1^0}{\partial x \partial y} + F_{62}\frac{\partial^2 K_2^0}{\partial x \partial y} + F_{66}\frac{\partial K_6^0}{\partial x \partial y} \\
&\quad + H_{61}\frac{\partial^2 K_1^2}{\partial x \partial y} + H_{62}\frac{\partial^2 K_2^2}{\partial x \partial y} + H_{66}\frac{\partial^2 K_6^2}{\partial x \partial y}
\end{aligned}
\tag{2.57}
$$

For a curved panel having a rectangular plane from, the Simply supported boundary conditions may be expressed as

at x=0,a

$$
\begin{aligned}
v(0,y) &= v(a,y) = 0 \\
w(0,y) &= w(a,y) = 0 \\
N_1(0,y) &= N_1(a,y) = 0 \\
M_1(0,y) &= M_1(a,y) = 0 \\
P_1(0,y) &= P_1(a,y) = 0 \\
\psi_y(0,y) &= \psi_y(a,y) = 0
\end{aligned}
$$

at y=0,b

$$
\begin{aligned}
u(x,0) &= u(x,b) = 0 \\
w(x,0) &= w(x,b) = 0 \\
N_2(x,0) &= N_2(x,b) = 0 \\
M_2(x,0) &= M_2(x,b) = 0 \\
P_2(x,0) &= P_2(x,b) = 0 \\
\psi_x(x,0) &= \psi_x(x,b) = 0
\end{aligned}
\tag{2.58}
$$

Where a and b denote the length along the x-and y-direction, respectively. For a full cylinder the boundary conditions on X are not there.

We assume the following Naviour type solution form that satisfies the boundary condition in eq (2.58)

$$
\begin{aligned}
u(x,y,t) &= \sum_{m=1}^{\infty}\sum_{n=1}^{\infty} U_{mn} cos\frac{m\pi x}{a} sin\frac{n\pi y}{b} sin\omega_{mn}t \\
v(x,y,t) &= \sum_{m=1}^{\infty}\sum_{n=1}^{\infty} V_{mn} sin\frac{m\pi x}{a} cos\frac{n\pi y}{b} sin\omega_{mn}t \\
w(x,y,t) &= \sum_{m=1}^{\infty}\sum_{n=1}^{\infty} W_{mn} sin\frac{m\pi x}{a} sin\frac{n\pi y}{b} sin\omega_{mn}t \\
\psi_x(x,y,t) &= \sum_{m=1}^{\infty}\sum_{n=1}^{\infty} \psi^1_{mn} cos\frac{m\pi x}{a} sin\frac{n\pi y}{b} sin\omega_{mn}t \\
\psi_y(x,y,t) &= \sum_{m=1}^{\infty}\sum_{n=1}^{\infty} \psi^2_{mn} sin\frac{m\pi x}{a} cos\frac{n\pi y}{b} sin\omega_{mn}t
\end{aligned}
\tag{2.59}
$$

Now we Fourier Transform the displacement function split in the three parts

$$
\int_{-\infty}^{+\infty} f(x) = \int_{-\infty}^{0} f(x) + \int_{0}^{1} f(x) + \int_{1}^{+\infty} f(x)
$$

Here integral$-\infty$ to 0 is zero because the displacement is undefined in the negative domain of the set of integers. The integral 0 to 1 is zero because m and n are not

defined for the range 0 to 1. Where N is maximum time limit, Substituting eq(2.59) into eq(2.54) we obtain

$$\begin{bmatrix} M_{11} & M_{12} & M_{13} & M_{14} & M_{15} \\ M_{21} & M_{22} & M_{23} & M_{24} & M_{25} \\ M_{31} & M_{32} & M_{33} & M_{34} & M_{35} \\ M_{41} & M_{42} & M_{43} & M_{44} & M_{45} \\ M_{51} & M_{52} & M_{53} & M_{54} & M_{55} \end{bmatrix} \begin{Bmatrix} \ddot{U}_{mn} \\ \ddot{V}_{mn} \\ \ddot{W}_{mn} \\ \ddot{\psi}^1_{mn} \\ \ddot{\psi}^2_{mn} \end{Bmatrix} + \begin{bmatrix} k_{11} & k_{12} & k_{13} & k_{14} & k_{15} \\ k_{21} & k_{22} & k_{23} & k_{24} & k_{25} \\ k_{31} & k_{32} & k_{33} & k_{34} & k_{35} \\ k_{41} & k_{42} & k_{43} & k_{44} & k_{45} \\ k_{51} & k_{52} & k_{53} & k_{54} & k_{55} \end{bmatrix} \begin{Bmatrix} U_{mn} \\ V_{mn} \\ W_{mn} \\ \psi^1_{mn} \\ \psi^2_{mn} \end{Bmatrix} = \begin{Bmatrix} 0 \\ 0 \\ Q_{mn} \\ 0 \\ 0 \end{Bmatrix} \tag{2.60}$$

for any m, n

Where Q_{mn} are the coefficients in the double Fourier expansion of the transverse load,

$$q(x,y) = \sum_{m=1}^{\infty} \sum_{n=1}^{\infty} Q_{mn} sin\frac{m\pi x}{a} sin\frac{n\pi y}{b} sin\omega_{mn} t \tag{2.61}$$

and the coefficients M_{ij} and k_{ij} $(i, j = 1, 2, \ldots, 5)$ are given in the Appendix

Equation(2.59) can be solved for $U_{mn}, V_{mn}, W_{mn}, \psi^1_{mn}, \psi^2_{mn}$ for each m and n, and then the solution is given by eq(2.58) are evaluated using a finite number of terms in the series. For free vibration analysis, eq(2.59) can be expressed as an eigenvalue equation

$$\left(\begin{bmatrix} k_{11} & k_{12} & k_{13} & k_{14} & k_{15} \\ k_{21} & k_{22} & k_{23} & k_{24} & k_{25} \\ k_{31} & k_{32} & k_{33} & k_{34} & k_{35} \\ k_{41} & k_{42} & k_{43} & k_{44} & k_{45} \\ k_{51} & k_{52} & k_{53} & k_{54} & k_{55} \end{bmatrix} - \omega^2_{mn} \begin{bmatrix} M_{11} & M_{12} & M_{13} & M_{14} & M_{15} \\ M_{21} & M_{22} & M_{23} & M_{24} & M_{25} \\ M_{31} & M_{32} & M_{33} & M_{34} & M_{35} \\ M_{41} & M_{42} & M_{43} & M_{44} & M_{45} \\ M_{51} & M_{52} & M_{53} & M_{54} & M_{55} \end{bmatrix} \right) \begin{Bmatrix} U_{mn} \\ V_{mn} \\ W_{mn} \\ \psi^1_{mn} \\ \psi^2_{mn} \end{Bmatrix} = 0 \tag{2.62}$$

Where ω is the frequency of natural vibration

2.6 Composite Material

From eq(2.49-2.50) re write Stiffness Matrix

$$\begin{Bmatrix} \sigma_{11} \\ \sigma_{22} \\ \tau_{12} \end{Bmatrix}_{(k)} = \begin{bmatrix} \bar{Q_{11}} & \bar{Q_{12}} & \bar{Q_{16}} \\ \bar{Q_{21}} & \bar{Q_{22}} & \bar{Q_{26}} \\ \bar{Q_{61}} & \bar{Q_{62}} & \bar{Q_{66}} \end{bmatrix}_{(k)} \begin{Bmatrix} \epsilon_{11} \\ \epsilon_{22} \\ \gamma_{12} \end{Bmatrix}_{(k)} \tag{2.63}$$

$$\begin{Bmatrix} \tau_{23} \\ \tau_{31} \end{Bmatrix}_{(k)} = \begin{bmatrix} \bar{Q_{44}} & \bar{Q_{45}} \\ \bar{Q_{54}} & \bar{Q_{55}} \end{bmatrix}_{(k)} \begin{Bmatrix} \gamma_{23} \\ \gamma_{31} \end{Bmatrix}_{(k)} \tag{2.64}$$

Here

$$\bar{Q}_{16} = \bar{Q}_{61}$$

$$\bar{Q}_{26} = \bar{Q}_{62}$$

$$\bar{Q}_{45} = \bar{Q}_{54}$$

$\bar{Q}_{11}, \bar{Q}_{22}, \bar{Q}_{16}, \bar{Q}_{26}, \bar{Q}_{66}, \bar{Q}_{44}$, *and* $\bar{Q}_{55}$ we can get from Ref [21]. Substituting eq (2.62 to 2.64) in eq (2.51) after simplifying we can get response often satisfying boundary condition.

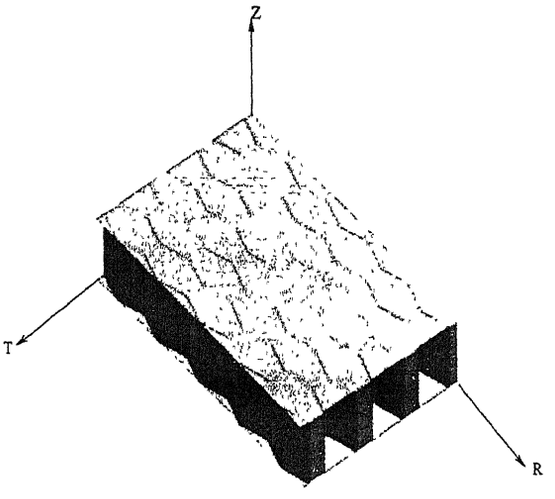

(a)

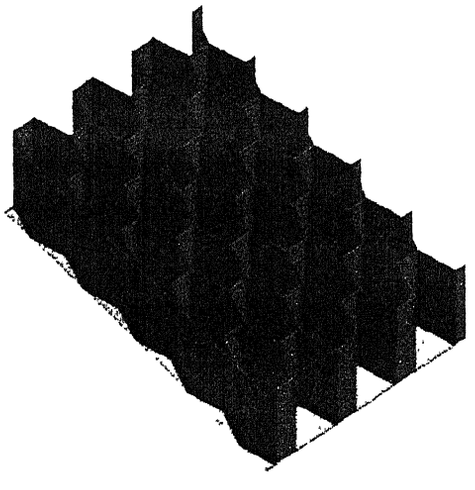

(b)

Figure 2.5: Honeycomb structure

(a) with Both face skins (b) Top face skin removed.

Chapter 3

Solution Approach

3.1 Eigen Value Problem

The System is assumed to vibrate in the principal mode with the displacements as expressed in eq (2.59). where the shape functions $u(x,y,t), v(x,y,t), w(x,y,t), \psi_x(x,y,t)$ *and* $\psi_y(x,y,t)$ satisfy the boundary conditions for the shell.

The Shape functions are initially assumed to be zero then constituted to wave forms. These can be expressed as in eq (2.59). where U, V, W, ψ^1 *and* ψ^2 are the displacement amplitudes sinusoidal functions with $(\frac{m\pi x}{a})$ and $(\frac{n\pi y}{b})$ as their arguments, respectively. Here m and n denote longitudinal and circumference wave numbers.

Eq (2.62) can be written in matrix notation

$$\Big([K] - \omega^2[M]\Big)\{\Delta\} = 0 \tag{3.1}$$

Where K and M are (5×5) square matrices and

$$\Delta = \begin{bmatrix} U_{mn} & V_{mn} & W_{mn} & \psi^1_{mn} & \psi^2_{mn} \end{bmatrix}^T \tag{3.2}$$

Here

$$\begin{aligned} [M]_t &= [M]_{c1} + [M]_H + [M]_{c2} \\ [K]_t &= [K]_{c1} + [K]_H + [K]_{c2} \end{aligned} \tag{3.3}$$

And

$$[P] = [M]_t^{-1}[K]_t \tag{3.4}$$

The subscription "c" denotes laminated panel and "H" denotes the honeycomb panel. Subscription "t" denotes total mass and stiffness matrices of the panel. Equation (3.1) can be expressed as

$$([P] - \lambda[I])\{\Delta\} = 0 \tag{3.5}$$

Where $\{\Delta\}$ is the amplitude vector and $\lambda = \omega^2$. The eigen value problem becomes

$$|[P] - \lambda[I]| = 0 \tag{3.6}$$

Expanding eq (3.6) we get a fifth order characteristic equation

$$\lambda^5 - B_1\lambda^4 - B_2\lambda^3 - B_3\lambda^2 - B_4\lambda - B_5 = 0 \tag{3.7}$$

Where B_1, B_2, B_3, B_4 *and* B_5 are the coefficient and are placed in Appendix [B]. From eq (3.7) for the deterministic problem eigen value solution is obtained in the usual manner with standard technique. However, the eigen value λ as well as the eigen vector $\{\Delta\}$ are random as the characteristic equation has random coefficients. The eigen value and eigen vector statistics in this case can not be found directly and more analysis is needed. A procedure is being outlined here.

3.2 Perturbation Approach

We write the random components as the sum of the mean value and the zero mean random part.

$$\lambda_n = \lambda_n^m + \lambda_n^r; \quad \{\Delta_n\} = \{\Delta_n^m\} + \{\Delta_n^r\}; \quad [K] = [K]^m + [K]^r \quad n = 1, \ldots, 5 \tag{3.8}$$

It can be seen that

$$\lambda_n^m = (\omega_n^m)^2 \qquad and \quad \lambda_n^r = 2\omega_n^m\omega_n^r + (\omega_n^r)^2 \qquad n = 1, \ldots, 5 \tag{3.9}$$

The subscription "r" denotes zero mean random part and "m" denotes the mean part of the parameters.

It is assumed that the random component are very small compared to the mean value for each parameter. Substituting eq (3.8) and eq (3.9) in eq(3.1) and collecting the terms of zero and first order small quantities

$$[K]^m\{\Delta_n^m\} = \lambda_n^m[M]\{\Delta_n^m\} \tag{3.10}$$

$$and \qquad ([K]^m - \lambda_n^m[M])\{\Delta_n^r\} = -([K]^r - \lambda_n^r[M])\{\Delta_n^m\} \tag{3.11}$$

Where [K] and [M] denote the total system quantities. Eq (3.10) is in the mean and the mean values of the eigen value and eigen vectors are obtained in the usual manner with the help of any standard procedure.

The eigen vector are orthogonal with each other and would satisfy the condition

$$\{\Delta_n^m\}^T[M]\{\Delta_l^m\} = \delta_{nl} \qquad and \qquad \{\Delta_n^m\}^T[K]\{\Delta_l^m\} = \lambda_n^m\delta_{nl} \qquad n = 1,\ldots,5 \tag{3.12}$$

All eigen values are assumed to be distinct. In the given space the eigen vectors form a complete orthogonal set and any vector in the space can be expressed in terms of these. Hence, the random component

$$\{\Delta_n^r\} = \sum_{l=1}^{5} c_{nl}\{\Delta_l\}^m \qquad\qquad c_{nn} = 0 \tag{3.13}$$

Here c_{nl} are unknown random coefficients and have to be evaluated.

Substituting eq (3.13) in eq (3.11)

$$\sum_{l=1}^{5}([K]^m - \lambda_n^m[M])\,c_{nl}\{\Delta_l^m\} = -([K]^r - \lambda_n^r[M])\{\Delta_n^m\} \tag{3.14}$$

Premultiply by$\{\Delta_n^m\}^T$ eq (3.14) becomes

$$\sum_{l=1}^{5}\{\Delta_n^m\}^T([K]^m - \lambda_n^m[M])\,c_{nl}\{\Delta_l^m\} = \{\Delta_n^m\}^T([K]^r - \lambda_n^r[M])\{\Delta_n^m\}$$

$$or \qquad \sum_{l=1}^{5}\left[\{\Delta_n^m\}^T[K]^m\{\Delta_l^m\}c_{nl} - \lambda_n^m c_{nl}\{\Delta_n^m\}^T[M]\{\Delta_l^m\}\right]$$

$$= +\{\Delta_n^m\}^T[K]^r\{\Delta_n^m\} - \lambda_n^r\{\Delta_n^m\}^T[M]\{\Delta_n^m\}$$

$$or \qquad \sum_{l=1}^{5}[\lambda_n^m\delta_{nl}c_{nl} - \lambda_n^m c_{nl}\delta_{nl}] = +\{\Delta_n^m\}^T[K]^r\{\Delta_n^m\} - \lambda_n^r 1$$

$$or \qquad \lambda_n^r = \{\Delta_n^m\}^T[K]^r\{\Delta_n^m\} \tag{3.15}$$

Premultiplying eq (3.14) by $\{\Delta_k^m\}^T$ with $k \neq n$

$$\sum_{l=1}^{5}\{\Delta_k^m\}^T([K]^m - \lambda_n^m[M])\,c_{nl}\{\Delta_l^m\} = \{\Delta_k^m\}^T([K]^r - \lambda_n^r[M])\{\Delta_n^m\}$$

$$or \qquad \sum_{l=1}^{5}\left[\{\Delta_k^m\}^T[K]^m\{\Delta_l^m\}c_{nl} - \lambda_n^m c_{nl}\{\Delta_k^m\}^T[M]\{\Delta_l^m\}\right]$$

$$= +\{\Delta_k^m\}^T[K]^r\{\Delta_l^m\} - \lambda_n^r\{\Delta_k^m\}^T[M]\{\Delta_n^m\}$$

$$or \qquad \sum_{l=1}^{5}[\lambda_k^m \delta_{kl} c_{nl} - \lambda_n^m c_{nl}\delta_{kl}] = +\{\Delta_k^m\}^T [K]^r \{\Delta_n^m\} - \lambda_n^r \delta_{kn}$$

$$or \qquad [c_{nk}](\lambda_k^m - \lambda_n^m) = +\{\Delta_k^m\}^T [K]^r \{\Delta_n^m\}$$

$$[c_{nk}] = \frac{\{\Delta_k^m\}^T [K]^r \{\Delta_n^m\}}{\lambda_k^m - \lambda_n^m} \tag{3.16}$$

using eq (3.16) in eq (3.13)

$$\{\Delta_n^r\} = \sum_{l=1}^{5} \frac{\{\Delta_l^m\}^T [K]^r \{\Delta_n^m\}}{\lambda_l^m - \lambda_n^m} \{\Delta_l^m\} \qquad l \neq n \tag{3.17}$$

Variance of λ_n and $\{\Delta_n\}$ can be obtained from eq (3.15) and eq (3.17). Consider the RHS of eq (3.15) and let

$$\{\Delta_n^m\}^T = [q_{n1} \quad q_{n2} \quad q_{n3} \quad q_{n4} \quad q_{n5}]$$

Then

$$\{\Delta_n^m\}^T [K]^r \{\Delta_n^m\} = \sum_{l=1}^{5}\sum_{j=1}^{5} q_{nl}^m k_{lj}^r q_{nj}^m = \sum_{l=1}^{5}\sum_{j=1}^{5} q_{nl}^m q_{nj}^m k_{lj}^r$$

Hence from eq (3.15)

$$\{\lambda_n^r\}^2 = \sum_{l=1}^{5}\sum_{j=1}^{5} q_{nl}^m q_{nj}^m k_{lj}^r \sum_{s=1}^{5}\sum_{t=1}^{5} q_{ns}^m q_{nt}^m k_{st}^r$$

$$or \qquad \{\lambda_n^r\}^2 = \sum_{l=1}^{5}\sum_{j=1}^{5}\sum_{s=1}^{5}\sum_{t=1}^{5} q_{nl}^m q_{nj}^m q_{ns}^m q_{nt}^m k_{lj}^r k_{st}^r$$

$$Var\{\lambda_n^r\} = \sum_{l=1}^{5}\sum_{j=1}^{5}\sum_{s=1}^{5}\sum_{t=1}^{5} q_{nl}^m q_{nj}^m q_{ns}^m q_{nt}^m cov\left(k_{lj}^r k_{st}^r\right) \tag{3.18}$$

The zero mean random parts of elements of stiffness matrix k_{ij}^r are expanded in Taylor Series. Using a single step Taylor series in-terms of the basic material properties likes E_{11}, E_{22} etc,

$$k_{ij}^r = \sum_{l=1}^{\eta} \frac{\partial k_{ij}^m}{\partial {A_l}^m} A_l^r + \sum_{l=1}^{\eta} \frac{\partial k_{ij}^r}{\partial {A_l}^m} A_l^r \tag{3.19}$$

Where A_l are the basic Material properties and η is the number of basic material properties. The second and higher order terms in eq (3.19) has been dropped because there are very small compared to the first order terms. Further, the second set of terms are very small compared to the first set and may be ignored in evaluation.

3.3 FEM Approach

The random problem can be solved by using finite element method (FEM) with Monte Carlo simulation. In this approach the structure is discretised in to finite elements with nodes. The system properties and external loading at each node is obtained by computer simulation of numbers that first this given statistical distributions. The problem in solved repeatedly to obtain a sample of the response statistics. This sample is analysed to obtain the response.

These steps are being described below for the present problem

3.3.1 Generating Random Number

The material properties, used as basic variables, have been generated assuming them to be Gaussian. The random numbers are generated first in the range -1 to +1 in the normal distribution curve. After that for analysis we are assuming the basic material properties to have a input mean value and input of standard deviation value. The generated numbers are modified to have the desired mean and SD. New basic material properties are generated for each cycle of solution. These basic material values are the input value of the FEM package for repeated solution.

3.3.2 Modelling

Geometric modelling has been performed using MSC-Patran package. The geometric model used is shown in Fig (3.1). This model has three set of surfaces. The top and bottom surfaces are laminated surfaces while the middle surface is honeycomb structure.

The most distinctive feature of the finite element method that separates it from others is the division of a given domain into a set of simple sub-domains called finite element. Any geometric shape that allows computation of the solution or approximation can be used as a finite element. Finite element discretization is represented as a collection of a finite number of n sub-domains, namely line, surface and volume segments. Each sub-domain is called an element. The collection of elements is called finite element mesh. The elements are connected to each other at points called nodes.

FEM mesh used for this problem contains approximately 4600 sub-domain each sub-domain contains four noded quadratic rectangular shell elements. After generating elements in different parts of the structure it is required to merge them together. This becomes necessary as this model contains different surface and different material properties. When we are generating elements it will created two node identity in the same location. For avoiding this we need to do an equivalence operation in the finite element model. After merging the finite element model it becomes a single geometry. Each nodes has been assumed to possess 5 degrees of freedom-three translational and two rotational. The FEM model is shown in Fig (3.2)

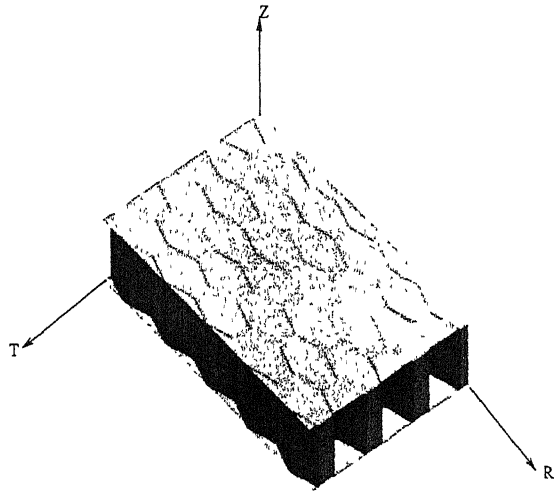

(a)

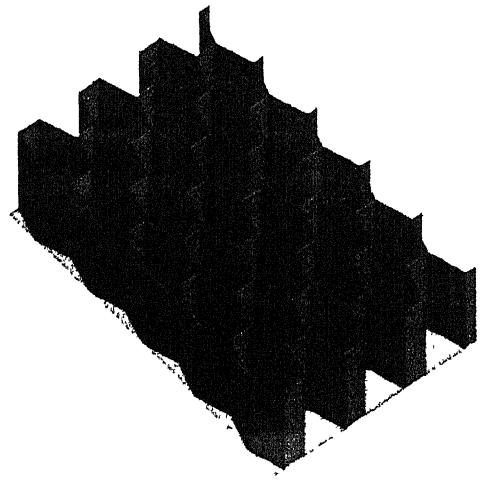

(b)

Figure 3.1: Honeycomb structure

(a) with Both face skins (b) Top face skin removed.

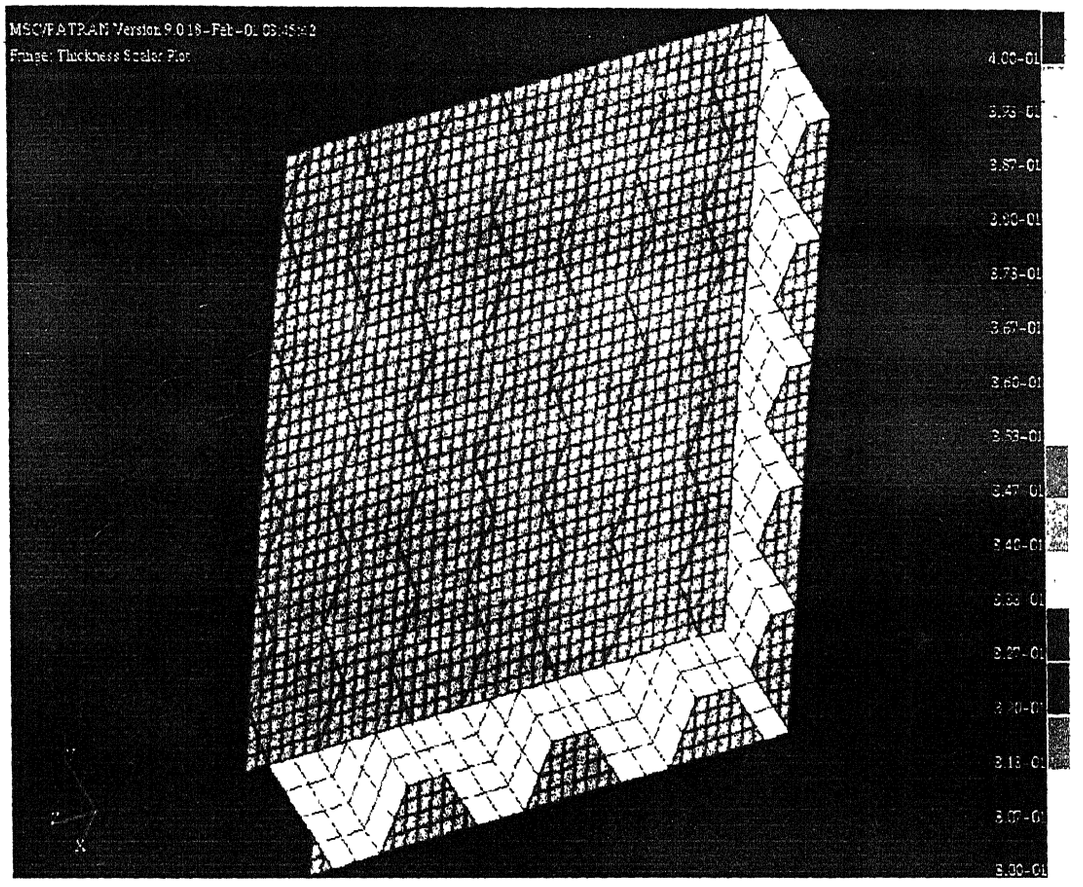

Figure 3.2: FEM Model of Honeycomb structure

Chapter 4

Results And Discussion

The solution approaches discussed in the previous chapter have been used to obtain the natural frequencies of honeycomb sandwich laminated cylinder, simply supported at the two ends. The sandwich is assumed to have facing laminates on the two sides with a hexagonal honeycomb core layer. The facing laminates have each lamina of the same thickness. The core is of aluminium and the facing is taken to be graphite epoxy. The mean material properties adopted for generating the results are Material properties for equivalent solid aluminium core: $E_s = 72395\ N/mm^2$, $G_s = 27578.8\ N/mm^2$, $\nu = 0.3125$, $\rho = 2.79567 * 10^{-}6\ \ Kg/mm^3$.
Material properties for Graphite/epoxy:$E_{11} = 134000\ N/mm^2$, $E_{22} = 10200\ N/mm^2$, $G_{12} = 5520\ \ N/mm^2$, $G_{23} = 3430\ \ N/mm^2$, $G_{31} = 5520\ \ N/mm^2$, $\nu_{12} = 0.3$, $\rho = 1.577 * 10^{-6}\ \ Kg/mm^3$.

The natural frequencies have been nondimensionalized as

$$\bar{\omega} = \omega \frac{R^2}{h} \sqrt{\frac{\rho}{E_{22}}}$$

Where ω is the natural frequency
R is the radius of the cylinder.
h is the total thickness of the laminate
ρ is the density of Graphite/epoxy
E_{22} is the material properties of Graphite/epoxy
$\bar{\omega}$ is the nondimenalized natural frequency

4.1 Validation

Validation has been sought for the approach by comparison of results with published data. For this, only the mean value has been compared as information on variance is not available in literature. Table (4.1) contains non dimensionalized natural frequency obtained by the present work and its comparison with Ref [20]. It can be seen that the results exhibit a close agreement.

4.2 Natural frequency statistics

The perturbation approach discussed in the chapter 3 has been used to find the mean and the variance of the first five natural frequencies. Three stacking sequences for the facing layer: (1)-[$0^o/90^o/90^o/0^o/H/0^o/90^o/90^o/90^o$], (2)-[$0^o/90^o/0^o/90^o/H/0^o/90^o/90^o/90^o$] and (3)-[$90^o/0^o/H/0^o/90^o$] have been studied for different length to radius (L/R) ratios and different thicknesses. Behaviour of the nondimensionalized mean and variance are presented below.

4.2.1 Mean frequency

Table (4.2 to 4.7) present the first five natural frequencies for different length ratios. There are different lay up sequences with each layer thickness 0.1 mm. Mode shape number m and n are selected from 1,2 and 3 in all possible combination. When we compare first mode shape m=n=1 for different L/R. We see that non-dimensional natural frequencies decrease as L/R increases. This may be because stiffness decreases and mass increases with increases in L/R. Comparing mode shapes m=1,n=2 and m=2,n=1 it can be seen that for m=1,n=2 non dimensional natural frequency is higher. It indicates that change in mode shape in y-direction is dominant for natural frequency. This behaviour is common to men other layup combinations.

The natural frequency is seen to increase with thickness, as expected, for all the three layup sequences. The third layup sequences has the highest natural frequency while the second has the smallest. The anti-symmetric case has $[B_{ij}] \neq 0$ and it may effect this region for increase or decrease in non dimensional frequencies. Table 4.4

also presents a symmetric lay up sequence case. But the lay up has lower number of layers compared with the other tables. The general behaviour discussed above are the same for the Tables (4.5) to (4.7) where the honey comb thickness changes but the L/R is constant.

4.3 Natural Frequency Variance

The results are presented graphically for changes in the square of SD/mean of the natural frequencies with changes in SD/mean of the input variables. Study has been conducted for the three layup sequences. However the results are presented only for the first layup in details because of the high space requirement. The study has been conducted first with each input variable changing alone, one by one, and then with all of them changing simultaneously. The variation in input SD/mean is taken from 0 to 20%.

Fig (4.1) to (4.27) for the first layup and figure 4.28 for the second layup show that the variance of natural frequencies change linearly with the basic material property SD. The main reason for this may be due to the inherent linearsation in the first order perturbation approach as well as in the one term Taylor series expansion employed in the analysis.

4.3.1 Only E_{11} Changing

Fig (4.1) to (4.3) shows the effect of randomness in E_{11} on the variance of the natural frequency. E_{11}^{r} has a most pre dominant effect on the SD of the square natural frequencies as compared to the other input variable. More over as seen from these curves first natural frequencies are dominant compared to the 2^{nd} and higher natural frequencies. This indicate that the effect of randomness is very high in the first mode. When we consider increasing mode shape natural frequency variances are reducing compared to the first mode shape. Comparison of m=1,n=3 and m=3,n=1 shows that y-direction mode shape has dominant effect on natural frequency variance. It is indicated that effect of randomness is very high in that direction. With L/R increase non dimensional SD squared natural frequencies increase. The general behaviour for

the lay up sequences $0^o/90^o/0^o/90^o/H/0^o/90^o/90^o/0^o$ is similar except that there is differences in frequencies.

4.3.2 Only E_{22} Changing

Fig (4.4) to (4.6) show that the variance of the natural frequencies increases linearly with the input of random value E_{22}. Comparison indicates that for mode shape m=1,n=1 the first five non dimensionalized natural frequencies variances are dominant. Other natural frequencies have very low variances compared to the first natural frequencies. Another combination of mode shape m=1,n=1,2,3 the first mode shape m=1,n=1 also indicates a higher variation. It's valid through out the combination of mode shape and L/R ratio. The behaviour for the lay up sequences $0^o/90^o/0^o/90^o/H/0^o/90^o/90^o/0^o$ is also similar to the first lay up except for differences in frequency values.

4.3.3 Only G_{12} Changing

Fig (4.7) to (4.9) show that variance of the natural frequencies increases linearly with the SD of input random value G_{12}. First natural frequencies variance is again dominant compared to second and higher natural frequencies. This observation is valid for different combination of the mode shape and L/R ratio. The dynamic behaviour for the lay up sequences $0^o/90^o/0^o/90^o/H/0^o/90^o/90^o/0^o$ is also similar.

4.3.4 Only G_{23} Changing

Fig (4.10) to (4.12) show that the variance of the natural frequencies increases linearly with the input random value G_{23}. Details follow the previous results. For the 4^{th} and 5^{th} natural frequencies values are very close for all mode shapes. This indicates that shear effect due to G_{23} is low. This is valid for different combination of mode shapes and L/R ratios. The dynamic behaviour for the lay up sequences $0^o/90^o/0^o/90^o/H/0^o/90^o/90^o/0^o$ is again similar.

4.3.5 Only G_{31} Changing

Fig (4.13) to (4.15) present the natural frequency variance with G_{31} only changing. The results follow the pattern of G_{23} variation. Again the dynamic behaviour for the lay up sequences $0^o/90^o/0^o/90^o/H/0^o/90^o/90^o/0^o$ is similar with only differences frequencies having different values.

4.3.6 Only E_s Changing

Fig (4.16) to (4.18) variance are for E_s only random. The natural frequencies of structure mode shape m=1,n=3 are the dominant natural frequencies. The effect is very high in the y-direction. The second and third non dimensionalized natural frequencies are above of the first natural frequency. These are for $L/R = 1.5$. The nature of the graph change with change in L/R ratio.

4.3.7 Only G_s Changing

Fig (4.19) to (4.21) present the results for only G_s having randomness. The fundamental natural frequencies of honeycomb structure mode shape m=1,n=1 is the dominant natural frequency. The effect is very high in the y-direction. The above behaviour changes with decrease in the L/R ratio. The frequency variance for the lay up sequences $0^o/90^o/0^o/90^o/H/0^o/90^o/90^o/0^o$ exhibits a similar nature with only differences in magnitude of the frequencies.

4.3.8 Only ν_{12} Changing

Fig (4.22) to (4.24) shows the results for ν_{12} only varying. The fundamental natural frequency variance for mode shape m=1,n=1 is the dominated natural frequency. The effect is very high in the y-direction. For the second and third natural frequencies the order of sequence of magnitudes of the mode shape is reversed with respect to the first natural frequency. With decrease in the L/R ratio the dominant mode changes, m=2,n=1 being dominant for $L/R = 1.0$ and m=3,n=1 for $L/R = 0.5$.

Table 4.1: Comparison of mean $\bar{\omega}$

Lay Up sequence	*Present work*		*J.N.Reddy [20]*	
	a/h=10	a/h=100	a/h=10	a/h=100
$0^o/90^o$	8.978141	9.712483	8.975	9.712
$0^o/90^o/0^o$	11.71697	15.039365	11.79	15.19
$0^o/90^o/90^o/0^o$	11.776354	15.188267	11.78	15.19

4.3.9 All Material Properties Simultaneously Random

The variance of the natural frequencies are plotted against the SD of material properties in Fig (4.25) to (4.27). The compared fundamental natural frequencies of honeycomb structure mode shape m=1,n=1 is the dominant natural frequency. The y direction mode has very high effect on the natural frequency variance. If compared to the first second and third non dimensionalized natural frequencies have reverse order of magnitudes. With change in L/R ratio the above behaviour changes for the honeycomb structure is shown in Fig (4.26) and (4.27). The dynamic behaviour for the lay up sequences $0^o/90^o/0^o/90^o/H/0^o/90^o/90^o/0^o$ is similar.

4.4 FEM Result

Fig (4.28) shows the plot using the FEM with Monte-Carlo simulation. A sample sets of 20 was analysed for the result. the large size of the problem requires 4 *hrs* for one point. The sample size, however is not large enough to be representative as indicated by the nature of the case and it was not possible to generate a large sample.

Table 4.2: Mean natural frequency for different L/R, lay up sequence(1)

Mode Shape	$0^o/90^o/90^o/0^o/H/0^o/90^o/90^o/0^o$		
	L/R=1.5	L/R=1.0	L/R=0.5
	$\bar{\omega}_i, i = 1, \ldots, 5$	$\bar{\omega}_i, i = 1, \ldots, 5$	$\bar{\omega}_i, i = 1, \ldots, 5$
m=1,n=1	227.171005	327.643420	550.343644
	1251.699907	1620.863005	2173.776609
	2068.663326	2485.669475	4491.111449
	223180.769586	223180.780103	223180.836911
	231671.576074	231680.442009	231728.307533
m=1,n=2	415.111843	550.344016	767.618573
	1828.939186	2173.777820	3421.960019
	3101.208623	4491.111425	8836.083742
	223180.794828	223180.836911	223181.064470
	231692.853281	231728.307517	231919.595005
m=1,n=3	550.344385	680.455598	906.860374
	2173.779033	2760.210425	4856.601120
	4491.111399	6653.311944	13218.327575
	223180.836911	223180.931665	223181.444818
	231728.307501	231808.043989	232237.777910
m=2,n=1	358.409705	528.029733	954.138765
	1334.313420	1791.958327	2374.885245
	2486.778188	2760.141615	4565.429197
	223182.286270	223182.295178	223182.343359
	231671.578847	231680.446282	231728.319845

Table 4.2: (Continued)

Mode Shape	$0^o/90^o/90^o/0^o/H/0^o/90^o/90^o/0^o$		
	L/R=1.5	L/R=1.0	L/R=0.5
	$\bar{\omega}_i, i = 1, \ldots, 5$	$\bar{\omega}_i, i = 1, \ldots, 5$	$\bar{\omega}_i, i = 1, \ldots, 5$
m=2,n=2	686.074178	954.139613	1369.390039
	2062.175534	2374.886212	3476.465713
	3256.809887	4565.429114	8866.241038
	223182.307656	223182.343359	223182.537385
	231692.859647	231728.319829	231919.638507
m=2,n=3	954.140461	1221.088877	1527.294495
	2374.887182	2867.108582	4874.474918
	4565.429029	6695.709334	13237.700387
	223182.343359	223182.423954	223182.865093
	231728.319813	231808.069482	232237.870168
m=3,n=1	423.728014	631.155806	1208.809303
	1432.008358	1948.058317	2721.534733
	3085.675040	3251.726421	4710.048147
	223184.814035	223184.820257	223184.854056
	231671.583469	231680.453395	231728.340373
m=3,n=2	832.887208	1208.810570	1937.991624
	2337.101310	2721.535494	3596.809944
	3582.331018	4710.047961	8918.417292
	223184.828993	223184.854056	223184.992168
	231692.870262	231728.340357	231919.710892
m=3,n=3	1208.811834	1659.094003	2185.491181
	2721.536254	3098.280886	4909.992944
	4710.047776	6771.353630	13270.516835
	223184.854056	223184.911043	223185.232117
	231728.340342	231808.111989	232238.023992

Table 4.3: Mean natural frequency for different L/R, lay up sequence(2)

Mode Shape	$0^o/90^o/0^o/90^o/H/0^o/90^o/90^o/0^o$		
	L/R=1.5	L/R=1.0	L/R=0.5
	$\bar{\omega}_i, i = 1, \ldots, 5$	$\bar{\omega}_i, i = 1, \ldots, 5$	$\bar{\omega}_i, i = 1, \ldots, 5$
m=1,n=1	222.855516	321.977084	544.304261
	1250.818722	1616.575003	2153.042833
	2066.958436	2484.137519	4490.636360
	225332.012723	225332.022608	225332.076060
	229579.785761	229588.760073	229637.210374
m=1,n=2	408.790928	544.304635	764.832394
	1819.690241	2153.044004	3364.004657
	3100.275615	4490.636335	8835.886370
	225332.036453	225332.076060	225332.291109
	229601.323027	229637.210359	229830.829400
m=1,n=3	544.305006	676.197275	905.595159
	2153.045178	2720.699332	4763.892141
	4490.636308	6653.035605	13218.200537
	225332.076060	225332.165430	225332.653400
	229637.210343	229717.919771	230152.871929
m=2,n=1	350.967391	517.506946	939.571039
	1334.012192	1790.236093	2360.488803
	2485.742301	2758.684607	4564.896553
	225333.526286	225333.532981	225333.569442
	229579.789819	229588.767210	229637.233906

Table 4.3: (Continued)

Mode Shape	$0^o/90^o/0^o/90^o/H/0^o/90^o/90^o/0^o$		
	L/R=1.5	L/R=1.0	L/R=0.5
	$\bar{\omega}_i, i = 1, \ldots, 5$	$\bar{\omega}_i, i = 1, \ldots, 5$	$\bar{\omega}_i, i = 1, \ldots, 5$
m=2,n=2	673.235105	939.571886	1361.763647
	2057.264838	2360.489735	3421.869080
	3255.720707	4564.896468	8866.037444
	225333.542383	225333.569442	225333.720244
	229601.334453	229637.233891	229830.914802
m=2,n=3	939.572732	1209.495359	1523.886919
	2360.490670	2833.082808	4782.964179
	4564.896382	6695.417502	13237.571576
	225333.569442	225333.631341	225333.987106
	229637.233876	229717.969781	230153.048823
m=3,n=1	414.693250	617.911182	1186.211460
	1431.911412	1947.530370	2714.059578
	3085.117285	3250.700391	4709.419210
	225336.048845	225336.050216	225336.058337
	229579.796586	229588.779104	229637.273160
m=3,n=2	815.842923	1186.212711	1921.600647
	2335.246843	2714.060317	3550.073743
	3581.204860	4709.419023	8918.202909
	225336.052210	225336.058337	225336.101976
	229601.353510	229637.273144	229831.057103
m=3,n=3	1186.213960	1636.048599	2178.819924
	2714.061057	3074.656795	4821.105997
	4709.418836	6771.034502	13270.385004
	225336.058337	225336.074415	225336.209699
	229637.273129	229718.053203	230153.343856

Table 4.4: Mean natural frequency for different L/R, lay up sequence(3)

Mode Shape	$90^o/0^o/H/0^o/90^o$		
	L/R=1.5	L/R=1.0	L/R=0.5
	$\bar{\omega}_i, i = 1, \ldots, 5$	$\bar{\omega}_i, i = 1, \ldots, 5$	$\bar{\omega}_i, i = 1, \ldots, 5$
m=1,n=1	277.546514	400.447120	717.440270
	1231.512680	1469.653621	1763.137796
	1983.809895	2493.473141	4600.358711
	215540.014275	215540.061561	215540.146558
	215548.049243	215558.295447	215613.779456
m=1,n=2	517.546930	717.440813	1036.250041
	1580.321471	1763.138499	2586.442502
	3159.837519	4600.358686	9059.410681
	215540.090374	215540.146558	215540.408666
	215572.675968	215613.779447	215835.529846
m=1,n=3	717.441356	918.549642	1182.996255
	1763.139197	2124.539398	3656.147965
	4600.358663	6820.772003	13552.687539
	215540.146558	215540.257431	215540.837931
	215613.779438	215706.224359	216204.177258
m=2,n=1	388.709035	536.205444	1012.643294
	1496.840694	1983.914046	2436.538841
	2718.580112	2927.011548	4698.708637
	215539.896063	215540.015533	215540.156070
	215549.912872	215560.086736	215615.514365

Table 4.4: (Continued)

Mode Shape	$90^o/0^o/H/0^o/90^o$		
	L/R=1.5	L/R=1.0	L/R=0.5
	$\bar{\omega}_i, i = 1, \ldots, 5$	$\bar{\omega}_i, i = 1, \ldots, 5$	$\bar{\omega}_i, i = 1, \ldots, 5$
m=2,n=2	694.780152	1012.644323	1787.200793
	2254.472189	2436.539218	2848.534304
	3381.967610	4698.708542	9098.474611
	215540.075564	215540.156070	215540.433604
	215574.435821	215615.514356	215837.245979
m=2,n=3	1012.645350	1450.989842	2108.551425
	2436.539593	2598.232382	3727.795131
	4698.708448	6875.885070	13577.739173
	215540.156070	215540.278307	215540.865816
	215615.514346	215707.946505	216205.884905
m=3,n=1	469.595400	607.656444	1109.196051
	1678.407943	2245.106409	3260.350769
	3719.319095	3803.910107	4926.335054
	215539.773959	215539.955241	215540.171153
	215552.943949	215563.055726	215618.406593
m=3,n=2	768.248933	1109.197199	2128.802737
	2749.994214	3260.351197	3549.191687
	3992.383691	4926.334819	9167.988489
	215540.054336	215540.171154	215540.474576
	215577.365398	215618.406584	215840.106547
m=3,n=3	1109.198346	1627.871529	2905.284143
	3260.351621	3442.606534	3978.288363
	4926.334587	6980.108038	13620.647249
	215540.171154	215540.312241	215540.911994
	215618.406574	215710.817553	216208.731225

Table 4.5: Mean natural frequency for different Web Thickness, lay up sequence(1)

Mode Shape	$0^o/90^o/90^o/0^o/H/0^o/90^o/90^o/0^o$		
	Thickness=0.3	Thickness=0.4	Thickness=0.5
	$\bar{\omega}_i, i = 1, \ldots, 5$	$\bar{\omega}_i, i = 1, \ldots, 5$	$\bar{\omega}_i, i = 1, \ldots, 5$
m=1,n=1	227.171005	244.069519	263.030256
	1251.699907	1341.239593	1397.811743
	2068.663326	2234.064423	2404.081059
	223180.769586	249709.882679	273679.367457
	231671.576074	257328.744608	280650.048367
m=1,n=2	415.111843	447.832763	487.659151
	1828.939186	1861.163378	1883.327867
	3101.208623	3558.285539	3966.609262
	223180.794828	249709.936861	273679.464754
	231692.853281	257354.652822	280680.049593
m=1,n=2	550.344385	599.477407	663.986306
	2173.779033	2217.895099	2249.234981
	4491.111399	5181.101772	5792.143978
	223180.836911	249710.027194	273679.626972
	231728.307501	257397.822596	280730.038470
m=2,n=1	358.409705	375.622287	390.300630
	1334.313420	1445.739427	1524.084937
	2486.778188	2633.911490	2787.811788
	223182.286270	249711.641153	273681.340420
	231671.578847	257328.749732	280650.056759

Table 4.5: (Continued)

Mode Shape	$0^o/90^o/90^o/0^o/H/0^o/90^o/90^o/0^o$		
	Thickness=0.3	Thickness=0.4	Thickness=0.5
	$\bar{\omega}_i, i = 1, \ldots, 5$	$\bar{\omega}_i, i = 1, \ldots, 5$	$\bar{\omega}_i, i = 1, \ldots, 5$
m=2,n=2	686.074178	718.316880	747.768978
	2062.175534	2105.884091	2133.898486
	3256.809887	3700.600092	4104.941705
	223182.307656	249711.689288	273681.429168
	231692.859647	257354.663656	280680.066133
m=2,n=3	954.140461	997.838583	1042.676006
	2374.887182	2412.933294	2441.842038
	4565.429029	5255.829465	5868.882707
	223182.343359	249711.769637	273681.577302
	231728.319813	257397.842856	280730.068423
m=3,n=1	423.728014	442.097286	455.942889
	1432.008358	1554.646191	1647.996454
	3085.675040	3228.271912	3375.990203
	223184.814035	249714.571891	273684.628631
	231671.583469	257328.758273	280650.070750
m=3,n=2	832.887208	868.448796	896.048728
	72337.101310	2423.188230	2473.730565
	3582.331018	3985.552629	4372.091336
	223184.828993	249714.609942	273684.703121
	231692.870262	257354.681722	280680.093712
m=3,n=3	1208.811834	1258.712205	1299.812094
	2721.536254	2759.720089	2788.918189
	4710.047776	5395.089821	6008.366973
	223184.854056	249714.673641	273684.827767
	231728.340342	257397.876641	280730.118375

Table 4.6: Mean natural frequency for different Web Thickness, lay up sequence(2)

Mode Shape	$0^o/90^o/0^o/90^o/H/0^o/90^o/90^o/0^o$		
	Thickness=0.3	Thickness=0.4	Thickness=0.5
	$\bar{\omega}_i, i = 1, \ldots, 5$	$\bar{\omega}_i, i = 1, \ldots, 5$	$\bar{\omega}_i, i = 1, \ldots, 5$
m=1,n=1	222.855516	239.436150	258.314104
	1250.818722	1339.797536	1395.895394
	2066.958436	2232.514121	2402.719802
	225332.012723	251634.428104	275436.482489
	229579.785761	255447.144531	278925.818106
m=1,n=2	408.790928	441.217378	481.038511
	1819.690241	1850.152147	1871.111758
	3100.275615	3557.537933	3965.968250
	225332.036453	251634.479884	275436.576363
	229601.323027	255473.314661	278956.077975
m=1,n=3	544.305006	593.369312	658.021488
	2153.045178	2193.992466	2223.136989
	4490.636308	5180.684953	5791.767812
	225332.076060	251634.566304	275436.733034
	229637.210343	255516.920544	279006.497418
m=2,n=1	350.967391	367.385401	381.582349
	1334.012192	1445.228674	1523.370657
	2485.742301	2632.872825	2786.827774
	225333.526286	251636.182433	275438.450353
	229579.789819	255447.151679	278925.829369

Table 4.6: (Continued)

Mode Shape	$0^o/90^o/0^o/90^o/H/0^o/90^o/90^o/0^o$		
	Thickness=0.3	Thickness=0.4	Thickness=0.5
	$\bar{\omega}_i, i = 1, \ldots, 5$	$\bar{\omega}_i, i = 1, \ldots, 5$	$\bar{\omega}_i, i = 1, \ldots, 5$
m=2,n=2	673.235105	704.271626	732.991570
	2057.264838	2099.717910	2126.902282
	3255.720707	3699.763764	4104.246584
	225333.542383	251636.222244	275438.527317
	229601.334453	255473.333437	278956.105742
m=2,n=3	939.572732	982.250223	1026.459805
	2360.490670	2395.986015	2423.182690
	4564.896382	5255.379548	5868.485368
	225333.569442	251636.289081	275438.656447
	229637.233876	255516.958338	279006.552050
m=3,n=1	414.693250	432.027639	445.191189
	1431.911412	1554.481064	1647.760379
	3085.117285	3227.681503	3375.399949
	225336.048845	251639.106257	275441.730057
	229579.796586	255447.163600	278925.848153
m=3,n=2	815.842923	849.541882	875.907645
	2335.246843	2420.588229	2470.623727
	3581.204860	3984.663738	4371.358784
	225336.052210	251639.126099	275441.778797
	229601.353510	255473.364761	278956.152074
m=3,n=3	1186.213960	1233.926887	1273.545434
	2714.061057	2750.657059	2778.808614
	4709.418836	5394.586855	6007.936827
	225336.058337	251639.160260	275441.861964
	229637.273129	255517.021396	279006.643219

Table 4.7: (Continued)

Mode Shape	$90^o/0^o/H/0^o/90^o$		
	Thickness=0.3	Thickness=0.4	Thickness=0.5
	$\bar{\omega}_i, i = 1, \ldots, 5$	$\bar{\omega}_i, i = 1, \ldots, 5$	$\bar{\omega}_i, i = 1, \ldots, 5$
m=2,n=2	694.780152	713.121854	729.172669
	2254.472189	2296.991193	2323.287469
	3381.967610	3826.227849	4235.475627
	215540.075564	243925.675222	269336.145775
	215574.435821	243966.441477	269382.493477
m=2,n=3	1012.645350	1039.845355	1064.352362
	2436.539593	2453.944665	2472.913093
	4698.708448	5403.903875	6030.752534
	215540.156070	243925.809434	269336.358801
	215615.514346	244015.285662	269438.144616
m=3,n=1	469.595400	481.156153	490.541235
	1678.407943	1828.528562	1950.694852
	3719.319095	3825.047251	3937.480315
	215539.773959	243925.317069	269335.717305
	215552.943949	243940.693154	269353.028169
m=3,n=2	768.248933	786.281473	800.237375
	2749.994214	2913.514825	3007.015376
	3992.383691	4315.748387	4659.862532
	215540.054336	243925.640868	269336.104008
	215577.365398	243969.764511	269386.169592
m=3,n=3	1109.198346	1135.451955	1155.587310
	3260.351621	3303.878696	3333.763607
	4926.334587	5604.327792	6220.720444
	215540.171154	243925.812158	269336.355883
	215618.406574	244018.570372	269441.780456

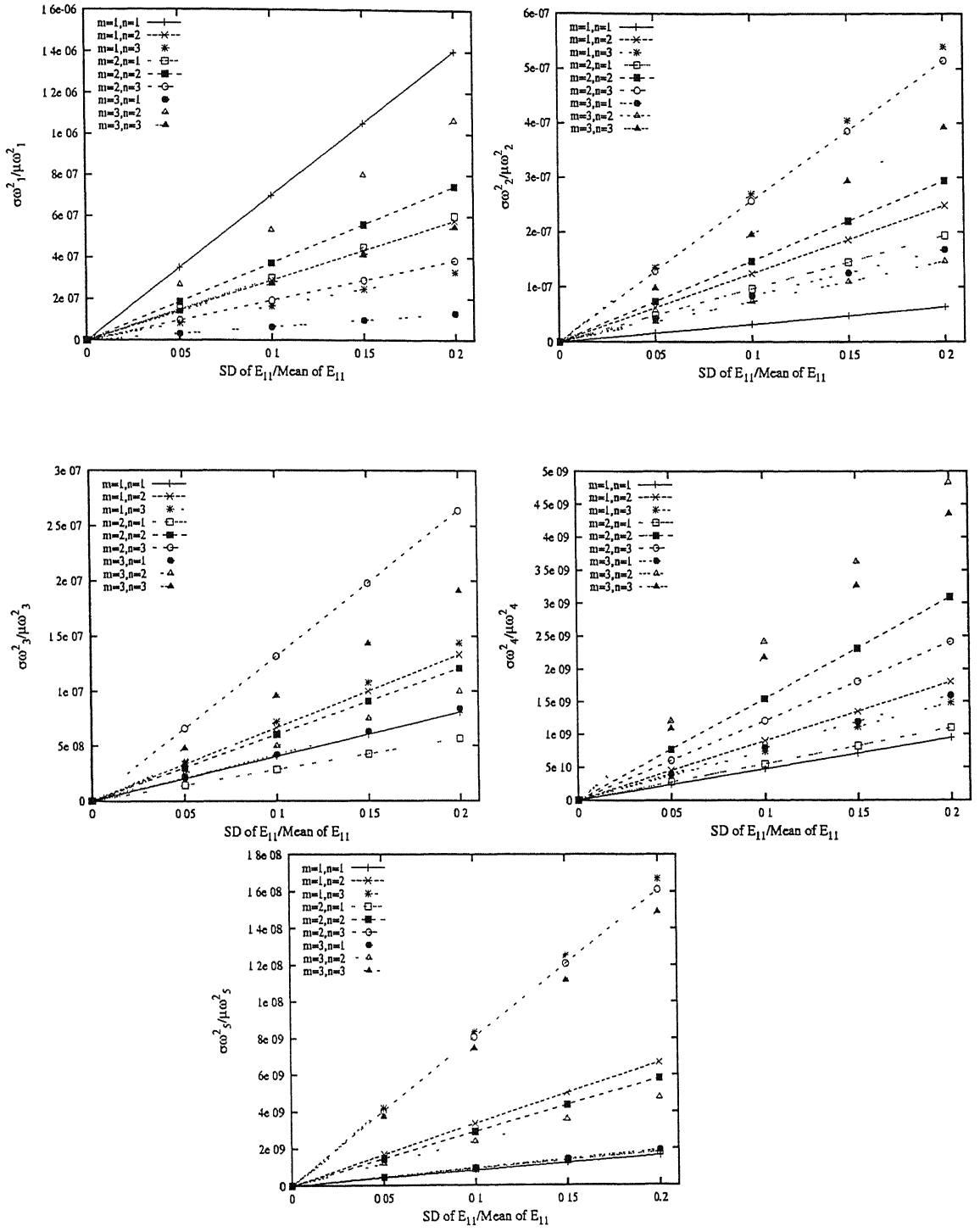

Figure 4.1: Variance of Natural Frequencies Vs SD of Input Random Variable E_{11}

$0^o/90^o/90^o/0^o/H/0^o/90^o/90^o/0^o$ L/R=1.5, Thickness=0.3

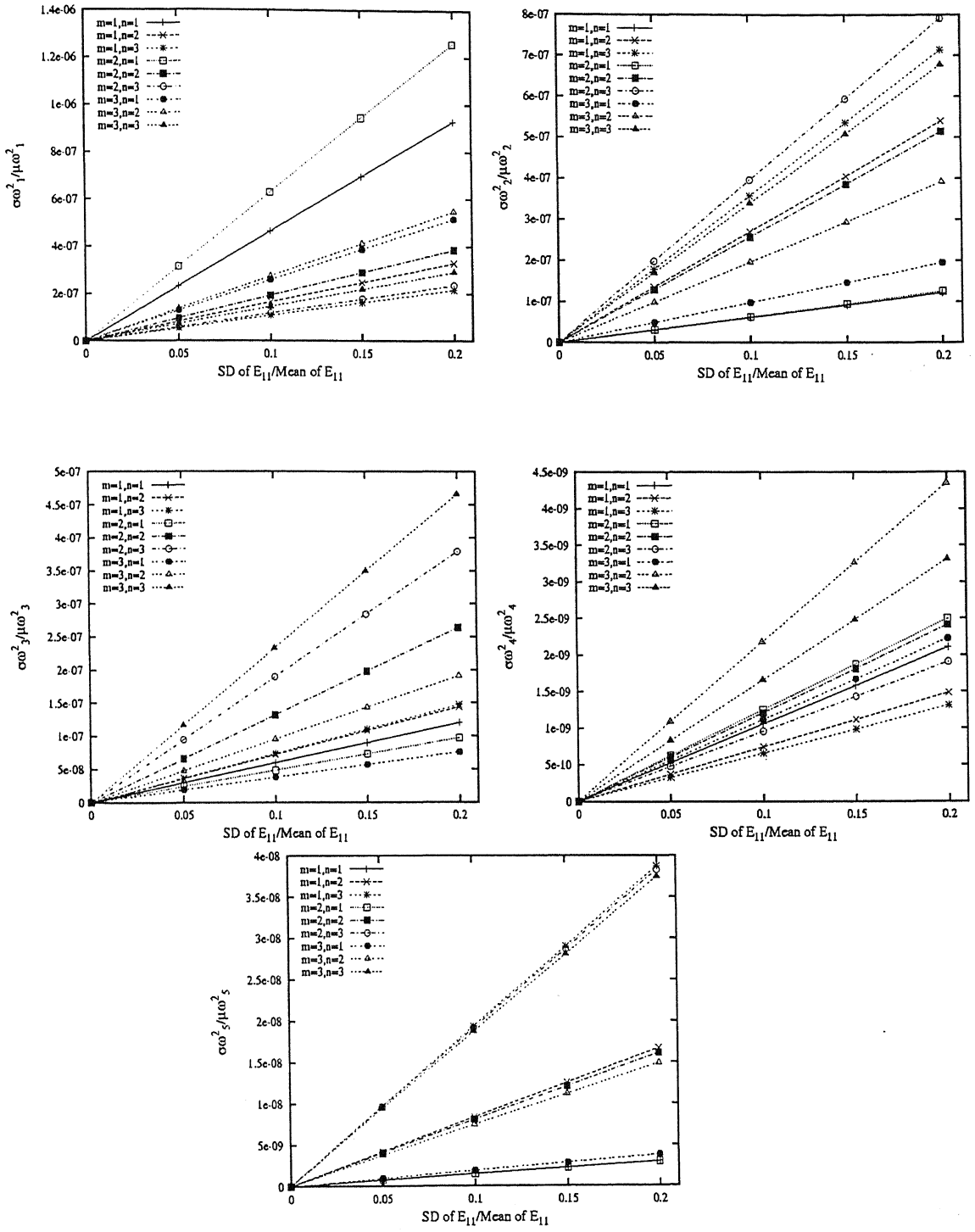

Figure 4.2: Variance of Natural Frequencies Vs SD of Input Random Variable E_{11}

$0^o/90^o/90^o/0^o/H/0^o/90^o/90^o/0^o$ L/R=1.0, Thickness=0.3

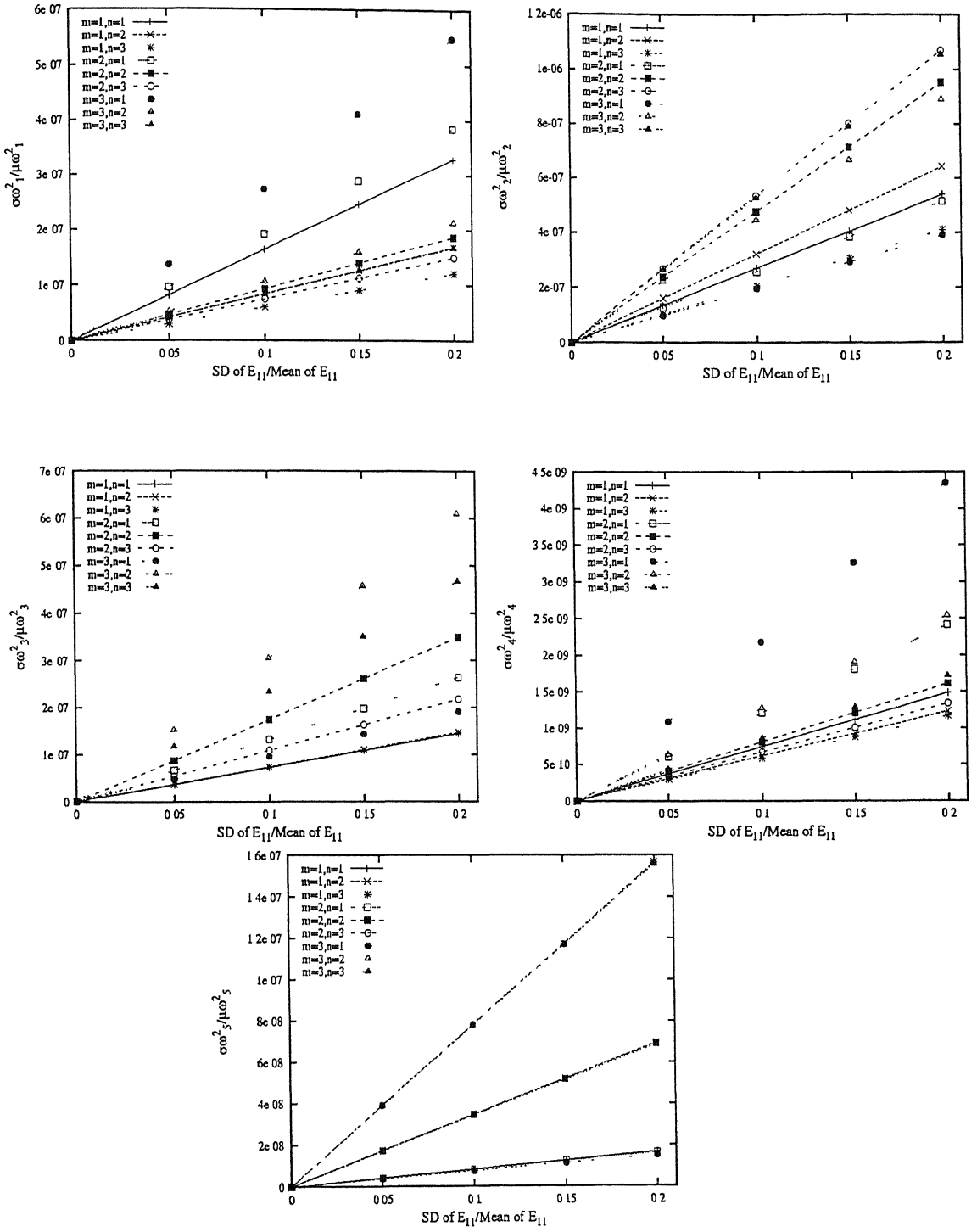

Figure 4.3: Variance of Natural Frequencies Vs SD of Input Random Variable E_{11}

$0^o/90^o/90^o/0^o/H/0^o/90^o/90^o/0^o$ L/R=0.5, Thickness=0.3

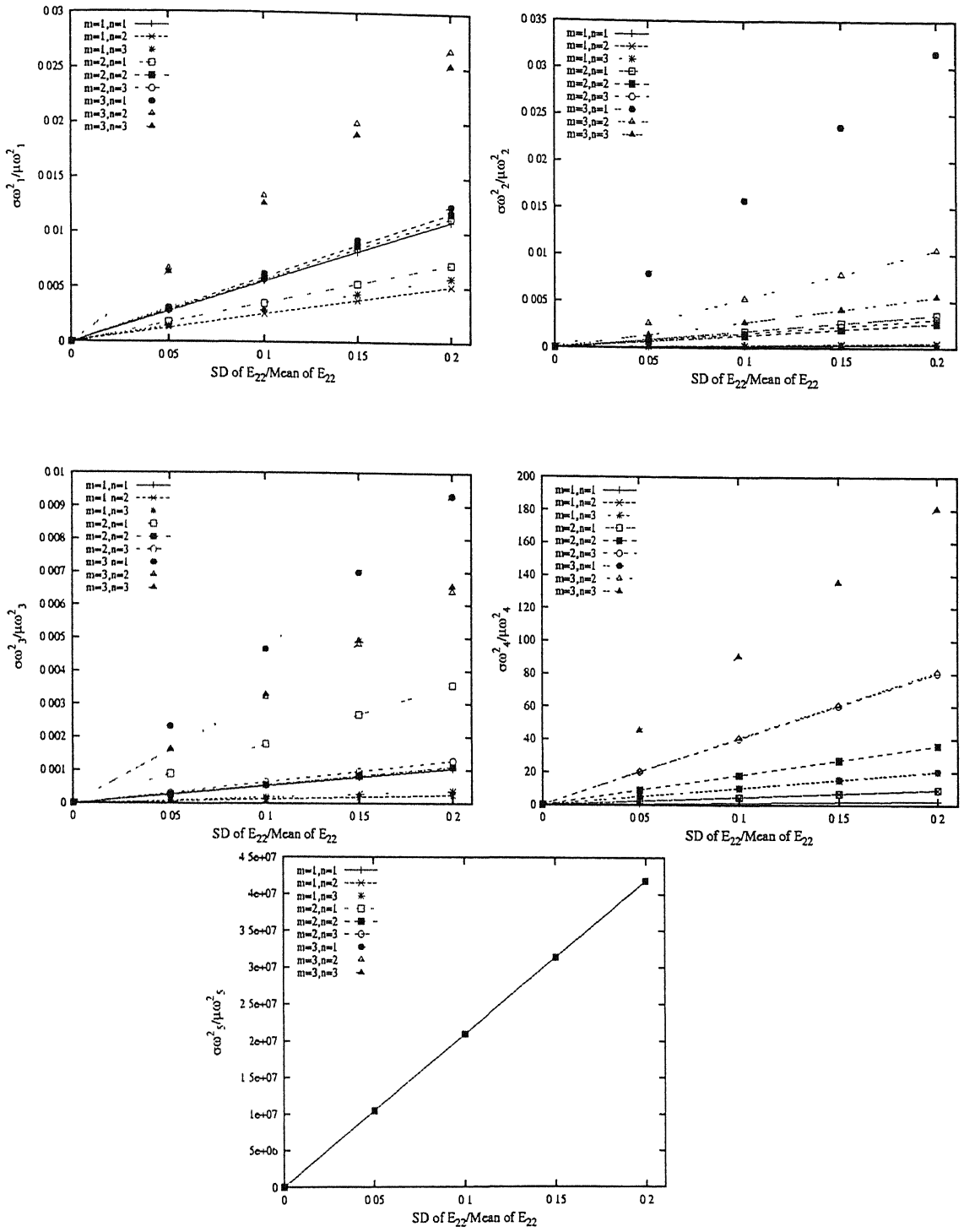

Figure 4.4: Variance of Natural Frequencies Vs SD of Input Random Variable E_{22}

$0^o/90^o/90^o/0^o/H/0^o/90^o/90^o/0^o$ L/R=1.5, Thickness=0.3

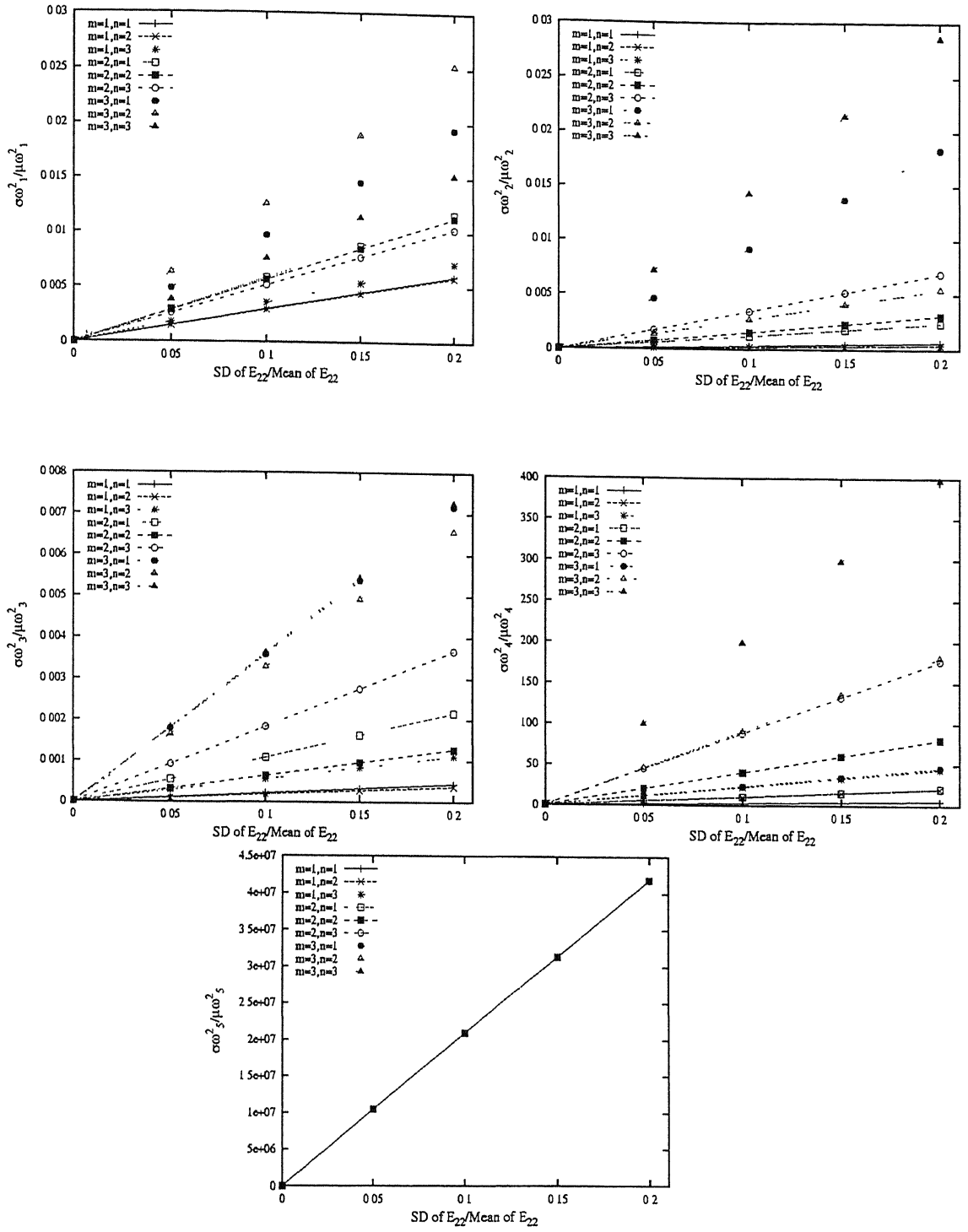

Figure 4.5: Variance of Natural Frequencies Vs SD of Input Random Variable E_{22}

$0^o/90^o/90^o/0^o/H/0^o/90^o/90^o/0^o$ L/R=1.0, Thickness=0.3

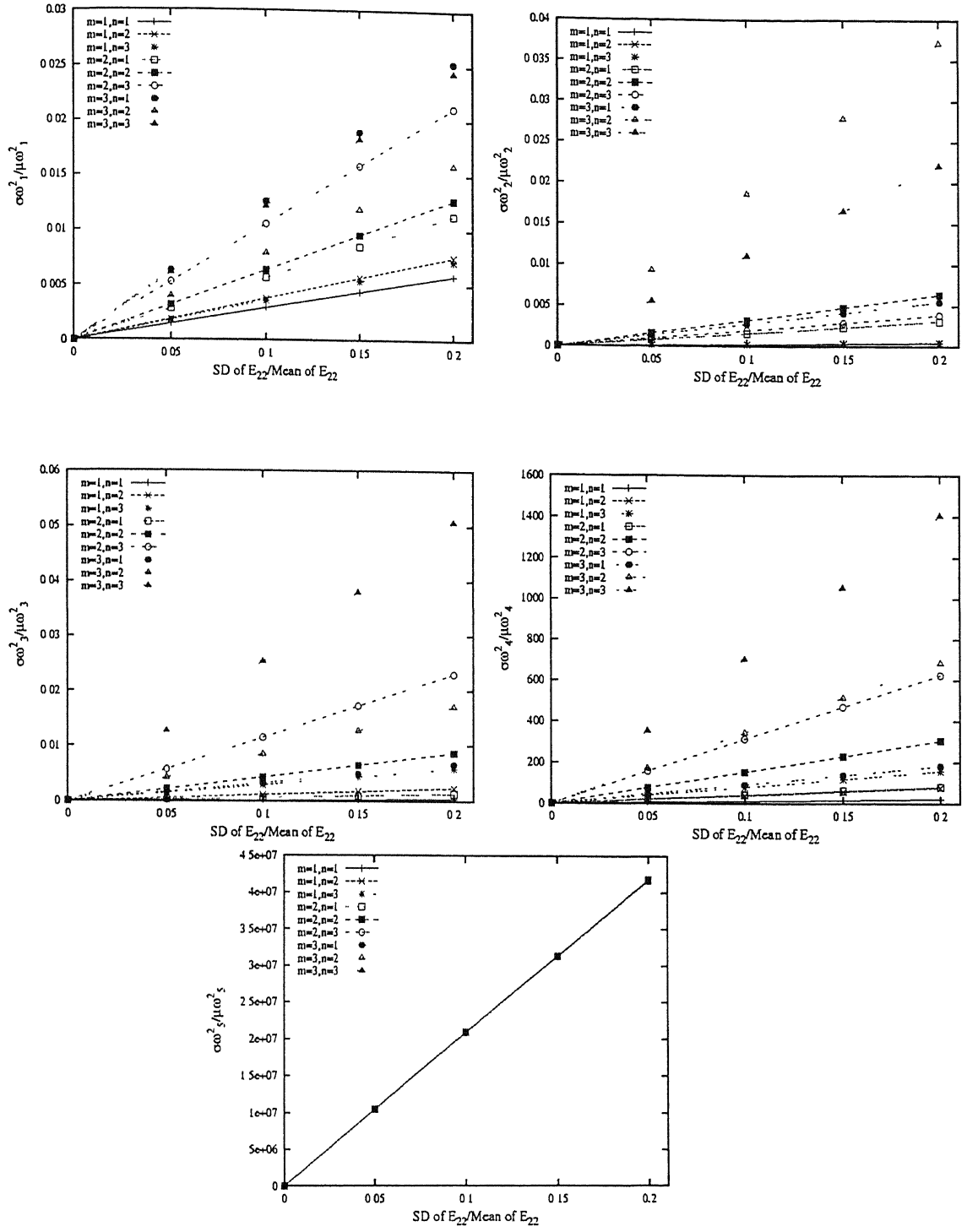

Figure 4.6: Variance of Natural Frequencies Vs SD of Input Random Variable E_{22}

$0^o/90^o/90^o/0^o/H/0^o/90^o/90^o/0^o$ L/R=0.5, Thickness=0.3

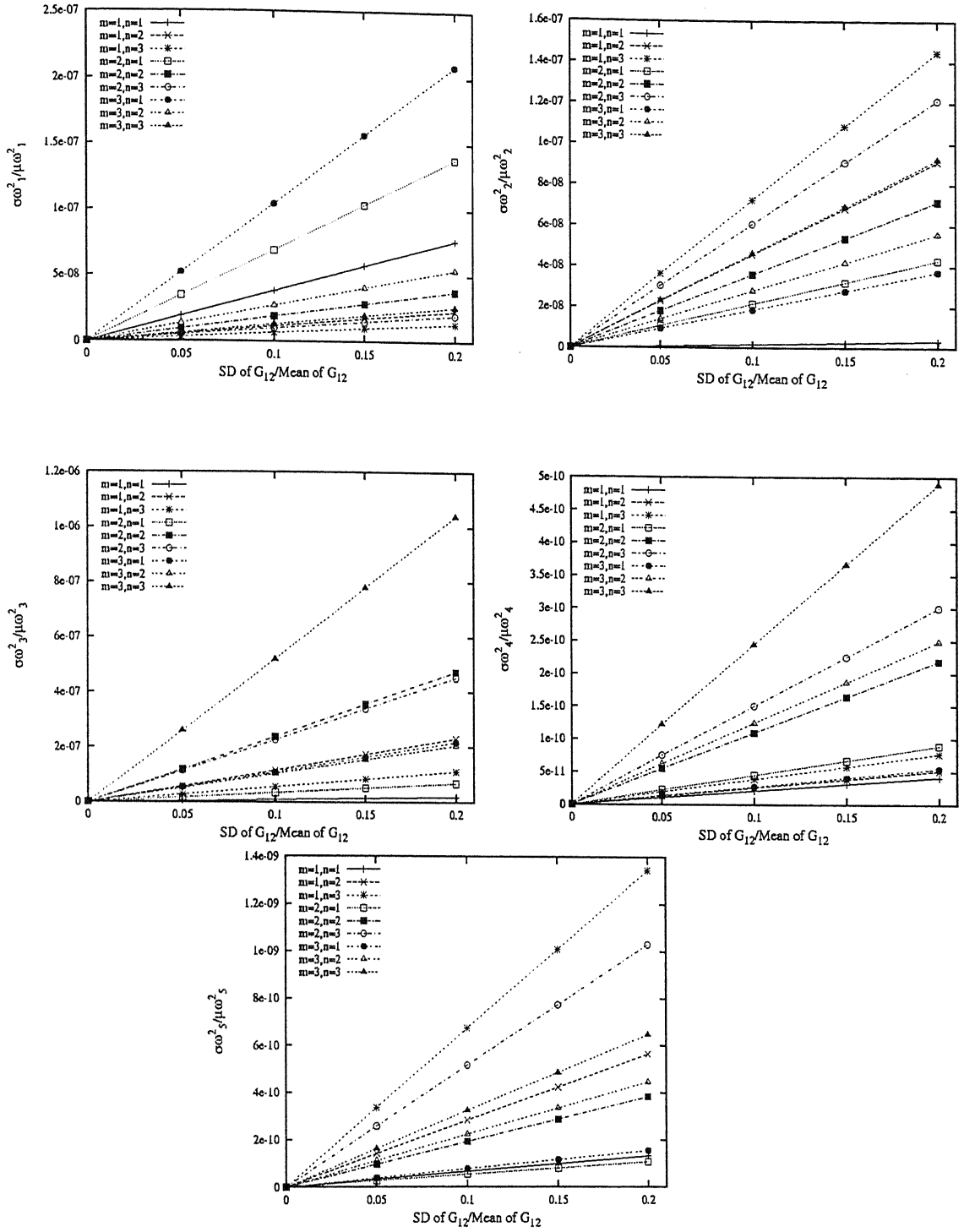

Figure 4.7: Variance of Natural Frequencies Vs SD of Input Random Variable G_{12}

$0^o/90^o/90^o/0^o/H/0^o/90^o/90^o/0^o$ L/R=1.5, Thickness=0.3

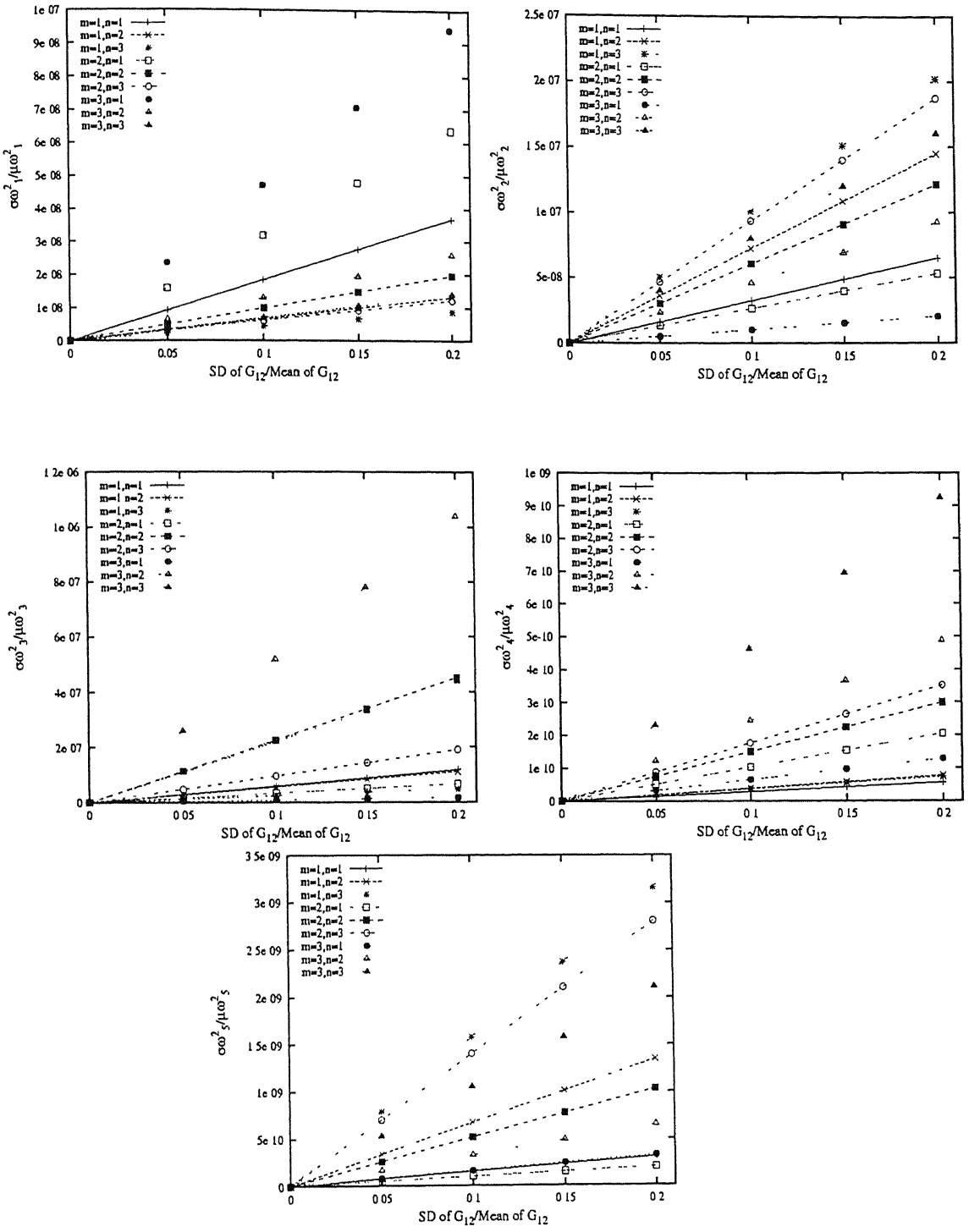

Figure 4.8: Variance of Natural Frequencies Vs SD of Input Random Variable G_{12}

$0^o/90^o/90^o/0^o/H/0^o/90^o/90^o/0^o$ L/R=1.0, Thickness=0.3

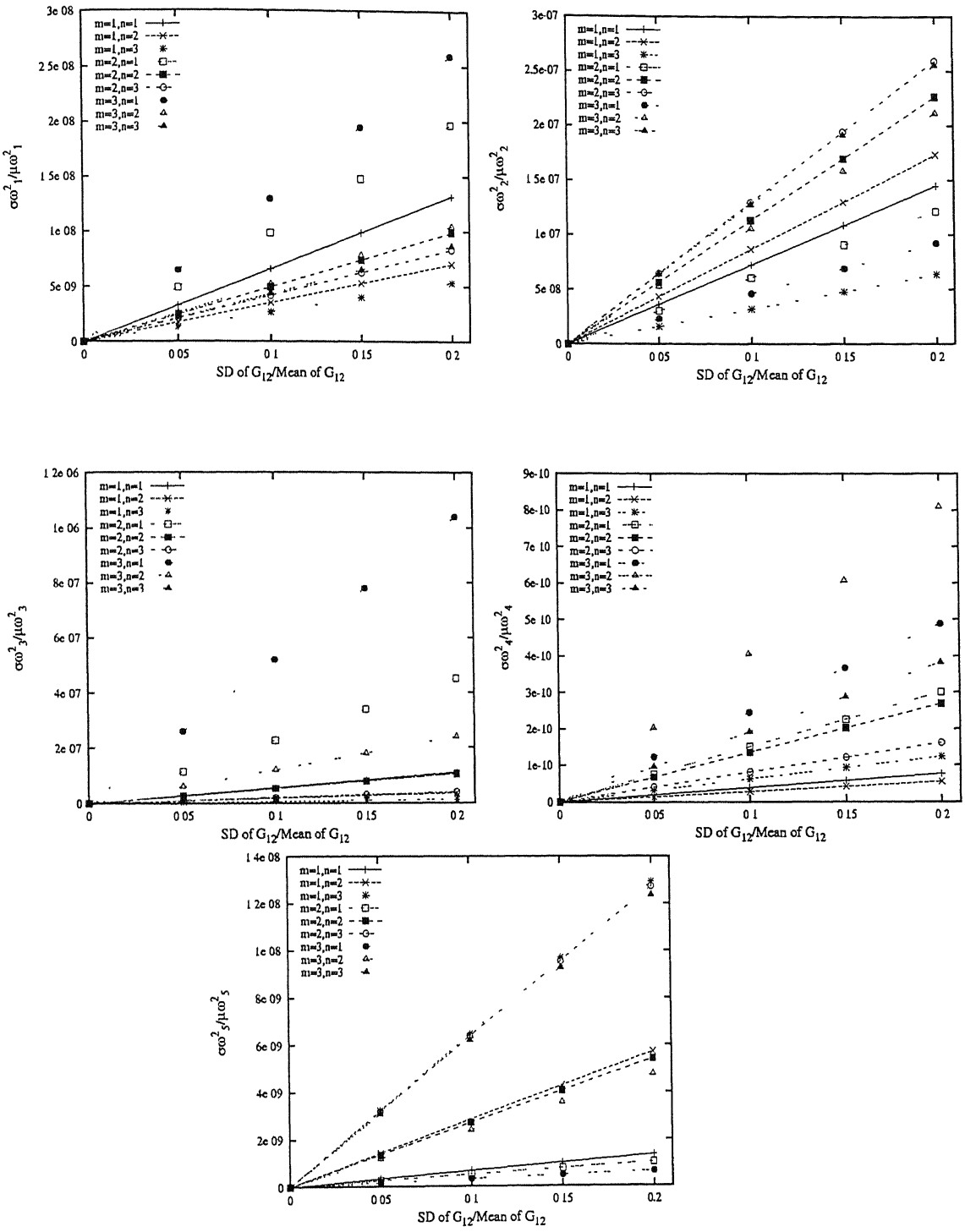

Figure 4.9: Variance of Natural Frequencies Vs SD of Input Random Variable G_{12}

$0^o/90^o/90^o/0^o/H/0^o/90^o/90^o/0^o$ L/R=0.5, Thickness=0.3

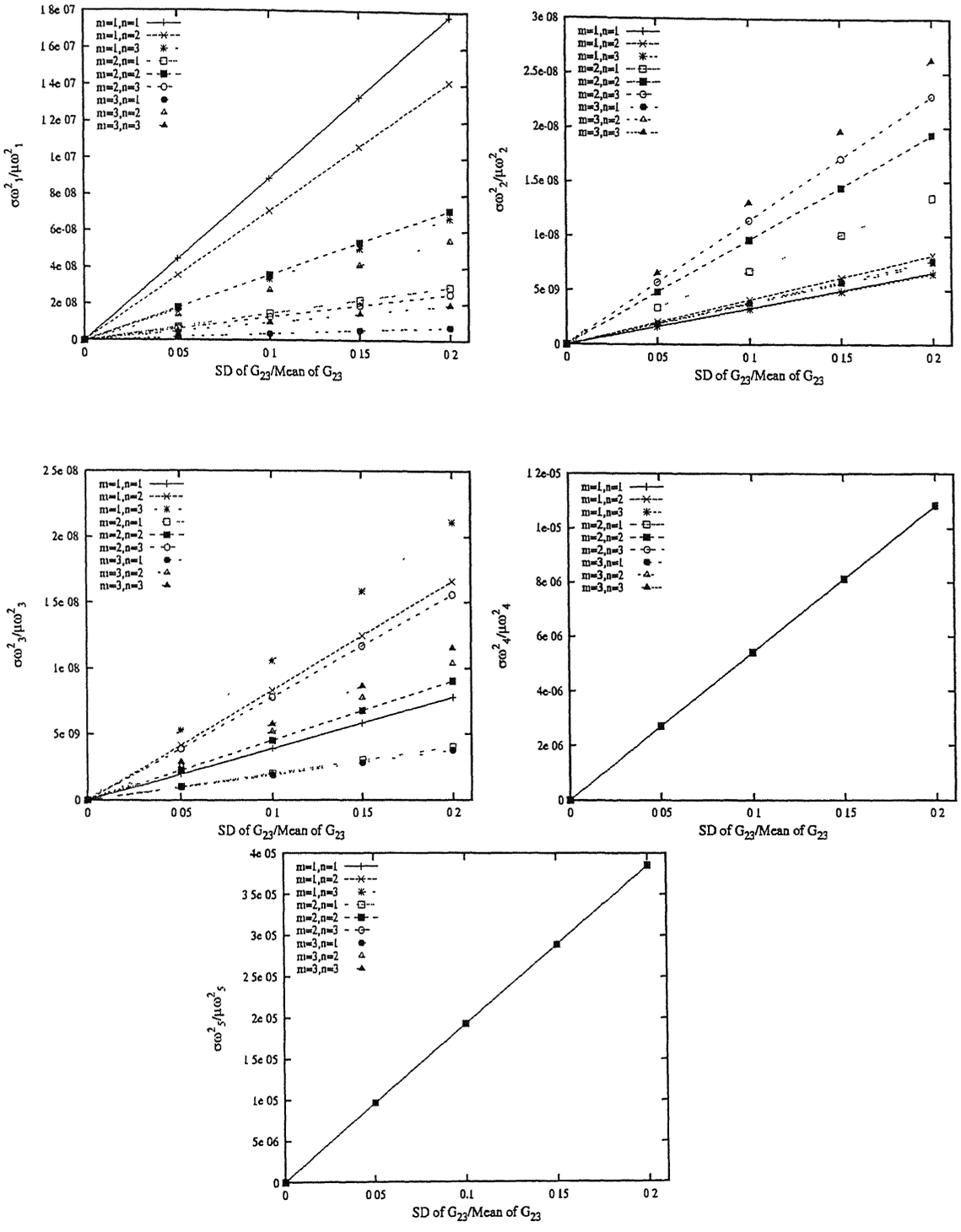

Figure 4.10: Variance of Natural Frequencies Vs SD of Input Random Variable G_{23}

$0^o/90^o/90^o/0^o/H/0^o/90^o/90^o/0^o$ L/R=1.5, Thickness=0.3

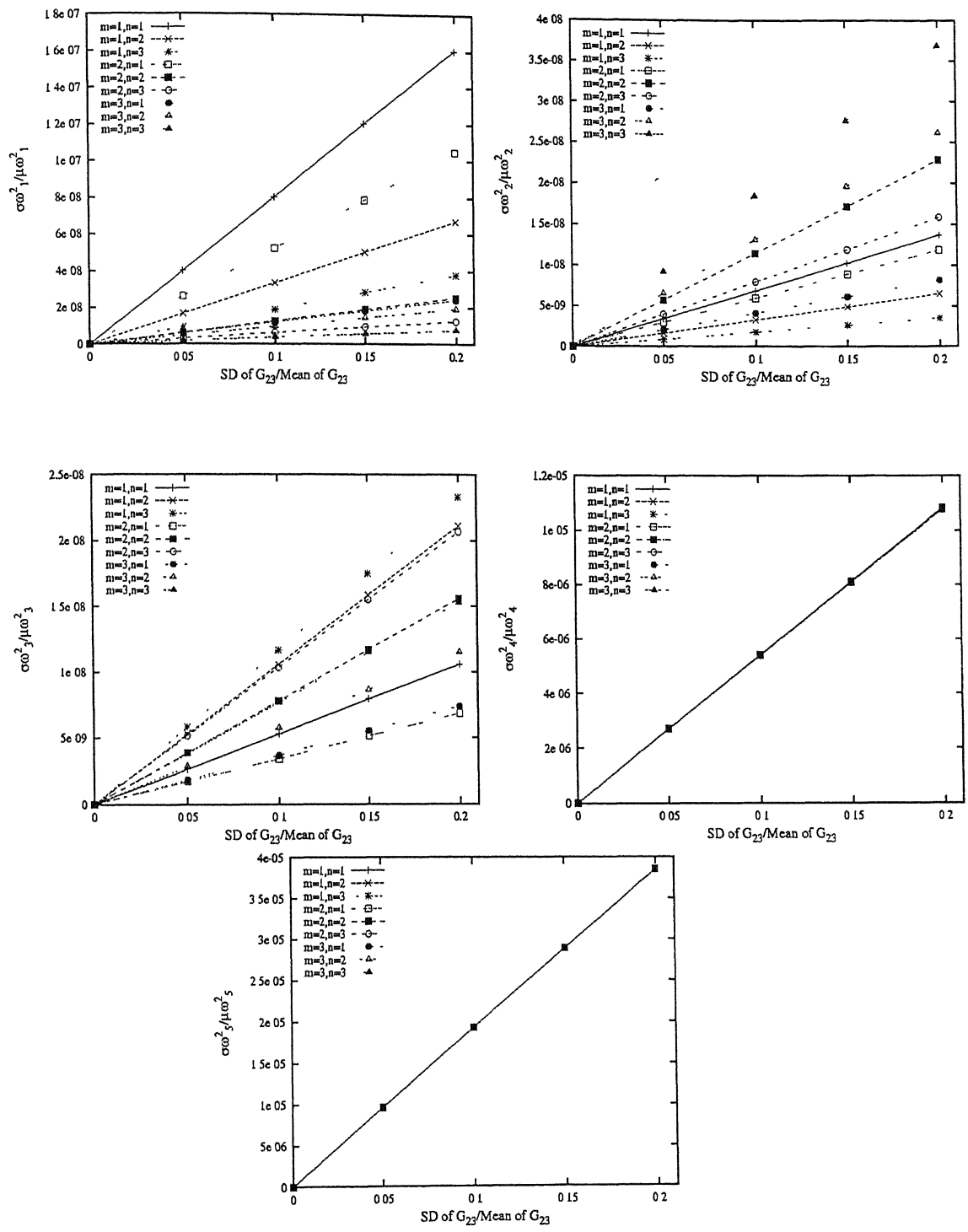

Figure 4.11: Variance of Natural Frequencies Vs SD of Input Random Variable G_{23} $0^o/90^o/90^o/0^o/H/0^o/90^o/90^o/0^o$ L/R=1.0, Thickness=0.3

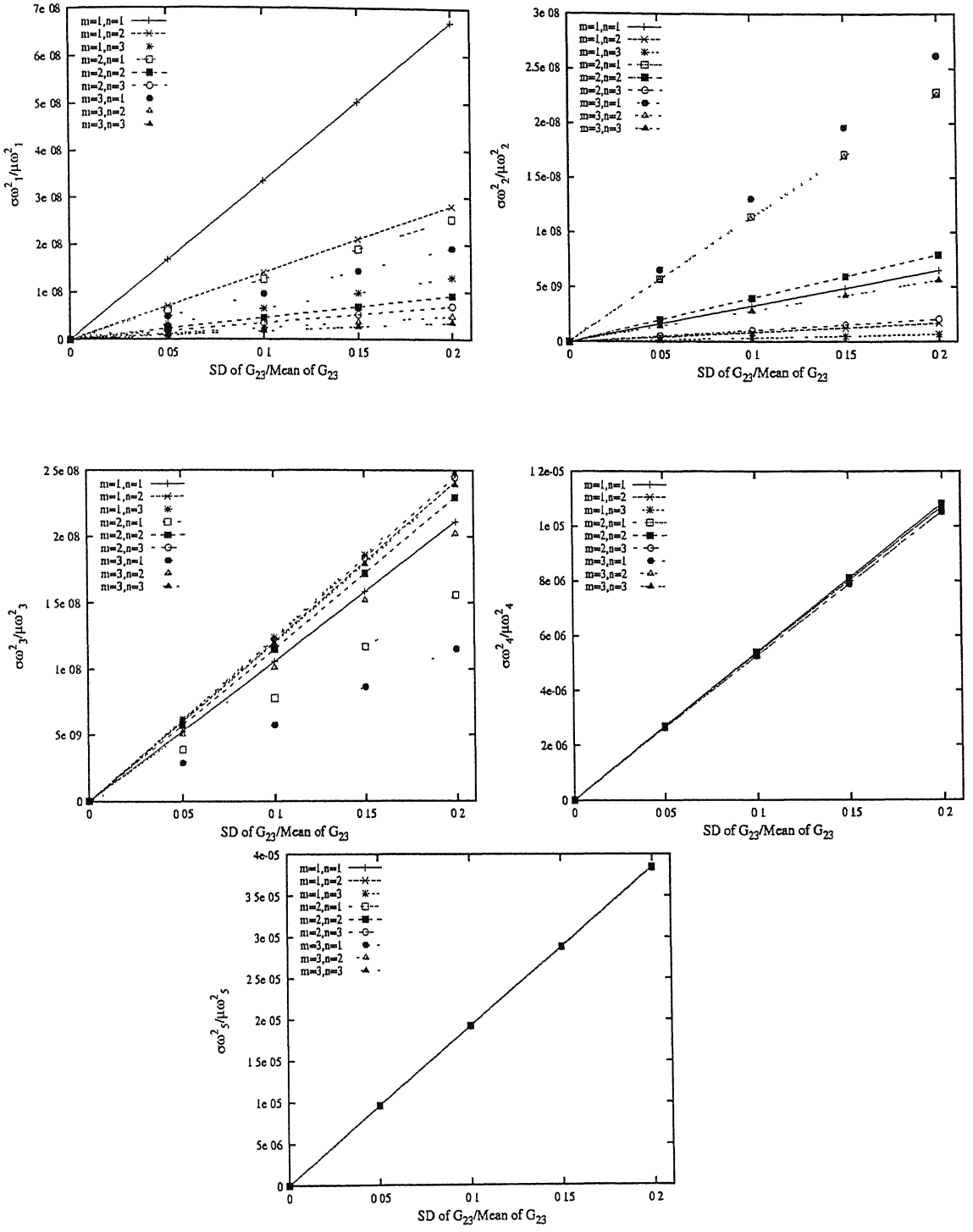

Figure 4.12: Variance of Natural Frequencies Vs SD of Input Random Variable G_{23}

$0^o/90^o/90^o/0^o/H/0^o/90^o/90^o/0^o$ L/R=0.5, Thickness=0.3

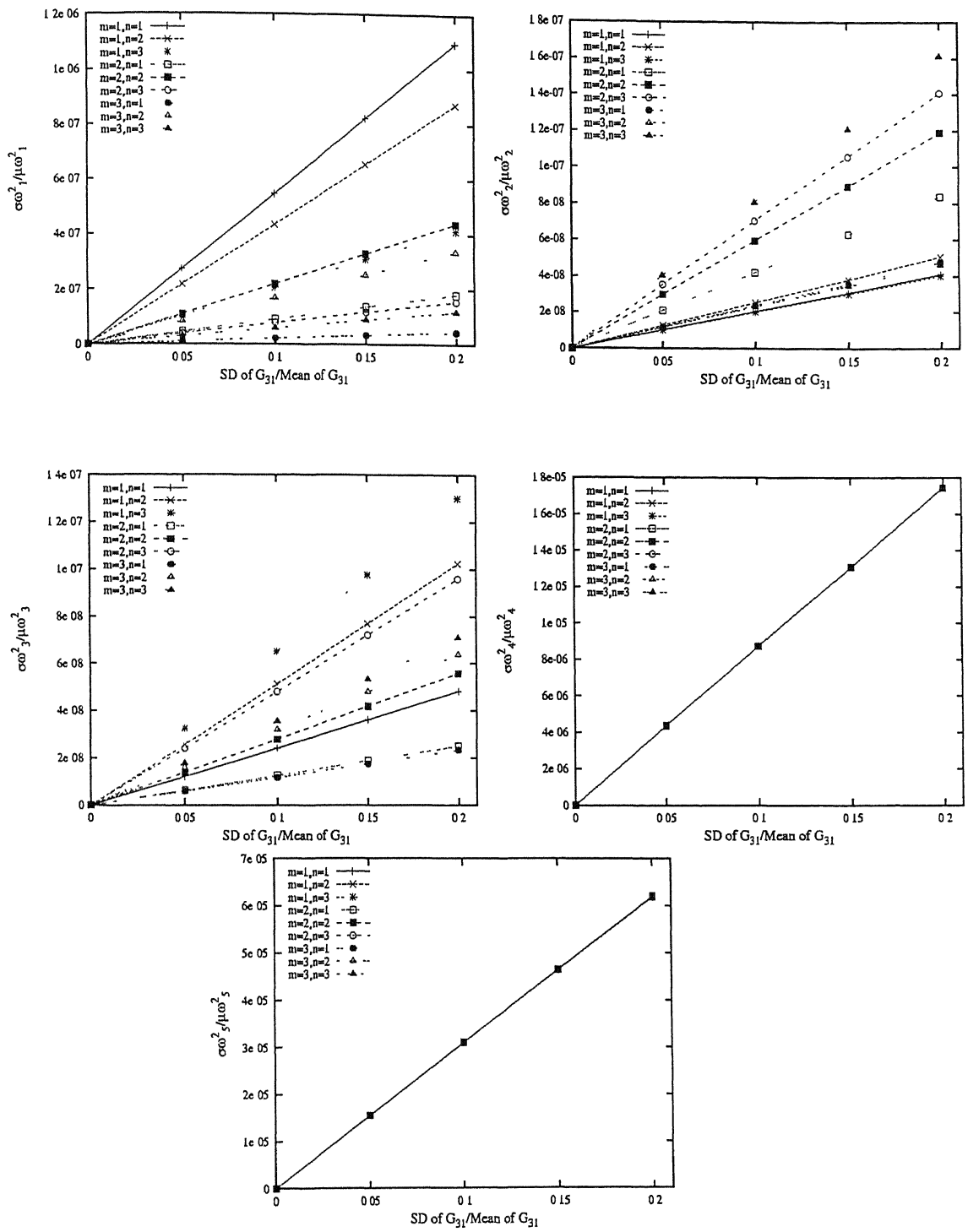

Figure 4.13: Variance of Natural Frequencies Vs SD of Input Random Variable G_{31}

$0^o/90^o/90^o/0^o/H/0^o/90^o/90^o/0^o$ L/R=1.5, Thickness=0.3

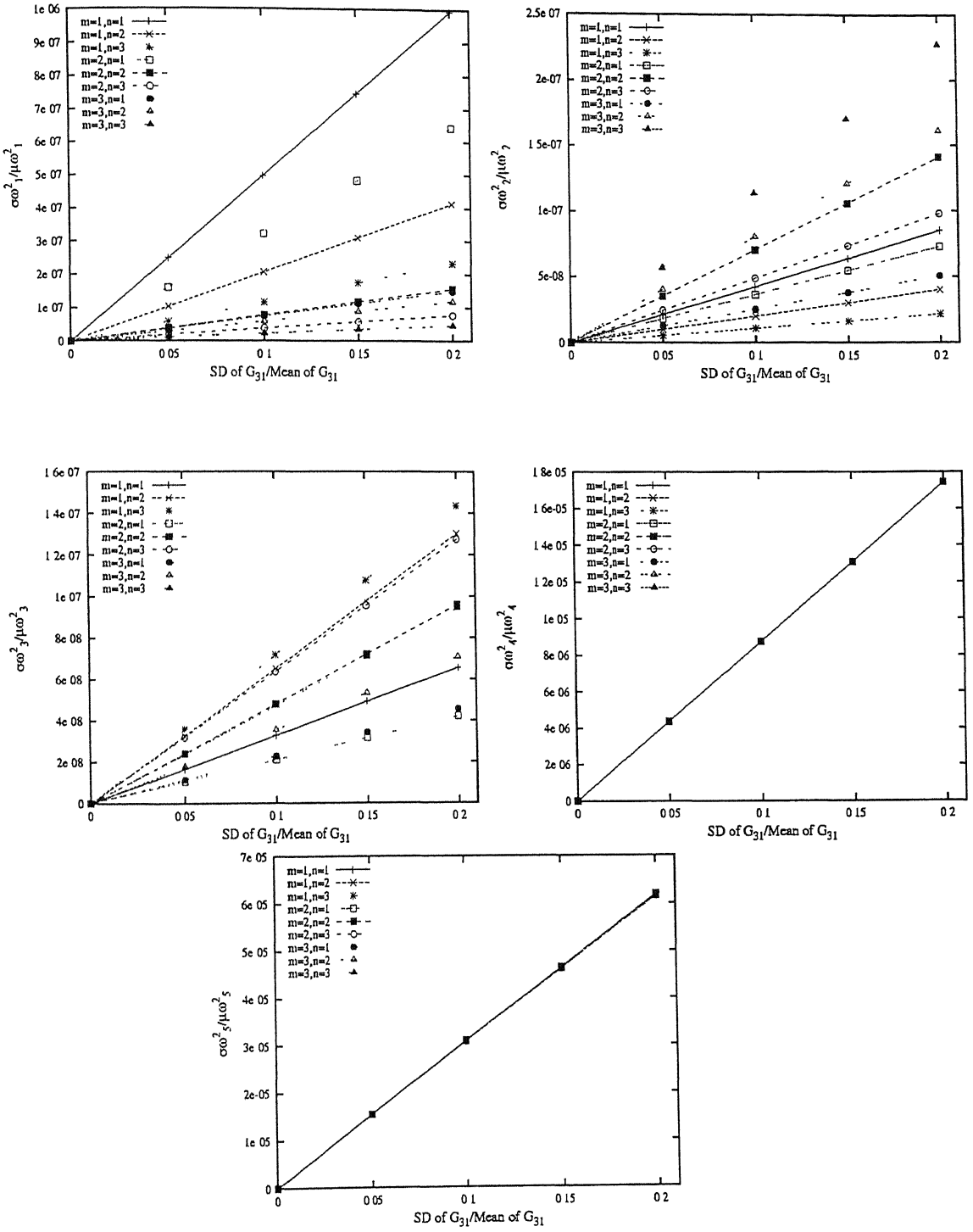

Figure 4.14: Variance of Natural Frequencies Vs SD of Input Random Variable G_{31}

$0^o/90^o/90^o/0^o/H/0^o/90^o/90^o/0^o$ L/R=1.0, Thickness=0.3

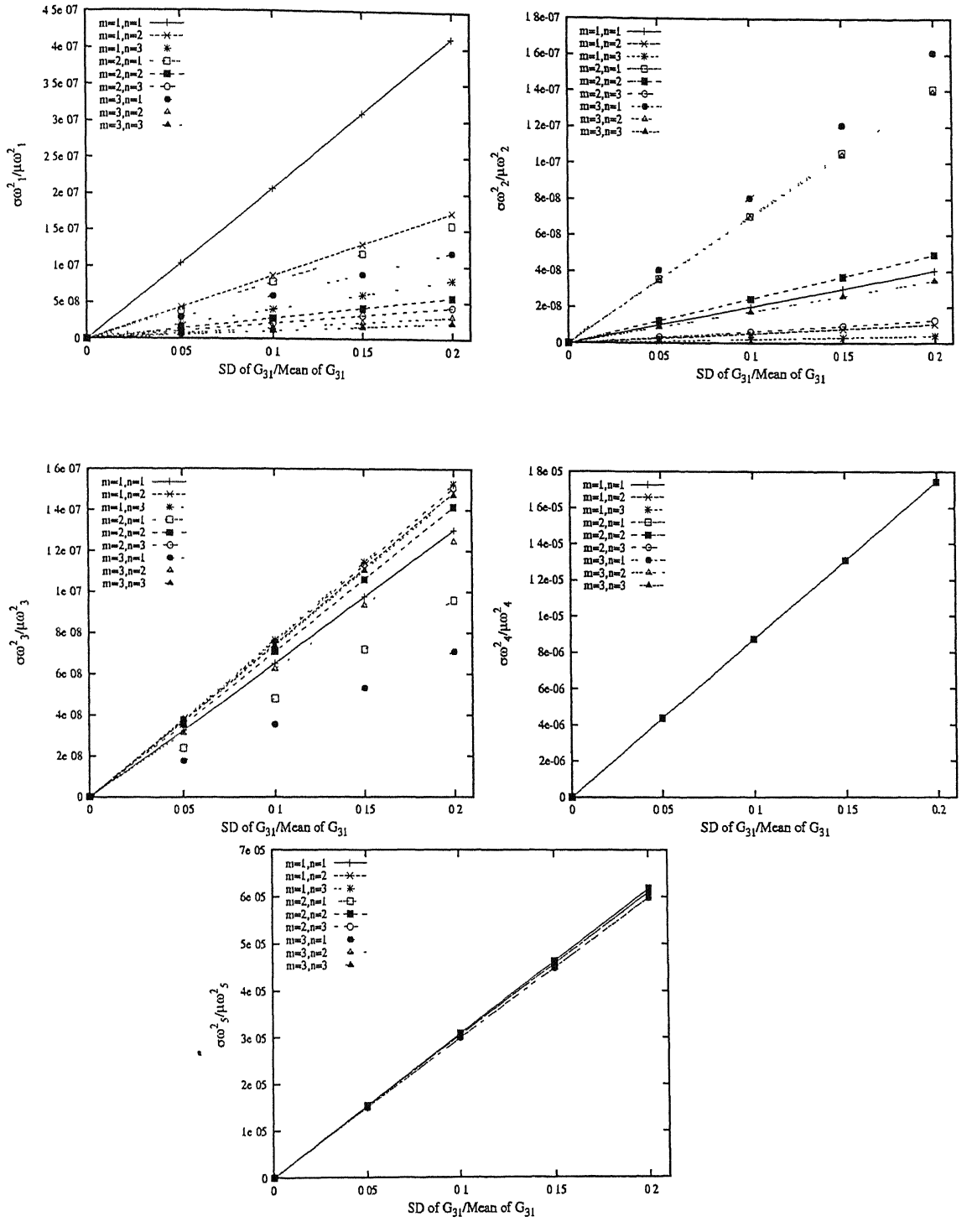

Figure 4.15: Variance of Natural Frequencies Vs SD of Input Random Variable G_{31}

$0^o/90^o/90^o/0^o/H/0^o/90^o/90^o/0^o$ L/R=0.5, Thickness=0.3

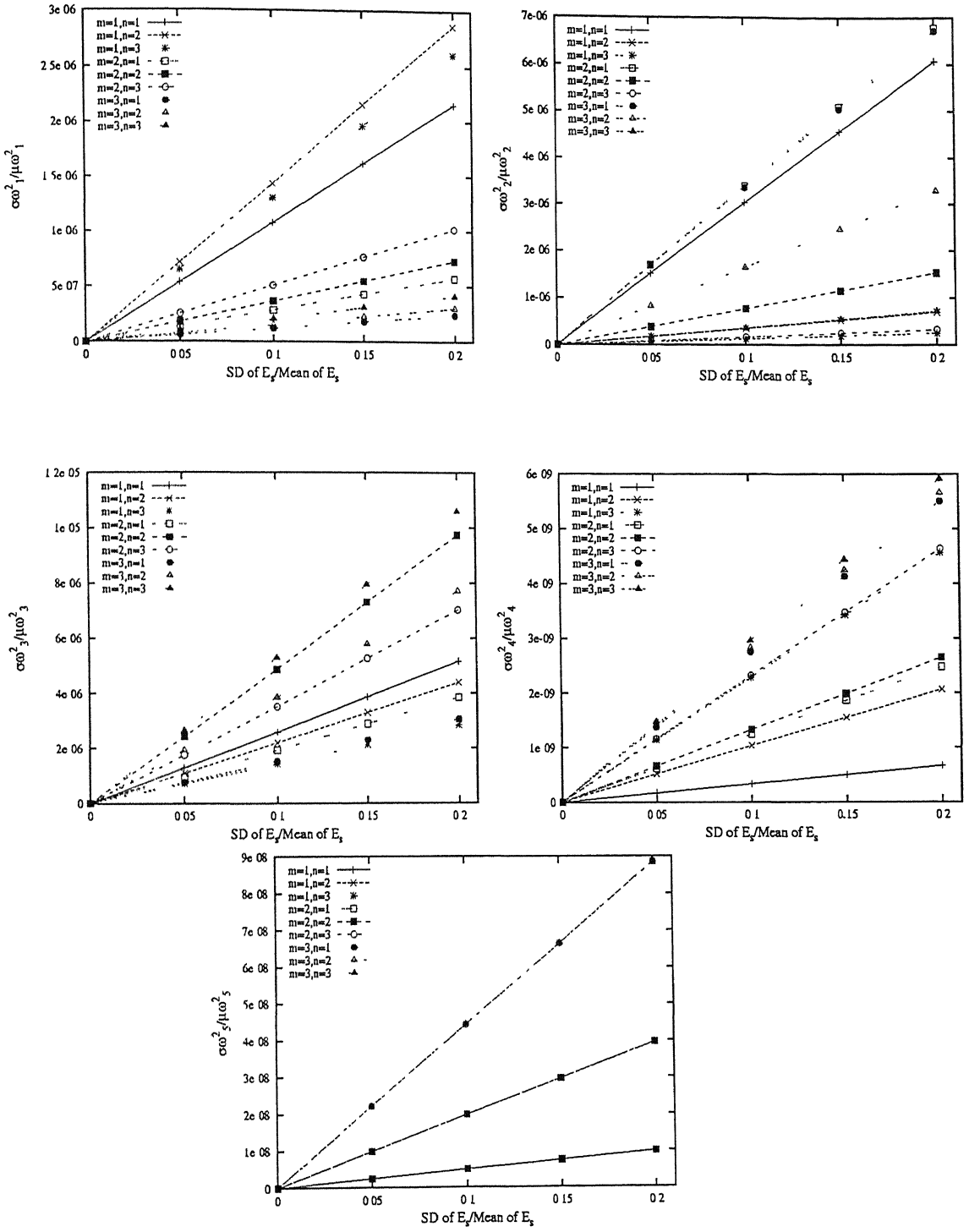

Figure 4.16: Variance of Natural Frequencies Vs SD of Input Random Variable E_s

$0^o/90^o/90^o/0^o/H/0^o/90^o/90^o/0^o$ L/R=1.5, Thickness=0.3

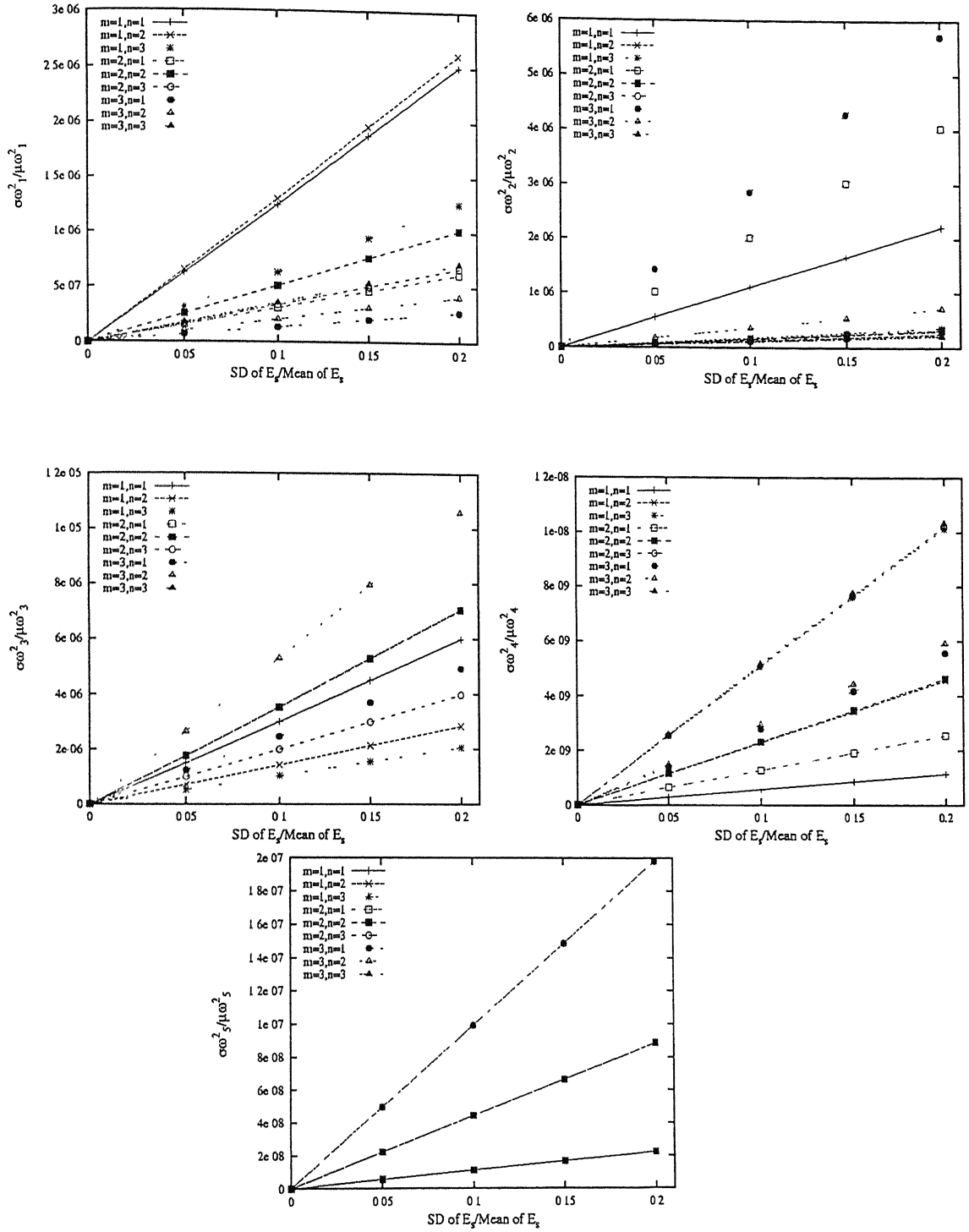

Figure 4.17: Variance of Natural Frequencies Vs SD of Input Random Variable E_s

$0^o/90^o/90^o/0^o/H/0^o/90^o/90^o/0^o$ L/R=1.0, Thickness=0.3

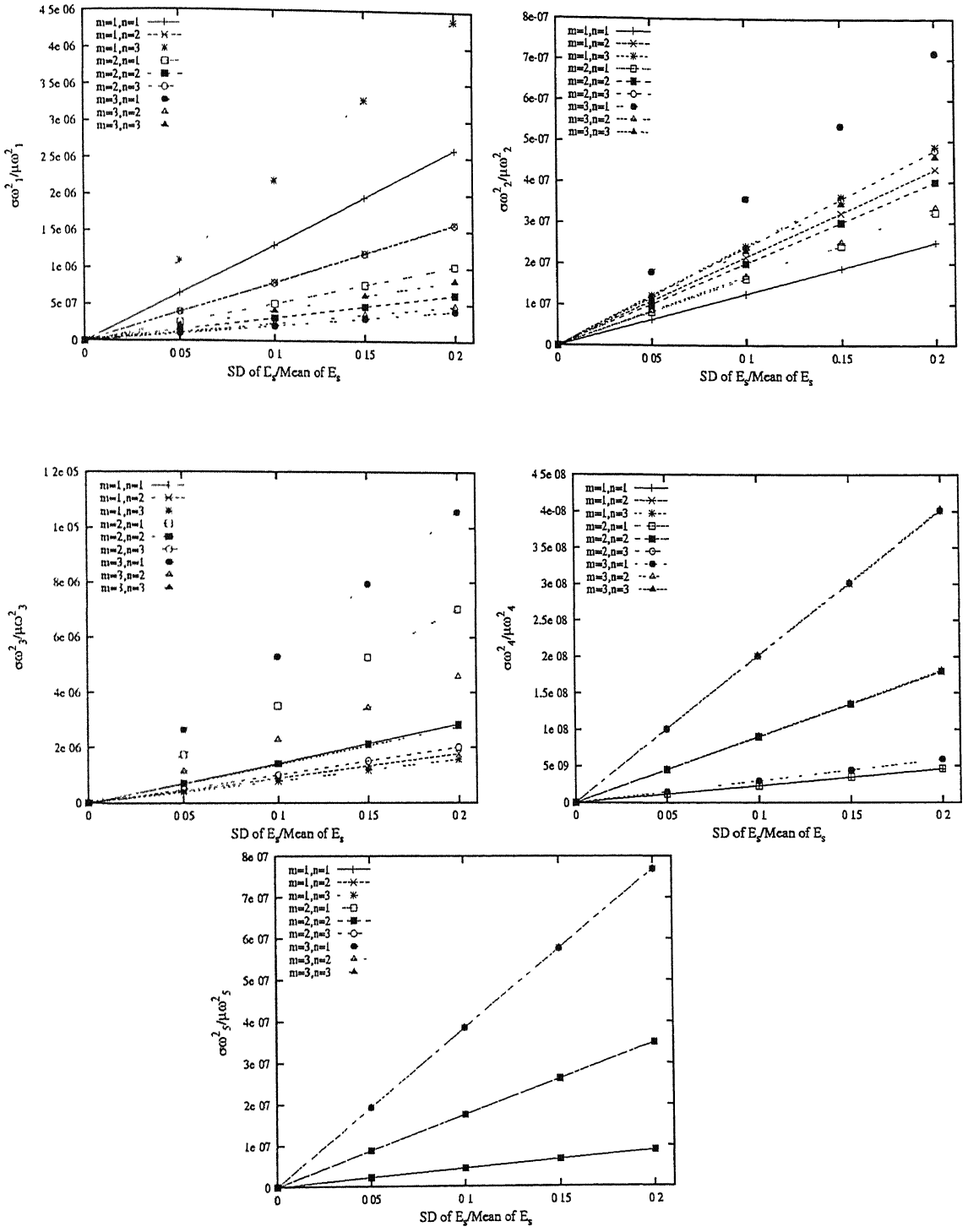

Figure 4.18: Variance of Natural Frequencies Vs SD of Input Random Variable E_s

$0^o/90^o/90^o/0^o/H/0^o/90^o/90^o/0^o$ L/R=0.5, Thickness=0.3

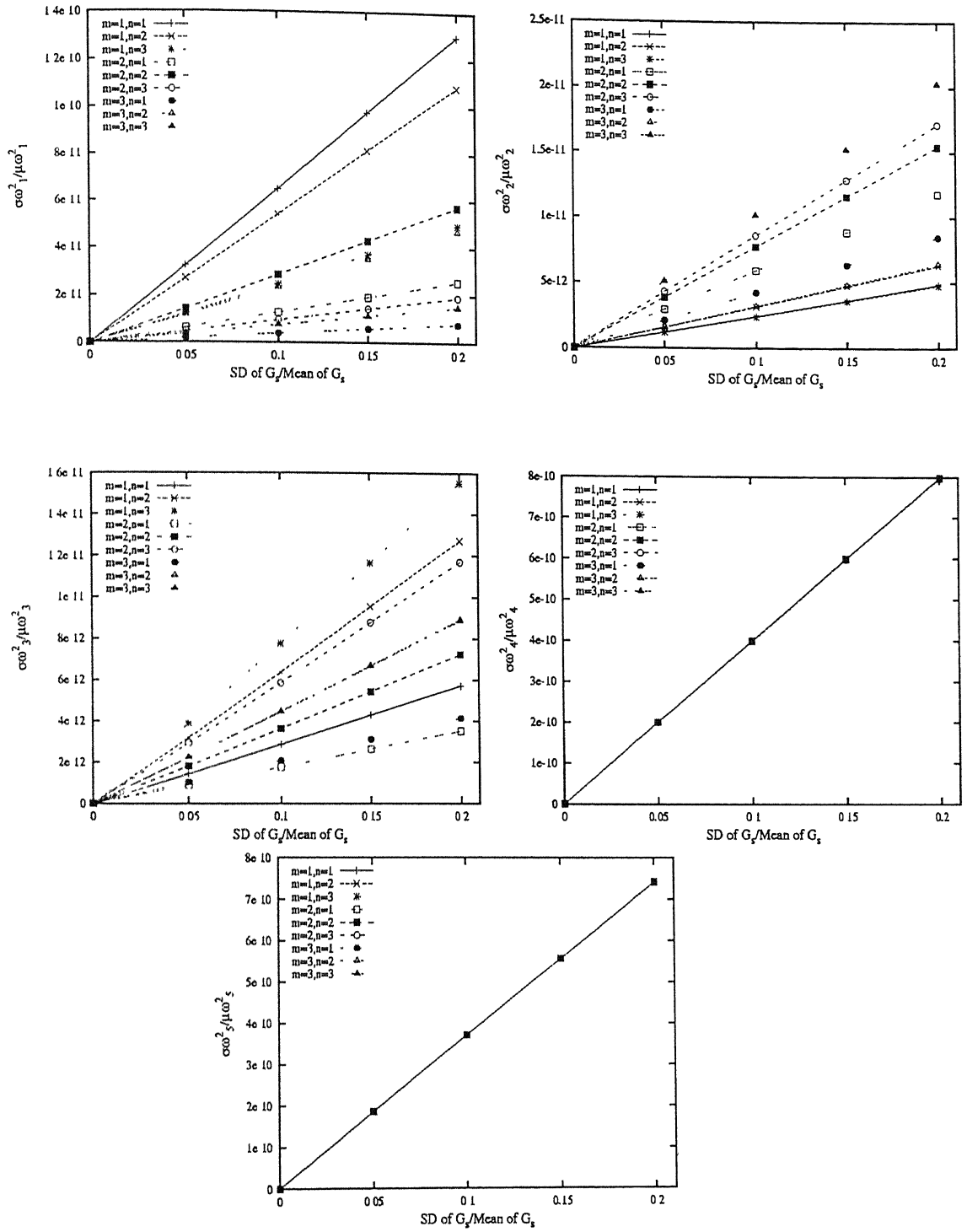

Figure 4.19: Variance of Natural Frequencies Vs SD of Input Random Variable G_s

$0^o/90^o/90^o/0^o/H/0^o/90^o/90^o/0^o$ L/R=1.5, Thickness=0.3

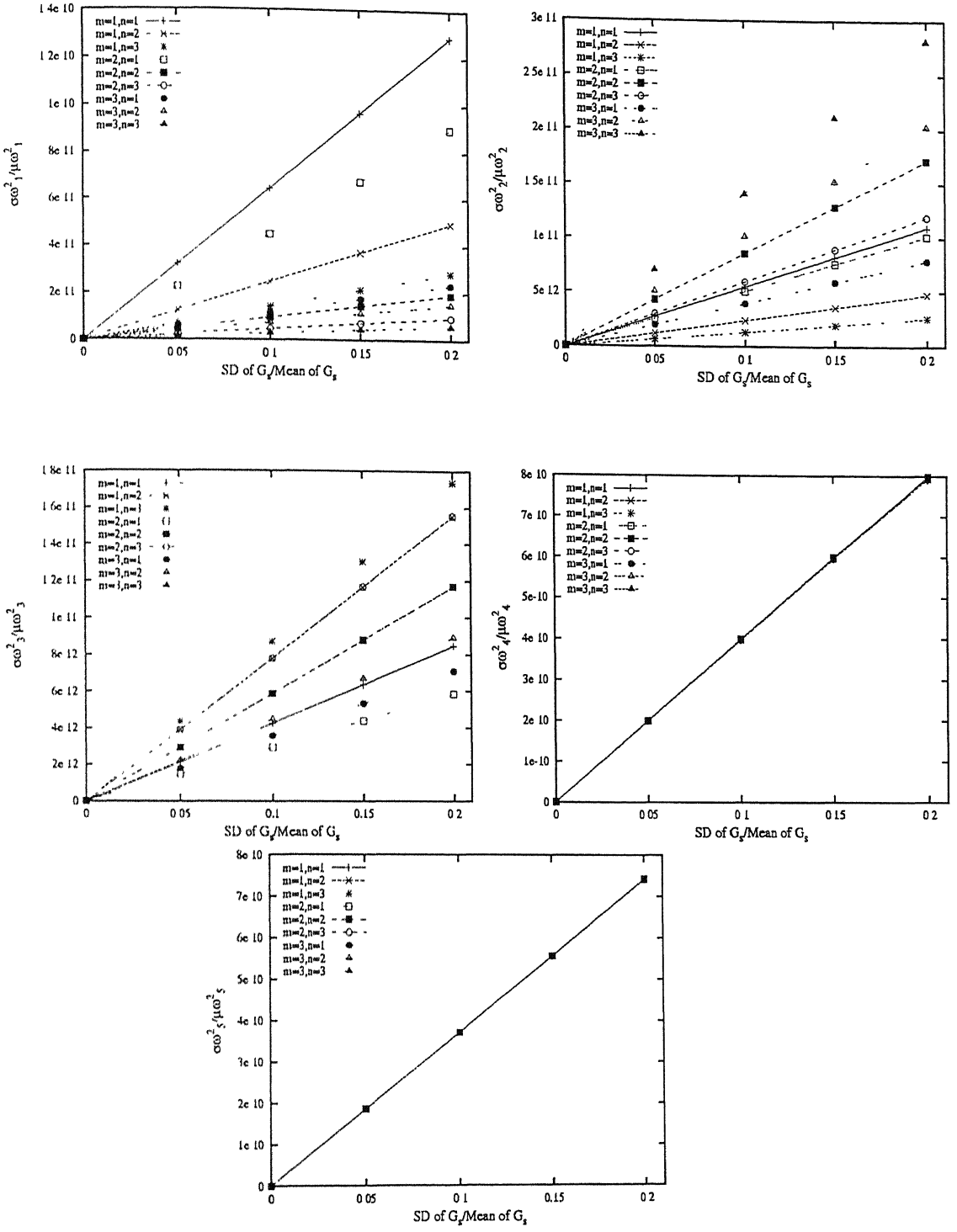

Figure 4.20: Variance of Natural Frequencies Vs SD of Input Random Variable G_s

$0^o/90^o/90^o/0^o/H/0^o/90^o/90^o/0^o$ L/R=1.0, Thickness=0.3

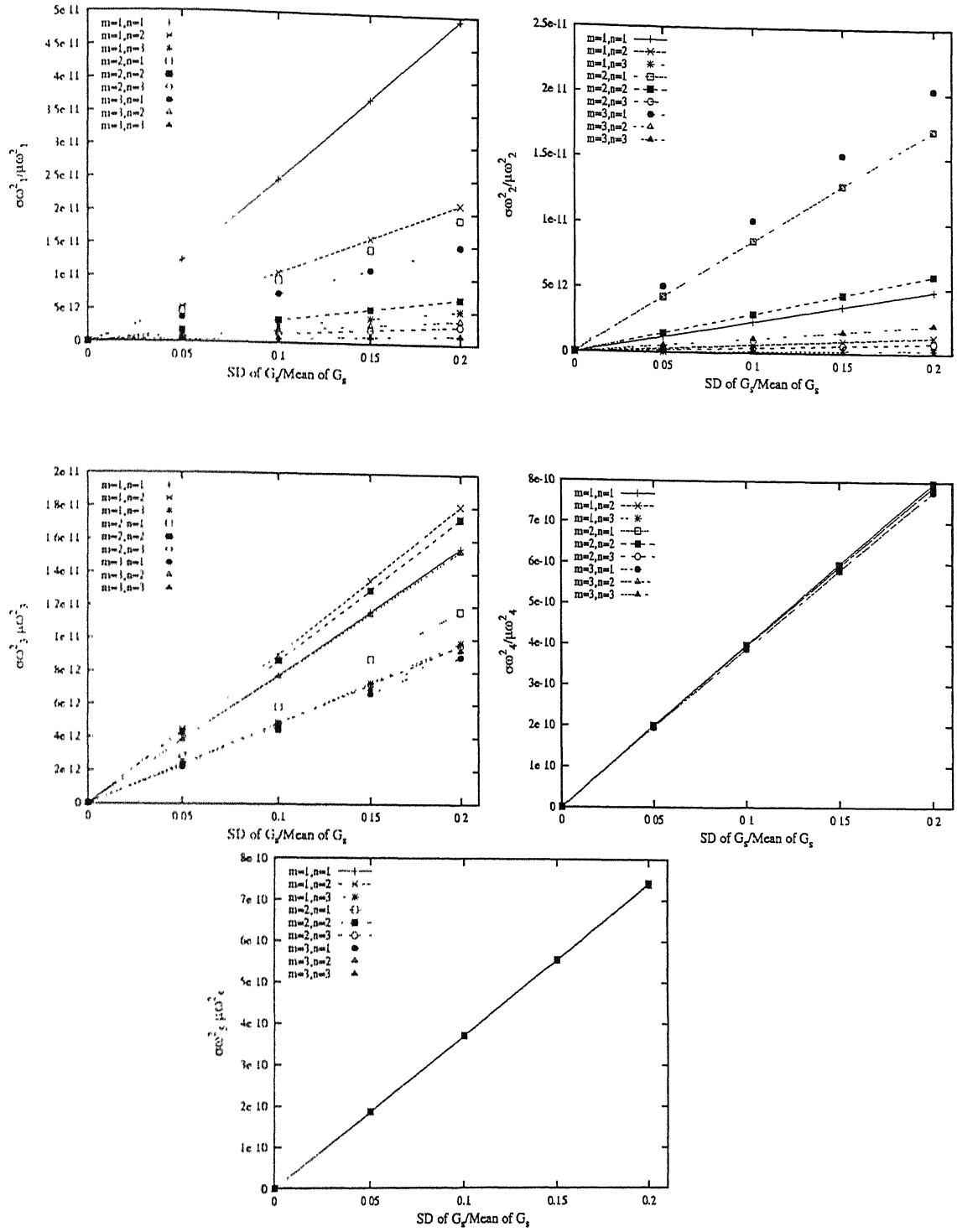

Figure 4.21: Variance of Natural Frequencies Vs SD of Input Random Variable G_s

$0^o/90^o/90^o/0^o/H/0^o/90^o/90^o/0^o$ L/R=0.5, Thickness=0.3

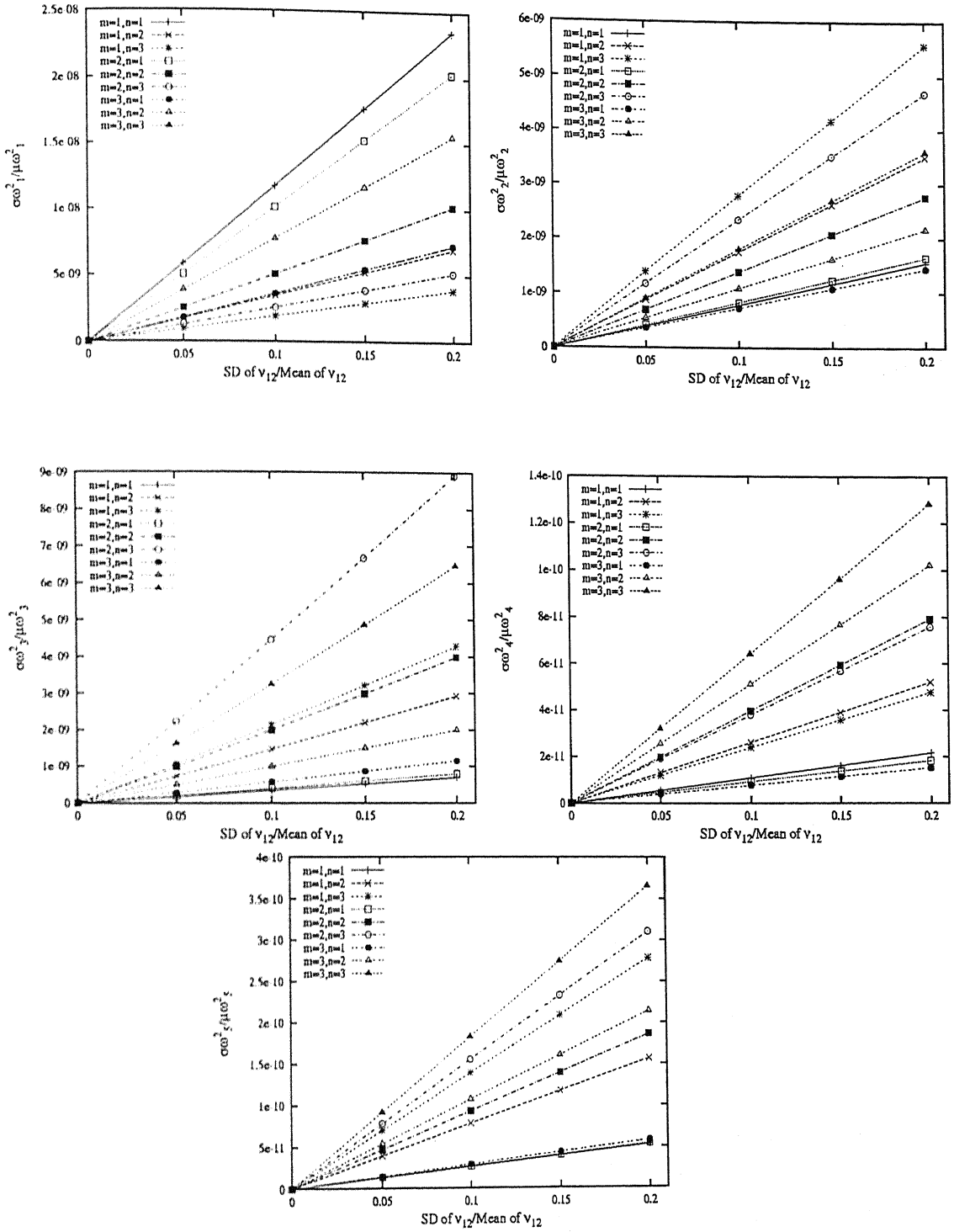

Figure 4.22: Variance of Natural Frequencies Vs SD of Input Random Variable ν_{12}

$0^o/90^o/90^o/0^o/H/0^o/90^o/90^o/0^o$ L/R=1.5, Thickness=0.3

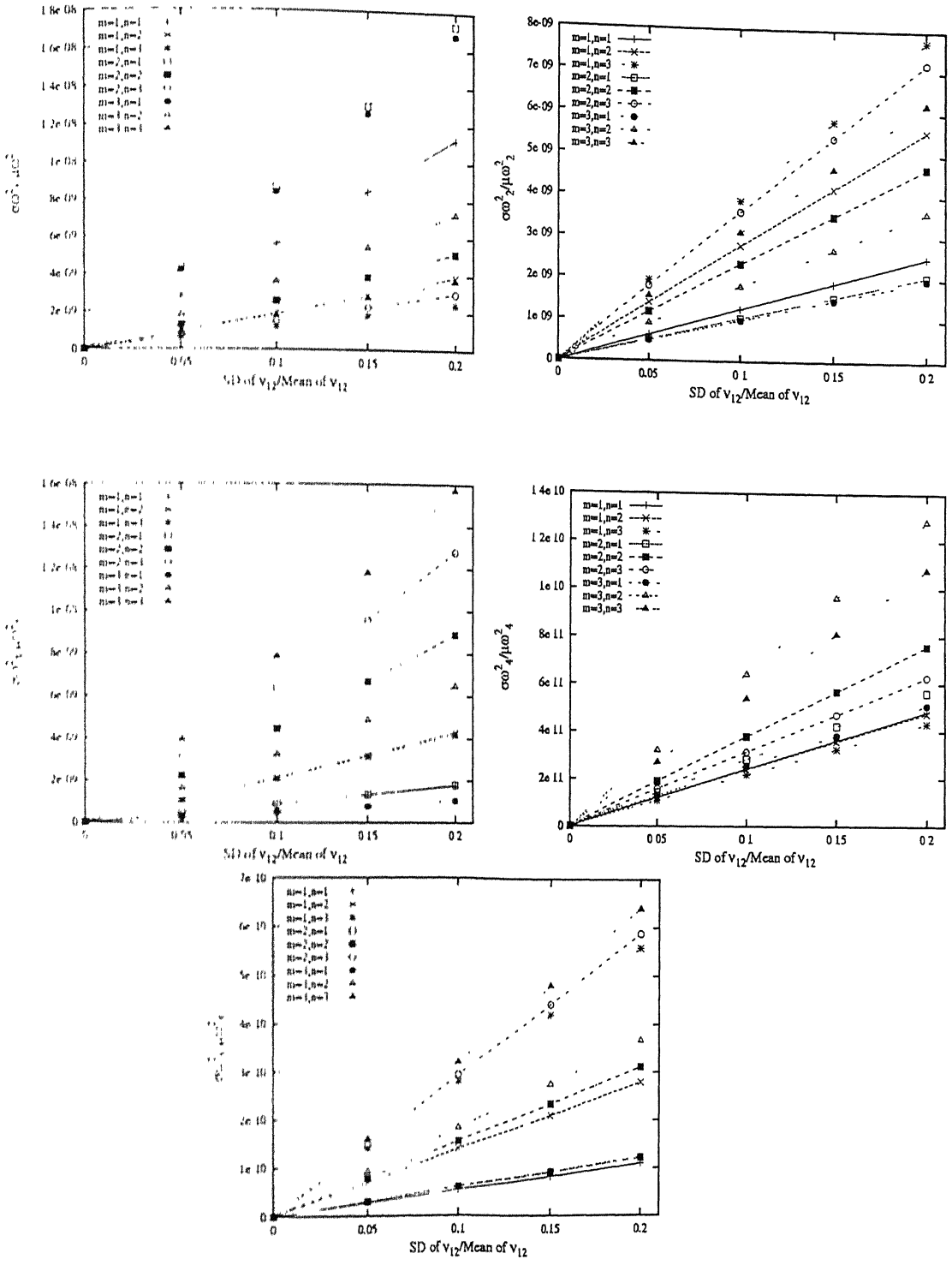

Figure 4.23: Variance of Natural Frequencies Vs SD of Input Random Variable ν_{12}

$0^o/90^o/90^o/0^o/H/0^o/90^o/90^o/0^o$ L/R=1.0, Thickness=0.3

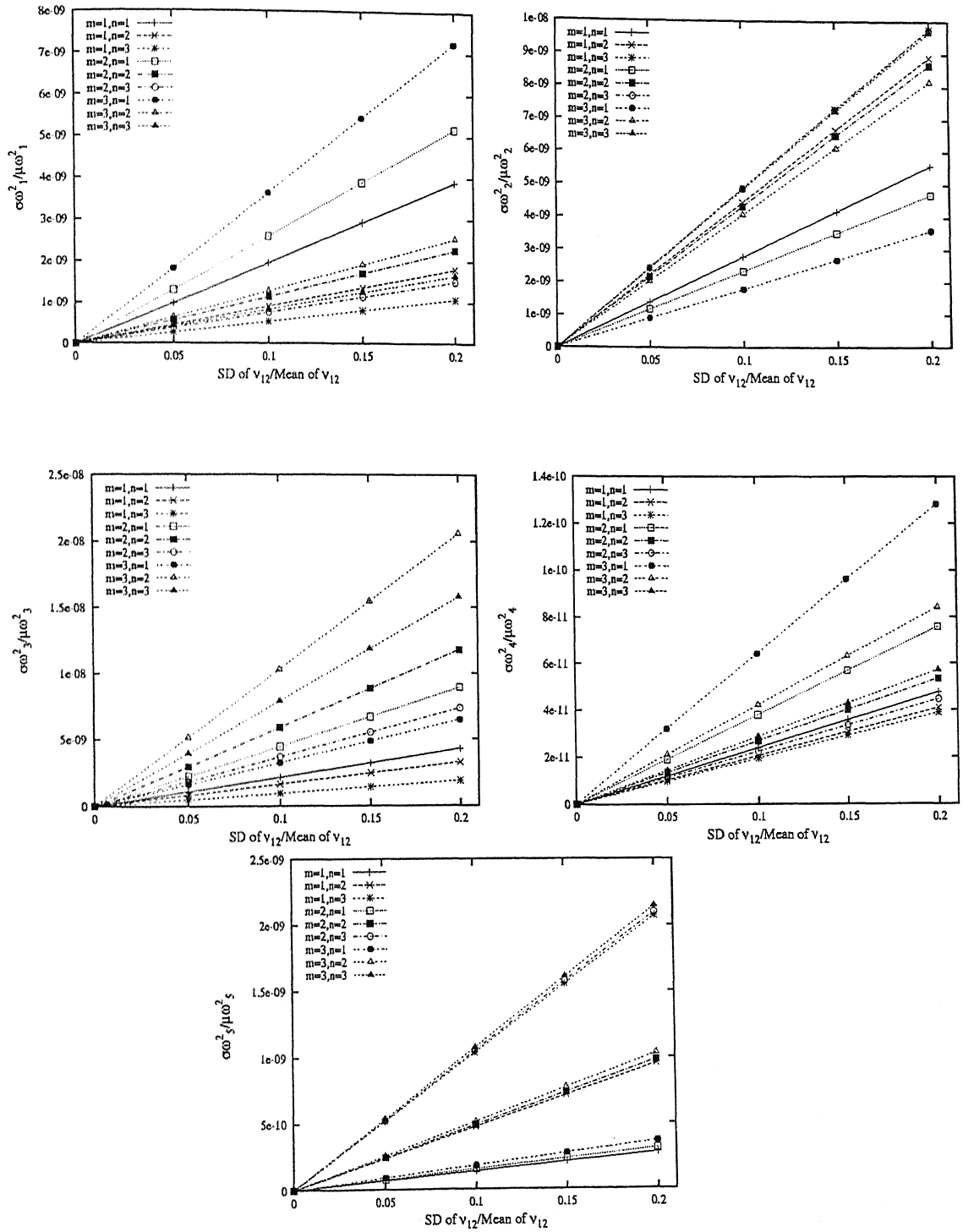

Figure 4.24: Variance of Natural Frequencies Vs SD of Input Random Variable ν_{12}

$0^o/90^o/90^o/0^o/H/0^o/90^o/90^o/0^o$ L/R=0.5, Thickness=0.3

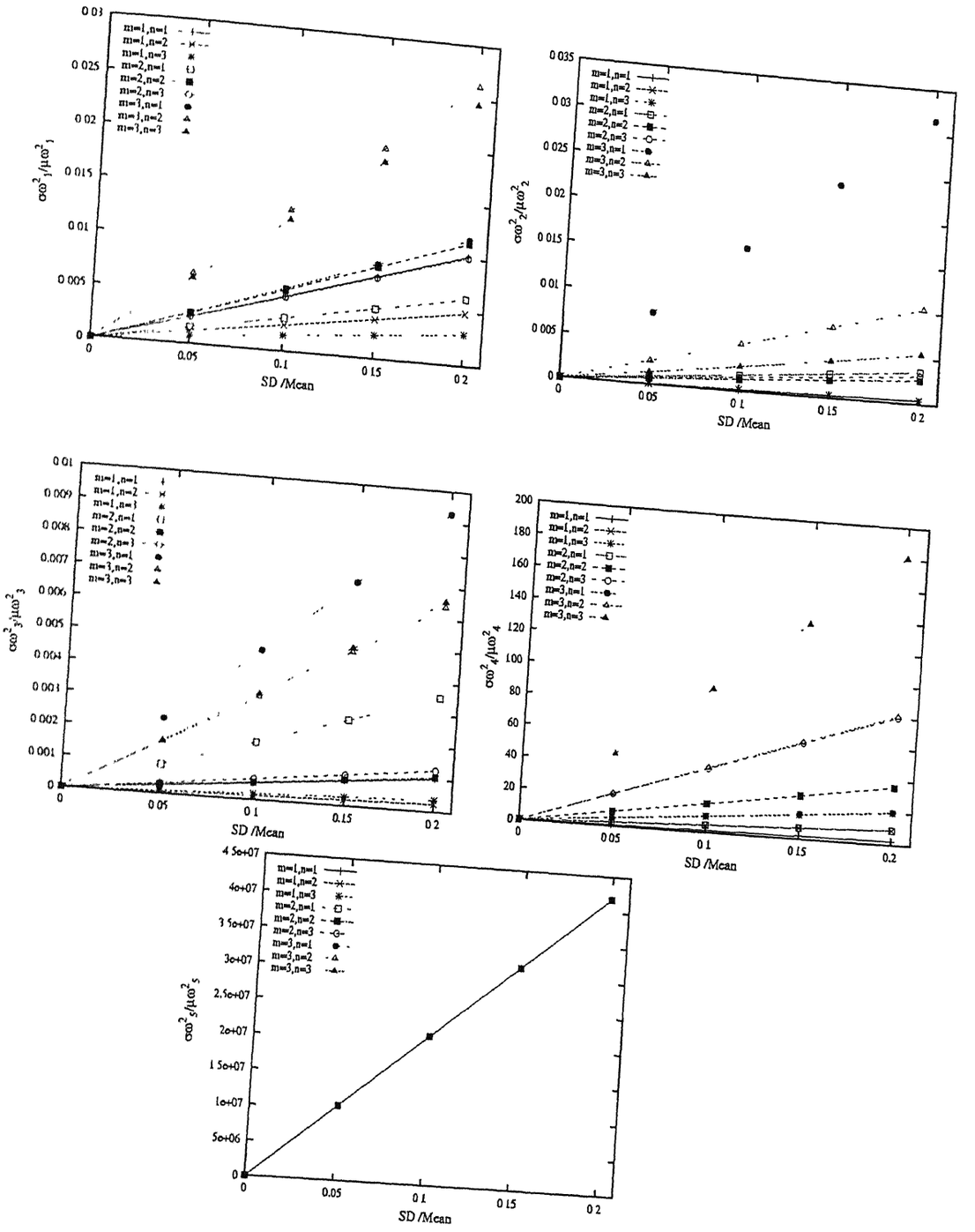

Figure 4.25: Variance of Natural Frequencies Vs SD all material properties $0^o/90^o/90^o/0^o/H/0^o/90^o/90^o/0^o$ L/R=1.5, Thickness=0.3

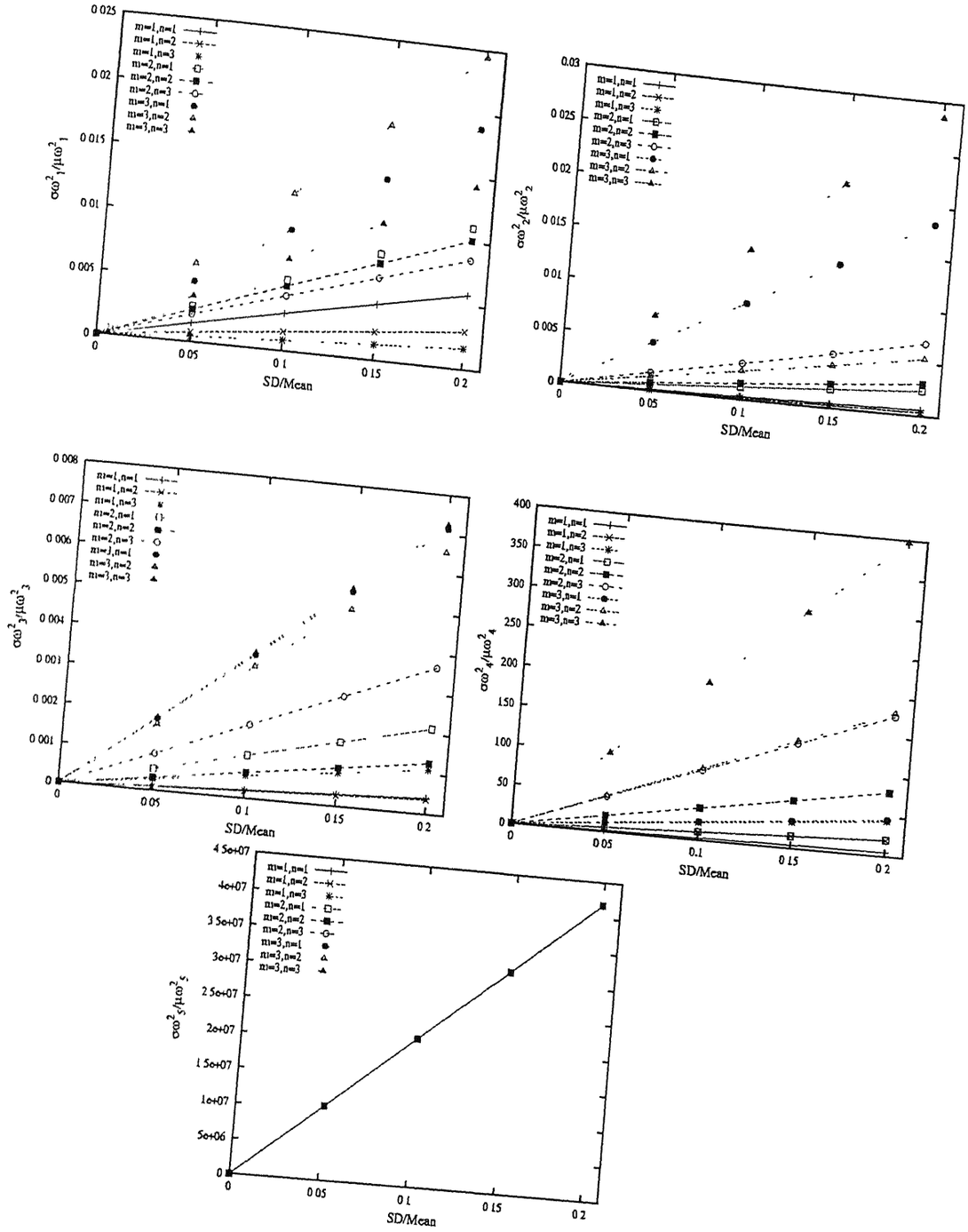

Figure 4.26: Variance of Natural Frequencies Vs SD all material properties $0^o/90^o/90^o/0^o/H/0^o/90^o/90^o/0^o$ L/R=1.0, Thickness=0.3

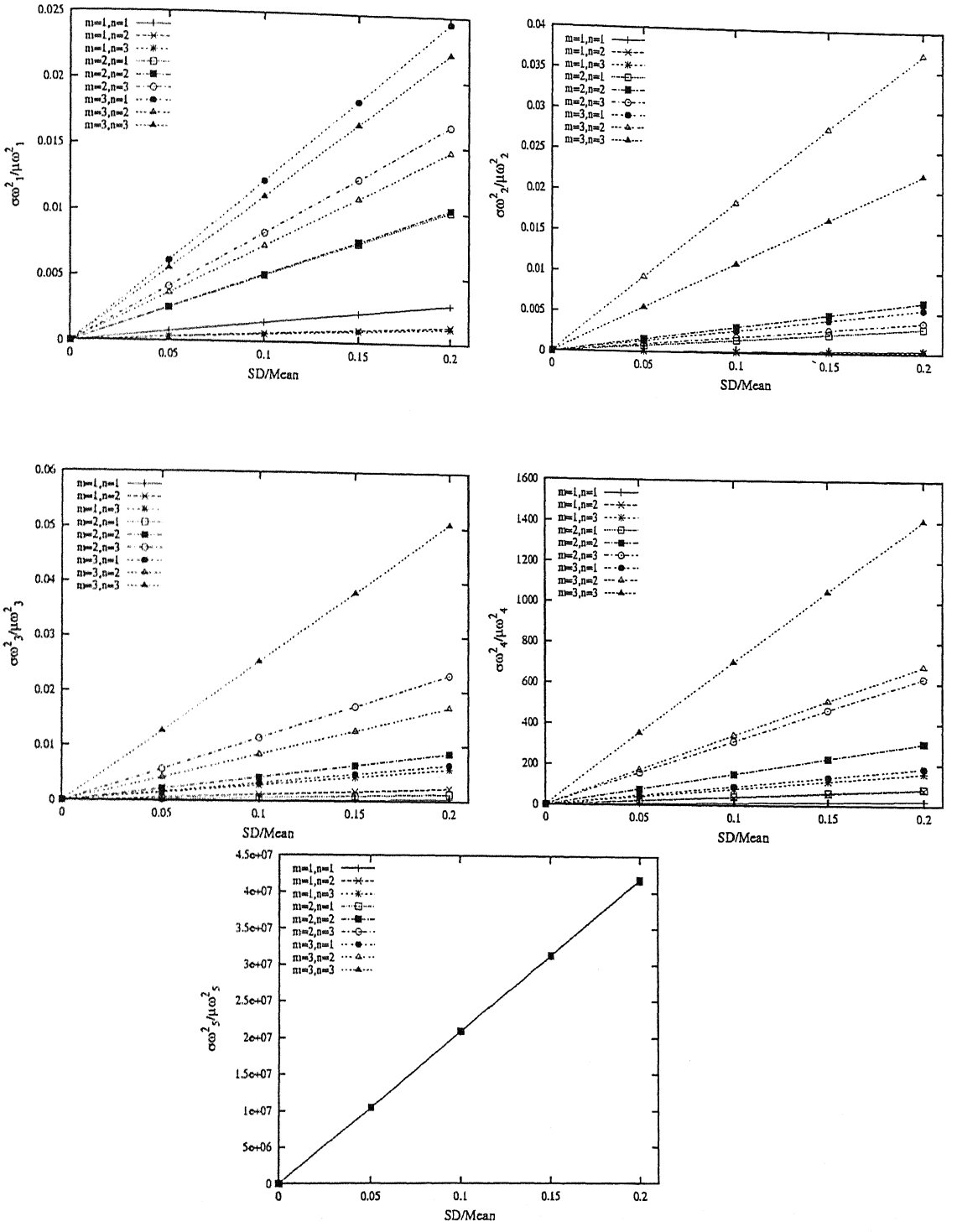

Figure 4.27: Variance of Natural Frequencies Vs SD all material properties

$0^o/90^o/90^o/0^o/H/0^o/90^o/90^o/0^o$ L/R=0.5, Thickness=0.3

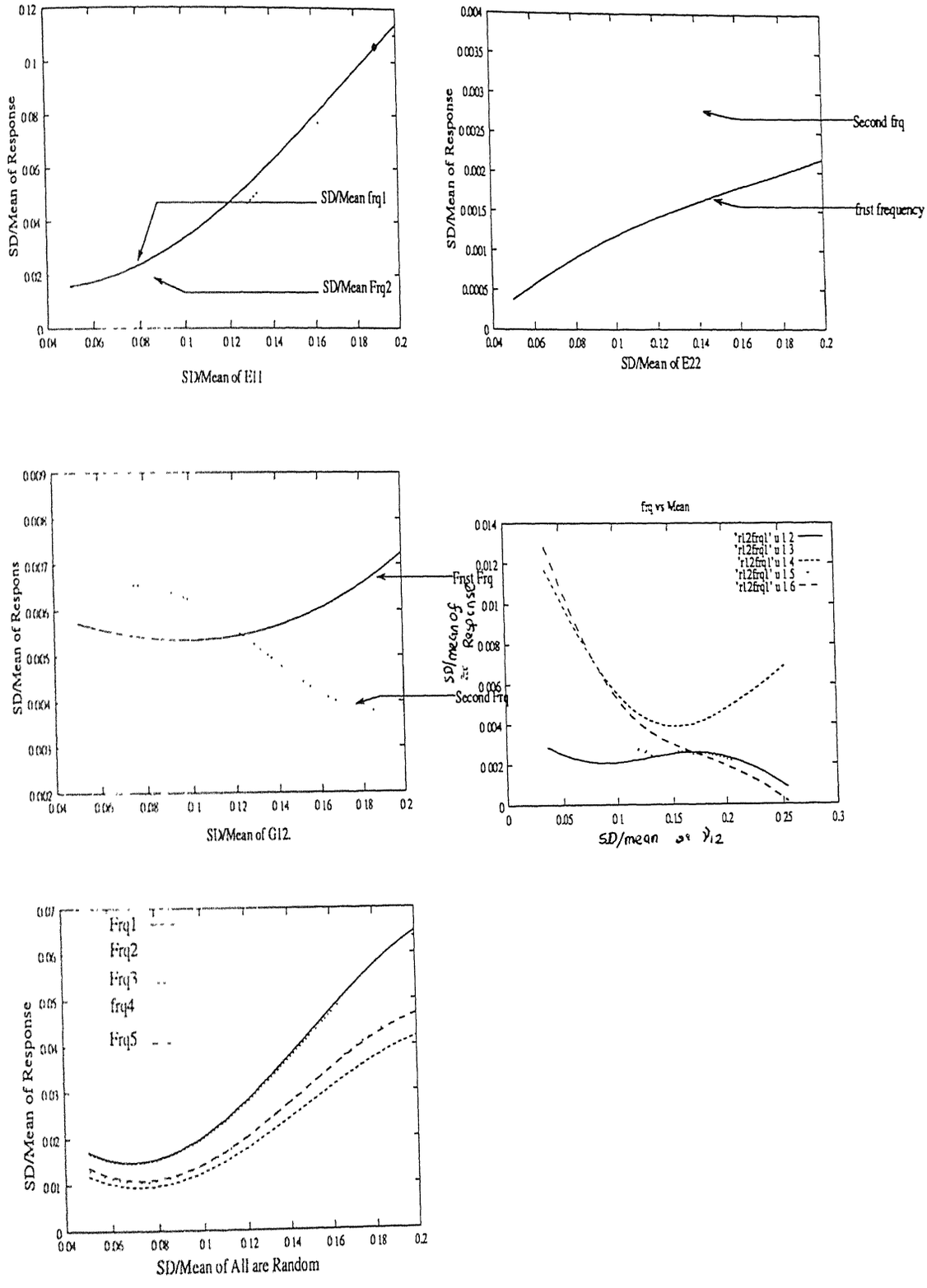

Figure 4.28: Natural Frequencies Vs Input Random Variable FEM Result

Chapter 5

Conclusion

The study analysis a honeycomb sandwich laminate composite cylinder. The honeycomb core is modified to an equivalent layer of uniform thickness homogeneous material. The material properties in the composite laminate as well as the core assumed to be random variables. Higher order shear effects have been included in the analysis. The laminate is processed for natural frequency by adopting a perturbation approach. The mean and various of the natural frequencies for different mode shapes have been evaluated. These are also evaluated by using Monte Carlo simulation with FEM. However the sample size generated could not be of representative size because of the large CPU time requirement.

The main conclusion reached on the basis of the above results are:

1. In general the first mode natural frequencies have the largest dispersion due to variation in the material properties.

2. Out of the facing layer material properties E_{22} has the largest effect of the natural frequency variance.

3. Amongst the material properties for the core E_s shows the largest effect on the natural frequencies.

4. The facing layer has a stronger effect on the cylinder natural frequencies than the core of the honey comb.

5. The material property ν_{12} for the facing layer has the smallest effect on the

natural frequencies. The sandwich cylinder shows low sensitivity to G_{23} and G_{31} also.

5.1 Suggestion for future work

The present study is limited to linear problem and use only first order perturbation. It would be interesting to study nonlinear large deflection problem with higher order perturbation procedure. The other related problem in the area are the study of the honeycomb sandwich cylinder. The study can continue to different types of cores with different thickness.

The FEM model attempted for the problem resulted in a very large size problem with large CPU time requirement. Some rethinking is required to have a smaller problem that can be economically handled.

Chapter 6

References

1. J.K. Paik, A.K. Thayamballi, G.S. Kim *"The sterngth characteristics of aluminum honeycomb sandwich panels"*, *Thin-walled Structures*, **35**(1999) pp. 205-231.

2. W. Becker, *"Closed-from analysis of thickness effect of regular honeycomb core material"*, *Composite Structures*, **48**(2000) pp. 67-70.

3. M.S. Hoo Fatt, K.S. Park, *"Perforation of honeycomb sandwich plates by projectiles"*, *Composites part A:applied science and manufacturing*, **Part A 31**(2000) pp. 889-899.

4. G.-Q. Li, *" Stress concentration and local behaviour of prestressed composite laminate/sandwich plates with overhangs in cylindrical bending"*, *Composite Structures*, **42**(1998) pp. 203-215.

5. D E. Glass, V.V. Raman, V.S. Venkat, S.N. Sankaran, *"Graphite/epoxy honeycomb core sandwich permeability under mechanical loads"*, *Composite Structures*, **44**(1999) pp. 253-261.

6. A. Petras, M.P.F. Sutcliffe, "Failure mode maps for honeycomb sandwich panels", *Composite Structures*, **44**(1999) pp. 237-252.

7. A. Muc, P. Zuchara, *"Buckling and failure analysis of FRP faced sandwich plates"*, *Composite Structures*, **48**(2000)pp. 145-150.

8. Y.B. Cho, R.C. Averill, *"First-order Zig-Zag sublaminate plate theory and finite element model for laminated composite and sandwich panels"*, *Composite Structures*, **50**(2000) pp. 1-15.

9. J.E. Shafizadeh, J.C. Seferis, *"Scaling of honeycomb compressive yeild stresses"*, *Composite part A:applied science and manufacturing*, **Part A 31**(2000) pp. 681-688.

10. X. Edward Guo, L.J. Gibson, *"Behavior of intact and damaged honeycombs: a finte element study"*, *International Journal of Mechanical Sciences*, **41**(1999) pp. 85-105.

11. W.S. Burton, A.K. Noor, *"Assessment of continum models for sandwich panel honeycomb cores"*, *Computer methods in applied Mechanics and engineering*, **145**(1997) pp. 341-360.

12. A.N. Palazotto, E.J. Herup, L.N.B. Gummadi, *"Finite element analysis of low-velocity impact on composite sandwich plates"*, *Composite Structures*, **49**(2000) pp. 209-227.

13. U.K. Vaidya, M.V. Hosur, D. Earl, S. Jeelani, *"Impact response of integrated hollow core sandwich composite panels"*, *Composite part A:applied science and manufacturing*, **Part A 31**(2000) pp. 761-772.

14. F. Meraghni, F. Desrumaux, M.L. Benzeggagh, *" Mechanical behaviour of cellur core for structural sandwich panels"*, *Composite part A:applied science and manufacturing*, **Part A 30**(1999) pp. 767-779.

15. I.M. Daniel, J.L. Abot, *"Fabrication, testing and analysis of composite sandwich beams"*, *Composite Science and Technology*, **60**(2000) pp. 2455-2463.

16. O.T. Thomsen, *"High-order theory for the analysis of multi-layer plate assemblies and its application for the analysis of sandwich panels with terminating plies"*, *Composite Structures*, **50**(2000) pp. 227-238.

17. B. Wang, M. Yang, *"Damping of honeycomb sanwich beams"*, *Journal of Meterials Processing Technology*, **105**(2000) pp. 67-72.

18. C. Chen, T.J. Lu, N.A. Fleck, *"Effect of inclusions and holes on the stiffness and strength of honeycombs"*, *International Journal of Mechanical Sciences*, **43**(2001) pp. 487 504.

19. J.N.Reddy, *"A simple higher order theory for laminated composite plates"*, *Transaction of the ASME, Journal of Applied Mechanics*, **51**(1984) pp. 745-752.

20. J.N.Reddy, C.F.Liu, *"A high-order shear deformation theory of laminated elastic shells"*, *International Journal of Engineering Science*, **23(3)**,(1985) pp. 319-330.

21. R.M.Jones, *"Mechanical of composite matrial"*, *Script*, **Washington DC, (1975).**

22. L.J.Gibson and M.F. Ashby, *"Cellular solids Structure & properties"*, **Pergamon press, (1988).**

Appendix A

A.1 Stiffness Matrix Coefficent

where $sin\omega t \quad sin\omega_{mn}t$

$$k_{11} = A_{11}\left\{\sum_{m=1}^{\infty}\sum_{n=1}^{\infty}\frac{m^2\pi^2}{a^2}U_{mn}cos\left(\frac{m\pi x}{a}\right)sin\left(\frac{n\pi y}{b}\right)sin\omega t\right\}$$

$$+ A_{16}\left\{\sum_{m=1}^{\infty}\sum_{n=1}^{\infty}\frac{mn\pi^2}{ab}U_{mn}sin\left(\frac{m\pi x}{a}\right)cos\left(\frac{n\pi y}{b}\right)sin\omega t\right\}$$

$$+ A_{61}\left\{\sum_{m=1}^{\infty}\sum_{n=1}^{\infty}\frac{mn\pi^2}{ab}U_{mn}sin\left(\frac{m\pi x}{a}\right)cos\left(\frac{n\pi y}{b}\right)sin\omega t\right\}$$

$$+ A_{66}\left\{\sum_{m=1}^{\infty}\sum_{n=1}^{\infty}\frac{n^2\pi^2}{b^2}U_{mn}cos\left(\frac{m\pi x}{a}\right)sin\left(\frac{n\pi y}{b}\right)sin\omega t\right\}$$

$$k_{12} = A_{12}\left\{\sum_{m=1}^{\infty}\sum_{n=1}^{\infty}\frac{mn\pi^2}{ab}V_{mn}cos\left(\frac{m\pi x}{a}\right)sin\left(\frac{n\pi y}{b}\right)sin\omega t\right\}$$

$$+ A_{16}\left\{\sum_{m=1}^{\infty}\sum_{n=1}^{\infty}\frac{m^2\pi^2}{a^2}V_{mn}sin\left(\frac{m\pi x}{a}\right)cos\left(\frac{n\pi y}{b}\right)sin\omega t\right\}$$

$$+ A_{62}\left\{\sum_{m=1}^{\infty}\sum_{n=1}^{\infty}\frac{n^2\pi^2}{b^2}V_{mn}sin\left(\frac{m\pi x}{a}\right)cos\left(\frac{n\pi y}{b}\right)sin\omega t\right\}$$

$$+ A_{66}\left\{\sum_{m=1}^{\infty}\sum_{n=1}^{\infty}\frac{mn\pi^2}{ab}V_{mn}cos\left(\frac{m\pi x}{a}\right)sin\left(\frac{n\pi y}{b}\right)sin\omega t\right\}$$

$$k_{13} = + \frac{A_{11}}{R_1}\left\{\sum_{m=1}^{\infty}\sum_{n=1}^{\infty}\frac{m\pi}{a}W_{mn}cos\left(\frac{m\pi x}{a}\right)sin\left(\frac{n\pi y}{b}\right)sin\omega t\right\}$$

$$+ \frac{A_{12}}{R_2}\left\{\sum_{m=1}^{\infty}\sum_{n=1}^{\infty}\frac{m\pi}{a}W_{mn}cos\left(\frac{m\pi x}{a}\right)sin\left(\frac{n\pi y}{b}\right)sin\omega t\right\}$$

$$+ \frac{A_{61}}{R_1}\left\{\sum_{m=1}^{\infty}\sum_{n=1}^{\infty}\frac{n\pi}{b}W_{mn}sin\left(\frac{m\pi x}{a}\right)cos\left(\frac{n\pi y}{b}\right)sin\omega t\right\}$$

$$+ \frac{A_{62}}{R_2}\left\{\sum_{m=1}^{\infty}\sum_{n=1}^{\infty}\frac{n\pi}{b}W_{mn}sin\left(\frac{m\pi x}{a}\right)cos\left(\frac{n\pi y}{b}\right)sin\omega t\right\}$$

$$+ \frac{4}{3h^2}E_{11}\left\{\sum_{m=1}^{\infty}\sum_{n=1}^{\infty}\frac{m^3\pi^3}{a^3}W_{mn}cos\left(\frac{m\pi x}{a}\right)sin\left(\frac{n\pi y}{b}\right)sin\omega t\right\}$$

$$+ \frac{4}{3h^2}E_{12}\left\{\sum_{m=1}^{\infty}\sum_{n=1}^{\infty}\frac{mn^2\pi^3}{ab^2}W_{mn}cos\left(\frac{m\pi x}{a}\right)sin\left(\frac{n\pi y}{b}\right)sin\omega t\right\}$$

$$+ \frac{4}{3h^2}E_{16}\left\{2\sum_{m=1}^{\infty}\sum_{n=1}^{\infty}\frac{m^2n\pi^3}{a^2b}W_{mn}sin\left(\frac{m\pi x}{a}\right)cos\left(\frac{n\pi y}{b}\right)sin\omega t\right\}$$

$$+ \frac{4}{3h^2}E_{61}\left\{\sum_{m=1}^{\infty}\sum_{n=1}^{\infty}\frac{m^2n\pi^3}{a^2b}W_{mn}sin\left(\frac{m\pi x}{a}\right)cos\left(\frac{n\pi y}{b}\right)sin\omega t\right\}$$

$$+ \frac{4}{3h^2}E_{62}\left\{\sum_{m=1}^{\infty}\sum_{n=1}^{\infty}\frac{n^3\pi^3}{b^3}W_{mn}sin\left(\frac{m\pi x}{a}\right)cos\left(\frac{n\pi y}{b}\right)sin\omega t\right\}$$

$$+ \frac{4}{3h^2}E_{66}\left\{2\sum_{m=1}^{\infty}\sum_{n=1}^{\infty}\frac{mn^2\pi^3}{ab^2}W_{mn}cos\left(\frac{m\pi x}{a}\right)sin\left(\frac{n\pi y}{b}\right)sin\omega t\right\}$$

$$k_{14} = -B_{11}\left\{\sum_{m=1}^{\infty}\sum_{n=1}^{\infty}\frac{m^2\pi^2}{a^2}\psi^1_{mn}cos\left(\frac{m\pi x}{a}\right)sin\left(\frac{n\pi y}{b}\right)sin\omega t\right\}$$

$$- B_{16}\left\{\sum_{m=1}^{\infty}\sum_{n=1}^{\infty}\frac{mn\pi^2}{ab}\psi^1_{mn}sin\left(\frac{m\pi x}{a}\right)cos\left(\frac{n\pi y}{b}\right)sin\omega t\right\}$$

$$- B_{61}\left\{\sum_{m=1}^{\infty}\sum_{n=1}^{\infty}\frac{mn\pi^2}{ab}\psi^1_{mn}sin\left(\frac{m\pi x}{a}\right)cos\left(\frac{n\pi y}{b}\right)sin\omega t\right\}$$

$$- B_{66}\left\{\sum_{m=1}^{\infty}\sum_{n=1}^{\infty}\frac{n^2\pi^2}{b^2}\psi^1_{mn}cos\left(\frac{m\pi x}{a}\right)sin\left(\frac{n\pi y}{b}\right)sin\omega t\right\}$$

$$+\frac{4}{3h^2}E_{11}\left\{\sum_{m=1}^{\infty}\sum_{n=1}^{\infty}\frac{m^2\pi^2}{a^2}\psi^1_{mn}cos\left(\frac{m\pi x}{a}\right)sin\left(\frac{n\pi y}{b}\right)sin\omega t\right\}$$

$$+\frac{4}{3h^2}E_{16}\left\{\sum_{m=1}^{\infty}\sum_{n=1}^{\infty}\frac{mn\pi^2}{ab}\psi^1_{mn}sin\left(\frac{m\pi x}{a}\right)cos\left(\frac{n\pi y}{b}\right)sin\omega t\right\}$$

$$+\frac{4}{3h^2}E_{61}\left\{\sum_{m=1}^{\infty}\sum_{n=1}^{\infty}\frac{mn\pi^2}{ab}\psi^1_{mn}sin\left(\frac{m\pi x}{a}\right)cos\left(\frac{n\pi y}{b}\right)sin\omega t\right\}$$

$$+\frac{4}{3h^2}E_{66}\left\{\sum_{m=1}^{\infty}\sum_{n=1}^{\infty}\frac{n^2\pi^2}{b^2}\psi^1_{mn}cos\left(\frac{m\pi x}{a}\right)sin\left(\frac{n\pi y}{b}\right)sin\omega t\right\}$$

$$K_{15}\cdot \quad B_{12}\left\{\sum_{m=1}^{\infty}\sum_{n=1}^{\infty}\frac{mn\pi^2}{ab}\psi^2_{mn}cos\left(\frac{m\pi x}{a}\right)sin\left(\frac{n\pi y}{b}\right)sin\omega t\right\}$$

$$B_{16}\left\{\sum_{m=1}^{\infty}\sum_{n=1}^{\infty}\frac{m^2\pi^2}{a^2}\psi^2_{mn}sin\left(\frac{m\pi x}{a}\right)cos\left(\frac{n\pi y}{b}\right)sin\omega t\right\}$$

$$B_{62}\left\{\sum_{m=1}^{\infty}\sum_{n=1}^{\infty}\frac{n^2\pi^2}{b^2}\psi^2_{mn}sin\left(\frac{m\pi x}{a}\right)cos\left(\frac{n\pi y}{b}\right)sin\omega t\right\}$$

$$- B_{66}\left\{\sum_{m=1}^{\infty}\sum_{n=1}^{\infty}\frac{mn\pi^2}{ab}\psi^2_{mn}cos\left(\frac{m\pi x}{a}\right)sin\left(\frac{n\pi y}{b}\right)sin\omega t\right\}$$

$$+\frac{4}{3h^2}E_{12}\left\{\sum_{m=1}^{\infty}\sum_{n=1}^{\infty}\frac{mn\pi^2}{ab}\psi^2_{mn}cos\left(\frac{m\pi x}{a}\right)sin\left(\frac{n\pi y}{b}\right)sin\omega t\right\}$$

$$+\frac{4}{3h^2}E_{16}\left\{\sum_{m=1}^{\infty}\sum_{n=1}^{\infty}\frac{m^2\pi^2}{a^2}\psi^2_{mn}sin\left(\frac{m\pi x}{a}\right)cos\left(\frac{n\pi y}{b}\right)sin\omega t\right\}$$

$$+\frac{4}{3h^2}E_{62}\left\{\sum_{m=1}^{\infty}\sum_{n=1}^{\infty}\frac{n^2\pi^2}{b^2}\psi^2_{mn}sin\left(\frac{m\pi x}{a}\right)cos\left(\frac{n\pi y}{b}\right)sin\omega t\right\}$$

$$+\frac{4}{3h^2}E_{66}\left\{\sum_{m=1}^{\infty}\sum_{n=1}^{\infty}\frac{mn\pi^2}{ab}\psi^2_{mn}cos\left(\frac{m\pi x}{a}\right)sin\left(\frac{n\pi y}{b}\right)sin\omega t\right\}$$

$$+\frac{4}{3h^2}E_{22}\left\{\sum_{m=1}^{\infty}\sum_{n=1}^{\infty}\frac{n^3\pi^3}{b^3}W_{mn}sin\left(\frac{m\pi x}{a}\right)cos\left(\frac{n\pi y}{b}\right)sin\omega t\right\}$$

$$+\frac{4}{3h^2}E_{26}\left\{2\sum_{m=1}^{\infty}\sum_{n=1}^{\infty}\frac{mn^2\pi^3}{ab^2}W_{mn}cos\left(\frac{m\pi x}{a}\right)sin\left(\frac{n\pi y}{b}\right)sin\omega t\right\}$$

$$+\frac{4}{3h^2}E_{61}\left\{\sum_{m=1}^{\infty}\sum_{n=1}^{\infty}\frac{m^3\pi^3}{a^3}W_{mn}cos\left(\frac{m\pi x}{a}\right)sin\left(\frac{n\pi y}{b}\right)sin\omega t\right\}$$

$$+\frac{4}{3h^2}E_{62}\left\{\sum_{m=1}^{\infty}\sum_{n=1}^{\infty}\frac{mn^2\pi^3}{ab^2}W_{mn}cos\left(\frac{m\pi x}{a}\right)sin\left(\frac{n\pi y}{b}\right)sin\omega t\right\}$$

$$+\frac{4}{3h^2}E_{66}\left\{2\sum_{m=1}^{\infty}\sum_{n=1}^{\infty}\frac{m^2n\pi^3}{a^2b}W_{mn}sin\left(\frac{m\pi x}{a}\right)cos\left(\frac{n\pi y}{b}\right)sin\omega t\right\}$$

$$k_{24}\quad B_{21}\left\{\sum_{m=1}^{\infty}\sum_{n=1}^{\infty}\frac{mn\pi^2}{ab}\psi^1_{mn}sin\left(\frac{m\pi x}{a}\right)cos\left(\frac{n\pi y}{b}\right)sin\omega t\right\}$$

$$-B_{26}\left\{\sum_{m=1}^{\infty}\sum_{n=1}^{\infty}\frac{n^2\pi^2}{b^2}\psi^1_{mn}cos\left(\frac{m\pi x}{a}\right)sin\left(\frac{n\pi y}{b}\right)sin\omega t\right\}$$

$$-B_{61}\left\{\sum_{m=1}^{\infty}\sum_{n=1}^{\infty}\frac{m^2\pi^2}{a^2}\psi^1_{mn}cos\left(\frac{m\pi x}{a}\right)sin\left(\frac{n\pi y}{b}\right)sin\omega t\right\}$$

$$-B_{66}\left\{\sum_{m=1}^{\infty}\sum_{n=1}^{\infty}\frac{mn\pi^2}{ab}\psi^1_{mn}sin\left(\frac{m\pi x}{a}\right)cos\left(\frac{n\pi y}{b}\right)sin\omega t\right\}$$

$$+\frac{4}{3h^2}E_{21}\left\{\sum_{m=1}^{\infty}\sum_{n=1}^{\infty}\frac{mn\pi^2}{ab}\psi^1_{mn}sin\left(\frac{m\pi x}{a}\right)cos\left(\frac{n\pi y}{b}\right)sin\omega t\right\}$$

$$+\frac{4}{3h^2}E_{26}\left\{\sum_{m=1}^{\infty}\sum_{n=1}^{\infty}\frac{n^2\pi^2}{b^2}\psi^1_{mn}cos\left(\frac{m\pi x}{a}\right)sin\left(\frac{n\pi y}{b}\right)sin\omega t\right\}$$

$$+\frac{4}{3h^2}E_{61}\left\{\sum_{m=1}^{\infty}\sum_{n=1}^{\infty}\frac{m^2\pi^2}{a^2}\psi^1_{mn}cos\left(\frac{m\pi x}{a}\right)sin\left(\frac{n\pi y}{b}\right)sin\omega t\right\}$$

$$+\frac{4}{3h^2}E_{66}\left\{\sum_{m=1}^{\infty}\sum_{n=1}^{\infty}\frac{mn\pi^2}{ab}\psi^1_{mn}sin\left(\frac{m\pi x}{a}\right)cos\left(\frac{n\pi y}{b}\right)sin\omega t\right\}$$

k_{25} $$B_{22}\left\{\sum_{m=1}^{\infty}\sum_{n=1}^{\infty}\frac{n^2\pi^2}{b^2}\psi_{mn}^2 sin\left(\frac{m\pi x}{a}\right)cos\left(\frac{n\pi y}{b}\right)sin\omega t\right\}$$

$$B_{26}\left\{\sum_{m=1}^{\infty}\sum_{n=1}^{\infty}\frac{mn\pi^2}{ab}\psi_{mn}^2 cos\left(\frac{m\pi x}{a}\right)sin\left(\frac{n\pi y}{b}\right)sin\omega t\right\}$$

$$B_{62}\left\{\sum_{m=1}^{\infty}\sum_{n=1}^{\infty}\frac{mn\pi^2}{ab}\psi_{mn}^2 cos\left(\frac{m\pi x}{a}\right)sin\left(\frac{n\pi y}{b}\right)sin\omega t\right\}$$

$$B_{66}\left\{\sum_{m=1}^{\infty}\sum_{n=1}^{\infty}\frac{m^2\pi^2}{a^2}\psi_{mn}^2 sin\left(\frac{m\pi x}{a}\right)cos\left(\frac{n\pi y}{b}\right)sin\omega t\right\}$$

$$+\frac{4}{3h^2}E_{22}\left\{\sum_{m=1}^{\infty}\sum_{n=1}^{\infty}\frac{n^2\pi^2}{b^2}\psi_{mn}^2 sin\left(\frac{m\pi x}{a}\right)cos\left(\frac{n\pi y}{b}\right)sin\omega t\right\}$$

$$+\frac{4}{3h^2}E_{26}\left\{\sum_{m=1}^{\infty}\sum_{n=1}^{\infty}\frac{mn\pi^2}{ab}\psi_{mn}^2 cos\left(\frac{m\pi x}{a}\right)sin\left(\frac{n\pi y}{b}\right)sin\omega t\right\}$$

$$+\frac{4}{3h^2}E_{62}\left\{\sum_{m=1}^{\infty}\sum_{n=1}^{\infty}\frac{mn\pi^2}{ab}\psi_{mn}^2 cos\left(\frac{m\pi x}{a}\right)sin\left(\frac{n\pi y}{b}\right)sin\omega t\right\}$$

$$+\frac{4}{3h^2}E_{66}\left\{\sum_{m=1}^{\infty}\sum_{n=1}^{\infty}\frac{m^2\pi^2}{a^2}\psi_{mn}^2 sin\left(\frac{m\pi x}{a}\right)cos\left(\frac{n\pi y}{b}\right)sin\omega t\right\}$$

k_{31} $$+\frac{A_{11}}{R_1}\left\{\sum_{m=1}^{\infty}\sum_{n=1}^{\infty}\frac{m\pi}{a}U_{mn}sin\left(\frac{m\pi x}{a}\right)sin\left(\frac{n\pi y}{b}\right)sin\omega t\right\}$$

$$-\frac{A_{16}}{R_1}\left\{\sum_{m=1}^{\infty}\sum_{n=1}^{\infty}\frac{n\pi}{b}U_{mn}cos\left(\frac{m\pi x}{a}\right)cos\left(\frac{n\pi y}{b}\right)sin\omega t\right\}$$

$$+\frac{A_{21}}{R_2}\left\{\sum_{m=1}^{\infty}\sum_{n=1}^{\infty}\frac{m\pi}{a}U_{mn}sin\left(\frac{m\pi x}{a}\right)sin\left(\frac{n\pi y}{b}\right)sin\omega t\right\}$$

$$-\frac{A_{26}}{R_2}\left\{\sum_{m=1}^{\infty}\sum_{n=1}^{\infty}\frac{n\pi}{b}U_{mn}cos\left(\frac{m\pi x}{a}\right)cos\left(\frac{n\pi y}{b}\right)sin\omega t\right\}$$

$$+\frac{4}{3h^2}E_{11}\left\{\sum_{m=1}^{\infty}\sum_{n=1}^{\infty}\frac{m^3\pi^3}{a^3}U_{mn}sin\left(\frac{m\pi x}{a}\right)sin\left(\frac{n\pi y}{b}\right)sin\omega t\right\}$$

$$\frac{4}{3h^2}E_{16}\left\{\sum_{m=1}^{\infty}\sum_{n=1}^{\infty}\frac{m^2n\pi^3}{a^2b}U_{mn}cos\left(\frac{m\pi x}{a}\right)cos\left(\frac{n\pi y}{b}\right)sin\omega t\right\}$$

$$+\frac{4}{3h^2}E_{21}\left\{\sum_{m=1}^{\infty}\sum_{n=1}^{\infty}\frac{mn^2\pi^3}{ab^2}U_{mn}sin\left(\frac{m\pi x}{a}\right)sin\left(\frac{n\pi y}{b}\right)sin\omega t\right\}$$

$$\frac{4}{3h^2}E_{26}\left\{\sum_{m=1}^{\infty}\sum_{n=1}^{\infty}\frac{n^3\pi^3}{b^3}U_{mn}cos\left(\frac{m\pi x}{a}\right)cos\left(\frac{n\pi y}{b}\right)sin\omega t\right\}$$

$$\frac{4}{3h^2}E_{61}\left\{\sum_{m=1}^{\infty}\sum_{n=1}^{\infty}\frac{m^2n\pi^3}{a^2b}U_{mn}cos\left(\frac{m\pi x}{a}\right)cos\left(\frac{n\pi y}{b}\right)sin\omega t\right\}$$

$$+\frac{4}{3h^2}E_{66}\left\{2\sum_{m=1}^{\infty}\sum_{n=1}^{\infty}\frac{mn^2\pi^3}{ab^2}U_{mn}sin\left(\frac{m\pi x}{a}\right)sin\left(\frac{n\pi y}{b}\right)sin\omega t\right\}$$

$$K_{32}\quad+\frac{A_{12}}{R_1}\left\{\sum_{m=1}^{\infty}\sum_{n=1}^{\infty}\frac{n\pi}{b}V_{mn}sin\left(\frac{m\pi x}{a}\right)sin\left(\frac{n\pi y}{b}\right)sin\omega t\right\}$$

$$\frac{A_{16}}{R_1}\left\{\sum_{m=1}^{\infty}\sum_{n=1}^{\infty}\frac{m\pi}{a}V_{mn}cos\left(\frac{m\pi x}{a}\right)cos\left(\frac{n\pi y}{b}\right)sin\omega t\right\}$$

$$+\frac{A_{22}}{R_2}\left\{\sum_{m=1}^{\infty}\sum_{n=1}^{\infty}\frac{n\pi}{b}V_{mn}sin\left(\frac{m\pi x}{a}\right)sin\left(\frac{n\pi y}{b}\right)sin\omega t\right\}$$

$$\frac{A_{26}}{R_2}\left\{\sum_{m=1}^{\infty}\sum_{n=1}^{\infty}\frac{m\pi}{a}V_{mn}cos\left(\frac{m\pi x}{a}\right)cos\left(\frac{n\pi y}{b}\right)sin\omega t\right\}$$

$$+\frac{4}{3h^2}E_{12}\left\{\sum_{m=1}^{\infty}\sum_{n=1}^{\infty}\frac{m^2n\pi^3}{a^2b}V_{mn}sin\left(\frac{m\pi x}{a}\right)sin\left(\frac{n\pi y}{b}\right)sin\omega t\right\}$$

$$\frac{4}{3h^2}E_{16}\left\{\sum_{m=1}^{\infty}\sum_{n=1}^{\infty}\frac{m^3\pi^3}{a^3}V_{mn}cos\left(\frac{m\pi x}{a}\right)cos\left(\frac{n\pi y}{b}\right)sin\omega t\right\}$$

$$+\frac{4}{3h^2}E_{22}\left\{\sum_{m=1}^{\infty}\sum_{n=1}^{\infty}\frac{n^3\pi^3}{b^3}V_{mn}sin\left(\frac{m\pi x}{a}\right)sin\left(\frac{n\pi y}{b}\right)sin\omega t\right\}$$

$$\frac{4}{3h^2}E_{26}\left\{\sum_{m=1}^{\infty}\sum_{n=1}^{\infty}\frac{mn^2\pi^3}{ab^2}V_{mn}cos\left(\frac{m\pi x}{a}\right)cos\left(\frac{n\pi y}{b}\right)sin\omega t\right\}$$

$$\frac{4}{3h^2}E_{62}\left\{\sum_{m=1}^{\infty}\sum_{n=1}^{\infty}\frac{mn^2\pi^3}{ab^2}V_{mn}cos\left(\frac{m\pi x}{a}\right)cos\left(\frac{n\pi y}{b}\right)sin\omega t\right\}$$

$$+\frac{4}{3h^2}E_{66}\left\{2\sum_{m=1}^{\infty}\sum_{n=1}^{\infty}\frac{m^2n\pi^3}{a^2b}V_{mn}sin\left(\frac{m\pi x}{a}\right)sin\left(\frac{n\pi y}{b}\right)sin\omega t\right\}$$

$$k_{33}\quad\frac{A_{11}}{R_1^2}\left\{\sum_{m=1}^{\infty}\sum_{n=1}^{\infty}W_{mn}sin\left(\frac{m\pi x}{a}\right)sin\left(\frac{n\pi y}{b}\right)sin\omega t\right\}$$

$$\frac{A_{12}}{R_1R_2}\left\{\sum_{m=1}^{\infty}\sum_{n=1}^{\infty}W_{mn}sin\left(\frac{m\pi x}{a}\right)sin\left(\frac{n\pi y}{b}\right)sin\omega t\right\}$$

$$\frac{A_{21}}{R_1R_2}\left\{\sum_{m=1}^{\infty}\sum_{n=1}^{\infty}W_{mn}sin\left(\frac{m\pi x}{a}\right)sin\left(\frac{n\pi y}{b}\right)sin\omega t\right\}$$

$$\frac{A_{22}}{R_2^2}\left\{\sum_{m=1}^{\infty}\sum_{n=1}^{\infty}W_{mn}sin\left(\frac{m\pi x}{a}\right)sin\left(\frac{n\pi y}{b}\right)sin\omega t\right\}$$

$$+A_{54}\left\{\sum_{m=1}^{\infty}\sum_{n=1}^{\infty}\frac{mn\pi^2}{ab}W_{mn}cos\left(\frac{m\pi x}{a}\right)cos\left(\frac{n\pi y}{b}\right)sin\omega t\right\}$$

$$A_{55}\left\{\sum_{m=1}^{\infty}\sum_{n=1}^{\infty}\frac{m^2\pi^2}{a^2}W_{mn}sin\left(\frac{m\pi x}{a}\right)sin\left(\frac{n\pi y}{b}\right)sin\omega t\right\}$$

$$A_{11}\left\{\sum_{m=1}^{\infty}\sum_{n=1}^{\infty}\frac{n^2\pi^2}{b^2}W_{mn}sin\left(\frac{m\pi x}{a}\right)sin\left(\frac{n\pi y}{b}\right)sin\omega t\right\}$$

$$+A_{45}\left\{\sum_{m=1}^{\infty}\sum_{n=1}^{\infty}\frac{mn\pi^2}{ab}W_{mn}cos\left(\frac{m\pi x}{a}\right)cos\left(\frac{n\pi y}{b}\right)sin\omega t\right\}$$

$$\frac{4}{h^2}D_{51}\left\{2\sum_{m=1}^{\infty}\sum_{n=1}^{\infty}\frac{mn\pi^2}{ab}W_{mn}cos\left(\frac{m\pi x}{a}\right)cos\left(\frac{n\pi y}{b}\right)sin\omega t\right\}$$

$$+\frac{4}{h^2}D_{55}\left\{2\sum_{m=1}^{\infty}\sum_{n=1}^{\infty}\frac{m^2\pi^2}{a^2}W_{mn}sin\left(\frac{m\pi x}{a}\right)sin\left(\frac{n\pi y}{b}\right)sin\omega t\right\}$$

$$+\frac{4}{h^2}D_{44}\left\{2\sum_{m=1}^{\infty}\sum_{n=1}^{\infty}\frac{n^2\pi^2}{b^2}W_{mn}sin\left(\frac{m\pi x}{a}\right)sin\left(\frac{n\pi y}{b}\right)sin\omega t\right\}$$

$$\frac{4}{h^2} D_{45} \left\{ 2 \sum_{m=1}^{\infty} \sum_{n=1}^{\infty} \frac{mn\pi^2}{ab} W_{mn} cos\left(\frac{m\pi x}{a}\right) cos\left(\frac{n\pi y}{b}\right) sin\omega t \right\}$$

$$\frac{4}{3h^2 R_1} E_{11} \left\{ 2 \sum_{m=1}^{\infty} \sum_{n=1}^{\infty} \frac{m^2\pi^2}{a^2} W_{mn} sin\left(\frac{m\pi x}{a}\right) sin\left(\frac{n\pi y}{b}\right) sin\omega t \right\}$$

$$\frac{4}{3h^2 R_1} E_{12} \left\{ 2 \sum_{m=1}^{\infty} \sum_{n=1}^{\infty} \frac{n^2\pi^2}{b^2} W_{mn} sin\left(\frac{m\pi x}{a}\right) sin\left(\frac{n\pi y}{b}\right) sin\omega t \right\}$$

$$\frac{4}{3h^2 R_2} E_{21} \left\{ 2 \sum_{m=1}^{\infty} \sum_{n=1}^{\infty} \frac{m^2\pi^2}{a^2} W_{mn} sin\left(\frac{m\pi x}{a}\right) sin\left(\frac{n\pi y}{b}\right) sin\omega t \right\}$$

$$\frac{4}{3h^2 R_2} E_{22} \left\{ 2 \sum_{m=1}^{\infty} \sum_{n=1}^{\infty} \frac{n^2\pi^2}{b^2} W_{mn} sin\left(\frac{m\pi x}{a}\right) sin\left(\frac{n\pi y}{b}\right) sin\omega t \right\}$$

$$+ \frac{4}{3h^2 R_1} E_{16} \left\{ 2 \sum_{m=1}^{\infty} \sum_{n=1}^{\infty} \frac{mn\pi^2}{ab} W_{mn} cos\left(\frac{m\pi x}{a}\right) cos\left(\frac{n\pi y}{b}\right) sin\omega t \right\}$$

$$+ \frac{4}{3h^2 R_2} E_{26} \left\{ 2 \sum_{m=1}^{\infty} \sum_{n=1}^{\infty} \frac{mn\pi^2}{ab} W_{mn} cos\left(\frac{m\pi x}{a}\right) cos\left(\frac{n\pi y}{b}\right) sin\omega t \right\}$$

$$+ \frac{4}{3h^2 R_1} E_{61} \left\{ 2 \sum_{m=1}^{\infty} \sum_{n=1}^{\infty} \frac{mn\pi^2}{ab} W_{mn} cos\left(\frac{m\pi x}{a}\right) cos\left(\frac{n\pi y}{b}\right) sin\omega t \right\}$$

$$+ \frac{4}{3h^2 R_2} E_{62} \left\{ 2 \sum_{m=1}^{\infty} \sum_{n=1}^{\infty} \frac{mn\pi^2}{ab} W_{mn} cos\left(\frac{m\pi x}{a}\right) cos\left(\frac{n\pi y}{b}\right) sin\omega t \right\}$$

$$+ \frac{16}{h^4} F_{54} \left\{ \sum_{m=1}^{\infty} \sum_{n=1}^{\infty} \frac{mn\pi^2}{ab} W_{mn} cos\left(\frac{m\pi x}{a}\right) cos\left(\frac{n\pi y}{b}\right) sin\omega t \right\}$$

$$+ \frac{16}{h^4} F_{55} \left\{ \sum_{m=1}^{\infty} \sum_{n=1}^{\infty} \frac{m^2\pi^2}{a^2} W_{mn} sin\left(\frac{m\pi x}{a}\right) sin\left(\frac{n\pi y}{b}\right) sin\omega t \right\}$$

$$\frac{16}{h^4} F_{44} \left\{ \sum_{m=1}^{\infty} \sum_{n=1}^{\infty} \frac{n^2\pi^2}{b^2} W_{mn} sin\left(\frac{m\pi x}{a}\right) sin\left(\frac{n\pi y}{b}\right) sin\omega t \right\}$$

$$+ \frac{16}{h^4} F_{45} \left\{ \sum_{m=1}^{\infty} \sum_{n=1}^{\infty} \frac{mn\pi^2}{ab} W_{mn} cos\left(\frac{m\pi x}{a}\right) cos\left(\frac{n\pi y}{b}\right) sin\omega t \right\}$$

$$-\frac{16}{9h^4}H_{11}\left\{\sum_{m=1}^{\infty}\sum_{n=1}^{\infty}\frac{m^4\pi^4}{a^4}W_{mn}sin\left(\frac{m\pi x}{a}\right)sin\left(\frac{n\pi y}{b}\right)sin\omega t\right\}$$

$$-\frac{16}{9h^4}H_{12}\left\{\sum_{m=1}^{\infty}\sum_{n=1}^{\infty}\frac{m^2n^2\pi^4}{a^2b^2}W_{mn}sin\left(\frac{m\pi x}{a}\right)sin\left(\frac{n\pi y}{b}\right)sin\omega t\right\}$$

$$+\frac{16}{9h^4}H_{16}\left\{2\sum_{m=1}^{\infty}\sum_{n=1}^{\infty}\frac{m^3n\pi^4}{a^3b}W_{mn}cos\left(\frac{m\pi x}{a}\right)cos\left(\frac{n\pi y}{b}\right)sin\omega t\right\}$$

$$-\frac{16}{9h^4}H_{21}\left\{\sum_{m=1}^{\infty}\sum_{n=1}^{\infty}\frac{m^2n^2\pi^4}{a^2b^2}W_{mn}sin\left(\frac{m\pi x}{a}\right)sin\left(\frac{n\pi y}{b}\right)sin\omega t\right\}$$

$$-\frac{16}{9h^4}H_{22}\left\{\sum_{m=1}^{\infty}\sum_{n=1}^{\infty}\frac{n^4\pi^4}{b^4}W_{mn}sin\left(\frac{m\pi x}{a}\right)sin\left(\frac{n\pi y}{b}\right)sin\omega t\right\}$$

$$+\frac{16}{9h^4}H_{26}\left\{2\sum_{m=1}^{\infty}\sum_{n=1}^{\infty}\frac{mn^3\pi^4}{ab^3}W_{mn}cos\left(\frac{m\pi x}{a}\right)cos\left(\frac{n\pi y}{b}\right)sin\omega t\right\}$$

$$+\frac{16}{9h^4}H_{61}\left\{2\sum_{m=1}^{\infty}\sum_{n=1}^{\infty}\frac{m^3n\pi^4}{a^3b}W_{mn}cos\left(\frac{m\pi x}{a}\right)cos\left(\frac{n\pi y}{b}\right)sin\omega t\right\}$$

$$+\frac{16}{9h^4}H_{62}\left\{2\sum_{m=1}^{\infty}\sum_{n=1}^{\infty}\frac{mn^3\pi^4}{ab^3}W_{mn}cos\left(\frac{m\pi x}{a}\right)cos\left(\frac{n\pi y}{b}\right)sin\omega t\right\}$$

$$-\frac{16}{9h^4}H_{66}\left\{2\sum_{m=1}^{\infty}\sum_{n=1}^{\infty}\frac{m^2n^2\pi^4}{a^2b^2}W_{mn}sin\left(\frac{m\pi x}{a}\right)sin\left(\frac{n\pi y}{b}\right)sin\omega t\right\}$$

$$k_{34}=+A_{45}\left\{\sum_{m=1}^{\infty}\sum_{n=1}^{\infty}\frac{n\pi}{b}\psi^1_{mn}cos\left(\frac{m\pi x}{a}\right)cos\left(\frac{n\pi y}{b}\right)sin\omega t\right\}$$

$$-A_{55}\left\{\sum_{m=1}^{\infty}\sum_{n=1}^{\infty}\frac{m\pi}{a}\psi^1_{mn}sin\left(\frac{m\pi x}{a}\right)sin\left(\frac{n\pi y}{b}\right)sin\omega t\right\}$$

$$-\frac{B_{11}}{R_1}\left\{\sum_{m=1}^{\infty}\sum_{n=1}^{\infty}\frac{m\pi}{a}\psi^1_{mn}sin\left(\frac{m\pi x}{a}\right)sin\left(\frac{n\pi y}{b}\right)sin\omega t\right\}$$

$$-\frac{B_{16}}{R_1}\left\{\sum_{m=1}^{\infty}\sum_{n=1}^{\infty}\frac{n\pi}{b}\psi^1_{mn}sin\left(\frac{m\pi x}{a}\right)sin\left(\frac{n\pi y}{b}\right)sin\omega t\right\}$$

$$+\frac{B_{21}}{R_2}\left\{\sum_{m=1}^{\infty}\sum_{n=1}^{\infty}\frac{m\pi}{a}\psi_{mn}^{1}sin\left(\frac{m\pi x}{a}\right)sin\left(\frac{n\pi y}{b}\right)sin\omega t\right\}$$

$$-\frac{B_{26}}{R_2}\left\{\sum_{m=1}^{\infty}\sum_{n=1}^{\infty}\frac{n\pi}{b}\psi_{mn}^{1}cos\left(\frac{m\pi x}{a}\right)cos\left(\frac{n\pi y}{b}\right)sin\omega t\right\}$$

$$-\frac{4}{h^2}D_{45}\left\{2\sum_{m=1}^{\infty}\sum_{n=1}^{\infty}\frac{n\pi}{b}\psi_{mn}^{1}cos\left(\frac{m\pi x}{a}\right)cos\left(\frac{n\pi y}{b}\right)sin\omega t\right\}$$

$$+\frac{4}{h^2}D_{55}\left\{2\sum_{m=1}^{\infty}\sum_{n=1}^{\infty}\frac{m\pi}{a}\psi_{mn}^{1}sin\left(\frac{m\pi x}{a}\right)sin\left(\frac{n\pi y}{b}\right)sin\omega t\right\}$$

$$-\frac{4}{3h^2R_1}E_{11}\left\{\sum_{m=1}^{\infty}\sum_{n=1}^{\infty}\frac{m\pi}{a}\psi_{mn}^{1}sin\left(\frac{m\pi x}{a}\right)sin\left(\frac{n\pi y}{b}\right)sin\omega t\right\}$$

$$+\frac{4}{3h^2R_1}E_{16}\left\{\sum_{m=1}^{\infty}\sum_{n=1}^{\infty}\frac{n\pi}{b}\psi_{mn}^{1}cos\left(\frac{m\pi x}{a}\right)cos\left(\frac{n\pi y}{b}\right)sin\omega t\right\}$$

$$-\frac{4}{3h^2R_2}E_{21}\left\{\sum_{m=1}^{\infty}\sum_{n=1}^{\infty}\frac{m\pi}{a}\psi_{mn}^{1}sin\left(\frac{m\pi x}{a}\right)sin\left(\frac{n\pi y}{b}\right)sin\omega t\right\}$$

$$+\frac{4}{3h^2R_2}E_{26}\left\{\sum_{m=1}^{\infty}\sum_{n=1}^{\infty}\frac{n\pi}{b}\psi_{mn}^{1}cos\left(\frac{m\pi x}{a}\right)cos\left(\frac{n\pi y}{b}\right)sin\omega t\right\}$$

$$-\frac{16}{h^4}F_{55}\left\{\sum_{m=1}^{\infty}\sum_{n=1}^{\infty}\frac{m\pi}{a}\psi_{mn}^{1}sin\left(\frac{m\pi x}{a}\right)sin\left(\frac{n\pi y}{b}\right)sin\omega t\right\}$$

$$+\frac{16}{h^4}F_{45}\left\{\sum_{m=1}^{\infty}\sum_{n=1}^{\infty}\frac{n\pi}{b}\psi_{mn}^{1}cos\left(\frac{m\pi x}{a}\right)cos\left(\frac{n\pi y}{b}\right)sin\omega t\right\}$$

$$+\frac{4}{3h^2}F_{11}\left\{\sum_{m=1}^{\infty}\sum_{n=1}^{\infty}\frac{m^3\pi^3}{a^3}\psi_{mn}^{1}sin\left(\frac{m\pi x}{a}\right)sin\left(\frac{n\pi y}{b}\right)sin\omega t\right\}$$

$$-\frac{4}{3h^2}F_{16}\left\{\sum_{m=1}^{\infty}\sum_{n=1}^{\infty}\frac{m^2n\pi^3}{a^2b}\psi_{mn}^{1}cos\left(\frac{m\pi x}{a}\right)cos\left(\frac{n\pi y}{b}\right)sin\omega t\right\}$$

$$+\frac{4}{3h^2}F_{21}\left\{\sum_{m=1}^{\infty}\sum_{n=1}^{\infty}\frac{mn^2\pi^3}{ab^2}\psi_{mn}^{1}sin\left(\frac{m\pi x}{a}\right)sin\left(\frac{n\pi y}{b}\right)sin\omega t\right\}$$

$$- \frac{4}{3h^2}F_{26}\left\{\sum_{m=1}^{\infty}\sum_{n=1}^{\infty}\frac{n^3\pi^3}{b^3}\psi_{mn}^1 cos\left(\frac{m\pi x}{a}\right)cos\left(\frac{n\pi y}{b}\right)sin\omega t\right\}$$

$$- \frac{4}{3h^2}F_{61}\left\{2\sum_{m=1}^{\infty}\sum_{n=1}^{\infty}\frac{m^2n\pi^3}{a^2b}\psi_{mn}^1 cos\left(\frac{m\pi x}{a}\right)cos\left(\frac{n\pi y}{b}\right)sin\omega t\right\}$$

$$+ \frac{4}{3h^2}F_{66}\left\{2\sum_{m=1}^{\infty}\sum_{n=1}^{\infty}\frac{mn^2\pi^3}{ab^2}\psi_{mn}^1 sin\left(\frac{m\pi x}{a}\right)sin\left(\frac{n\pi y}{b}\right)sin\omega t\right\}$$

$$- \frac{16}{9h^4}H_{11}\left\{\sum_{m=1}^{\infty}\sum_{n=1}^{\infty}\frac{m^3\pi^3}{a^3}\psi_{mn}^1 sin\left(\frac{m\pi x}{a}\right)sin\left(\frac{n\pi y}{b}\right)sin\omega t\right\}$$

$$+ \frac{16}{9h^4}H_{16}\left\{\sum_{m=1}^{\infty}\sum_{n=1}^{\infty}\frac{m^2n\pi^3}{a^2b}\psi_{mn}^1 cos\left(\frac{m\pi x}{a}\right)cos\left(\frac{n\pi y}{b}\right)sin\omega t\right\}$$

$$- \frac{16}{9h^4}H_{21}\left\{\sum_{m=1}^{\infty}\sum_{n=1}^{\infty}\frac{mn^2\pi^3}{ab^2}\psi_{mn}^1 sin\left(\frac{m\pi x}{a}\right)sin\left(\frac{n\pi y}{b}\right)sin\omega t\right\}$$

$$+ \frac{16}{9h^4}H_{26}\left\{\sum_{m=1}^{\infty}\sum_{n=1}^{\infty}\frac{n^3\pi^3}{b^3}\psi_{mn}^1 cos\left(\frac{m\pi x}{a}\right)cos\left(\frac{n\pi y}{b}\right)sin\omega t\right\}$$

$$+ \frac{16}{9h^4}H_{61}\left\{2\sum_{m=1}^{\infty}\sum_{n=1}^{\infty}\frac{m^2n\pi^3}{a^2b}\psi_{mn}^1 cos\left(\frac{m\pi x}{a}\right)cos\left(\frac{n\pi y}{b}\right)sin\omega t\right\}$$

$$- \frac{16}{9h^4}H_{66}\left\{2\sum_{m=1}^{\infty}\sum_{n=1}^{\infty}\frac{mn^2\pi^3}{ab^2}\psi_{mn}^1 sin\left(\frac{m\pi x}{a}\right)sin\left(\frac{n\pi y}{b}\right)sin\omega t\right\}$$

$$k_{35} = +A_{54}\left\{\sum_{m=1}^{\infty}\sum_{n=1}^{\infty}\frac{m\pi}{a}\psi_{mn}^2 cos\left(\frac{m\pi x}{a}\right)cos\left(\frac{n\pi y}{b}\right)sin\omega t\right\}$$

$$- A_{44}\left\{\sum_{m=1}^{\infty}\sum_{n=1}^{\infty}\frac{n\pi}{b}\psi_{mn}^2 sin\left(\frac{m\pi x}{a}\right)sin\left(\frac{n\pi y}{b}\right)sin\omega t\right\}$$

$$+ \frac{B_{12}}{R_1}\left\{\sum_{m=1}^{\infty}\sum_{n=1}^{\infty}\frac{n\pi}{b}\psi_{mn}^2 sin\left(\frac{m\pi x}{a}\right)sin\left(\frac{n\pi y}{b}\right)sin\omega t\right\}$$

$$- \frac{B_{16}}{R_1}\left\{\sum_{m=1}^{\infty}\sum_{n=1}^{\infty}\frac{m\pi}{a}\psi_{mn}^2 cos\left(\frac{m\pi x}{a}\right)cos\left(\frac{n\pi y}{b}\right)sin\omega t\right\}$$

$$+\frac{B_{22}}{R_2}\left\{\sum_{m=1}^{\infty}\sum_{n=1}^{\infty}\frac{n\pi}{b}\psi_{mn}^2 sin\left(\frac{m\pi x}{a}\right)sin\left(\frac{n\pi y}{b}\right)sin\omega t\right\}$$

$$-\frac{B_{26}}{R_2}\left\{\sum_{m=1}^{\infty}\sum_{n=1}^{\infty}\frac{m\pi}{a}\psi_{mn}^2 cos\left(\frac{m\pi x}{a}\right)cos\left(\frac{n\pi y}{b}\right)sin\omega t\right\}$$

$$-\frac{4}{h^2}D_{54}\left\{2\sum_{m=1}^{\infty}\sum_{n=1}^{\infty}\frac{m\pi}{a}\psi_{mn}^2 cos\left(\frac{m\pi x}{a}\right)cos\left(\frac{n\pi y}{b}\right)sin\omega t\right\}$$

$$+\frac{4}{h^2}D_{44}\left\{2\sum_{m=1}^{\infty}\sum_{n=1}^{\infty}\frac{n\pi}{b}\psi_{mn}^2 sin\left(\frac{m\pi x}{a}\right)sin\left(\frac{n\pi y}{b}\right)sin\omega t\right\}$$

$$-\frac{4}{3h^2R_1}E_{12}\left\{\sum_{m=1}^{\infty}\sum_{n=1}^{\infty}\frac{n\pi}{b}\psi_{mn}^2 sin\left(\frac{m\pi x}{a}\right)sin\left(\frac{n\pi y}{b}\right)sin\omega t\right\}$$

$$+\frac{4}{3h^2R_1}E_{16}\left\{\sum_{m=1}^{\infty}\sum_{n=1}^{\infty}\frac{m\pi}{a}\psi_{mn}^2 cos\left(\frac{m\pi x}{a}\right)cos\left(\frac{n\pi y}{b}\right)sin\omega t\right\}$$

$$-\frac{4}{3h^2R_2}E_{22}\left\{\sum_{m=1}^{\infty}\sum_{n=1}^{\infty}\frac{n\pi}{b}\psi_{mn}^2 sin\left(\frac{m\pi x}{a}\right)sin\left(\frac{n\pi y}{b}\right)sin\omega t\right\}$$

$$+\frac{4}{3h^2R_2}E_{26}\left\{\sum_{m=1}^{\infty}\sum_{n=1}^{\infty}\frac{m\pi}{a}\psi_{mn}^2 cos\left(\frac{m\pi x}{a}\right)cos\left(\frac{n\pi y}{b}\right)sin\omega t\right\}$$

$$-\frac{16}{h^4}F_{44}\left\{\sum_{m=1}^{\infty}\sum_{n=1}^{\infty}\frac{n\pi}{b}\psi_{mn}^2 sin\left(\frac{m\pi x}{a}\right)sin\left(\frac{n\pi y}{b}\right)sin\omega t\right\}$$

$$+\frac{16}{h^4}F_{54}\left\{\sum_{m=1}^{\infty}\sum_{n=1}^{\infty}\frac{m\pi}{a}\psi_{mn}^2 cos\left(\frac{m\pi x}{a}\right)cos\left(\frac{n\pi y}{b}\right)sin\omega t\right\}$$

$$+\frac{4}{3h^2}F_{12}\left\{\sum_{m=1}^{\infty}\sum_{n=1}^{\infty}\frac{m^2n\pi^3}{a^2b}\psi_{mn}^2 sin\left(\frac{m\pi x}{a}\right)sin\left(\frac{n\pi y}{b}\right)sin\omega t\right\}$$

$$-\frac{4}{3h^2}F_{16}\left\{\sum_{m=1}^{\infty}\sum_{n=1}^{\infty}\frac{m^3\pi^3}{a^3}\psi_{mn}^2 cos\left(\frac{m\pi x}{a}\right)cos\left(\frac{n\pi y}{b}\right)sin\omega t\right\}$$

$$+\frac{4}{3h^2}F_{22}\left\{\sum_{m=1}^{\infty}\sum_{n=1}^{\infty}\frac{m^3\pi^3}{b^3}\psi_{mn}^2 sin\left(\frac{m\pi x}{a}\right)sin\left(\frac{n\pi y}{b}\right)sin\omega t\right\}$$

$$- \frac{4}{3h^2} F_{26} \left\{ \sum_{m=1}^{\infty} \sum_{n=1}^{\infty} \frac{mn^2\pi^3}{ab^2} \psi_{mn}^2 cos\left(\frac{m\pi x}{a}\right) cos\left(\frac{n\pi y}{b}\right) sin\omega t \right\}$$

$$- \frac{4}{3h^2} F_{62} \left\{ 2 \sum_{m=1}^{\infty} \sum_{n=1}^{\infty} \frac{mn^2\pi^3}{ab^2} \psi_{mn}^2 cos\left(\frac{m\pi x}{a}\right) cos\left(\frac{n\pi y}{b}\right) sin\omega t \right\}$$

$$+ \frac{4}{3h^2} F_{66} \left\{ 2 \sum_{m=1}^{\infty} \sum_{n=1}^{\infty} \frac{m^2n\pi^3}{a^2b} \psi_{mn}^2 sin\left(\frac{m\pi x}{a}\right) sin\left(\frac{n\pi y}{b}\right) sin\omega t \right\}$$

$$- \frac{16}{9h^4} H_{12} \left\{ \sum_{m=1}^{\infty} \sum_{n=1}^{\infty} \frac{m^2n\pi^3}{a^2b} \psi_{mn}^2 sin\left(\frac{m\pi x}{a}\right) sin\left(\frac{n\pi y}{b}\right) sin\omega t \right\}$$

$$+ \frac{16}{9h^4} H_{16} \left\{ \sum_{m=1}^{\infty} \sum_{n=1}^{\infty} \frac{m^3\pi^3}{a^3} \psi_{mn}^2 cos\left(\frac{m\pi x}{a}\right) cos\left(\frac{n\pi y}{b}\right) sin\omega t \right\}$$

$$- \frac{16}{9h^4} H_{22} \left\{ \sum_{m=1}^{\infty} \sum_{n=1}^{\infty} \frac{n^3\pi^3}{b^3} \psi_{mn}^2 sin\left(\frac{m\pi x}{a}\right) sin\left(\frac{n\pi y}{b}\right) sin\omega t \right\}$$

$$+ \frac{16}{9h^4} H_{26} \left\{ \sum_{m=1}^{\infty} \sum_{n=1}^{\infty} \frac{mn^2\pi^3}{ab^2} \psi_{mn}^2 cos\left(\frac{m\pi x}{a}\right) cos\left(\frac{n\pi y}{b}\right) sin\omega t \right\}$$

$$+ \frac{16}{9h^4} H_{62} \left\{ 2 \sum_{m=1}^{\infty} \sum_{n=1}^{\infty} \frac{mn^2\pi^3}{ab^2} \psi_{mn}^2 cos\left(\frac{m\pi x}{a}\right) cos\left(\frac{n\pi y}{b}\right) sin\omega t \right\}$$

$$- \frac{16}{9h^4} H_{66} \left\{ 2 \sum_{m=1}^{\infty} \sum_{n=1}^{\infty} \frac{m^2n\pi^3}{a^2b} \psi_{mn}^2 sin\left(\frac{m\pi x}{a}\right) sin\left(\frac{n\pi y}{b}\right) sin\omega t \right\}$$

$$k_{41} = -B_{11} \left\{ \sum_{m=1}^{\infty} \sum_{n=1}^{\infty} \frac{m^2\pi^2}{a^2} U_{mn} cos\left(\frac{m\pi x}{a}\right) sin\left(\frac{n\pi y}{b}\right) sin\omega t \right\}$$

$$- B_{16} \left\{ \sum_{m=1}^{\infty} \sum_{n=1}^{\infty} \frac{mn\pi^2}{ab} U_{mn} sin\left(\frac{m\pi x}{a}\right) cos\left(\frac{n\pi y}{b}\right) sin\omega t \right\}$$

$$- B_{61} \left\{ \sum_{m=1}^{\infty} \sum_{n=1}^{\infty} \frac{mn\pi^2}{ab} U_{mn} sin\left(\frac{m\pi x}{a}\right) cos\left(\frac{n\pi y}{b}\right) sin\omega t \right\}$$

$$- B_{66} \left\{ \sum_{m=1}^{\infty} \sum_{n=1}^{\infty} \frac{n^2\pi^2}{b^2} U_{mn} cos\left(\frac{m\pi x}{a}\right) sin\left(\frac{n\pi y}{b}\right) sin\omega t \right\}$$

$$+\frac{4}{3h^2}E_{11}\left\{\sum_{m=1}^{\infty}\sum_{n=1}^{\infty}\frac{m^2\pi^2}{a^2}U_{mn}cos\left(\frac{m\pi x}{a}\right)sin\left(\frac{n\pi y}{b}\right)sin\omega t\right\}$$

$$+\frac{4}{3h^2}E_{16}\left\{\sum_{m=1}^{\infty}\sum_{n=1}^{\infty}\frac{mn\pi^2}{ab}U_{mn}sin\left(\frac{m\pi x}{a}\right)cos\left(\frac{n\pi y}{b}\right)sin\omega t\right\}$$

$$+\frac{4}{3h^2}E_{61}\left\{\sum_{m=1}^{\infty}\sum_{n=1}^{\infty}\frac{mn\pi^2}{ab}U_{mn}sin\left(\frac{m\pi x}{a}\right)cos\left(\frac{n\pi y}{b}\right)sin\omega t\right\}$$

$$+\frac{4}{3h^2}E_{66}\left\{\sum_{m=1}^{\infty}\sum_{n=1}^{\infty}\frac{n^2\pi^2}{b^2}U_{mn}cos\left(\frac{m\pi x}{a}\right)sin\left(\frac{n\pi y}{b}\right)sin\omega t\right\}$$

$$k_{42}=-B_{12}\left\{\sum_{m=1}^{\infty}\sum_{n=1}^{\infty}\frac{mn\pi^2}{ab}V_{mn}cos\left(\frac{m\pi x}{a}\right)sin\left(\frac{n\pi y}{b}\right)sin\omega t\right\}$$

$$-B_{16}\left\{\sum_{m=1}^{\infty}\sum_{n=1}^{\infty}\frac{m^2\pi^2}{a^2}V_{mn}sin\left(\frac{m\pi x}{a}\right)cos\left(\frac{n\pi y}{b}\right)sin\omega t\right\}$$

$$-B_{62}\left\{\sum_{m=1}^{\infty}\sum_{n=1}^{\infty}\frac{n^2\pi^2}{b^2}V_{mn}sin\left(\frac{m\pi x}{a}\right)cos\left(\frac{n\pi y}{b}\right)sin\omega t\right\}$$

$$-B_{66}\left\{\sum_{m=1}^{\infty}\sum_{n=1}^{\infty}\frac{mn\pi^2}{ab}V_{mn}cos\left(\frac{m\pi x}{a}\right)sin\left(\frac{n\pi y}{b}\right)sin\omega t\right\}$$

$$+\frac{4}{3h^2}E_{12}\left\{\sum_{m=1}^{\infty}\sum_{n=1}^{\infty}\frac{mn\pi^2}{ab}V_{mn}cos\left(\frac{m\pi x}{a}\right)sin\left(\frac{n\pi y}{b}\right)sin\omega t\right\}$$

$$+\frac{4}{3h^2}E_{16}\left\{\sum_{m=1}^{\infty}\sum_{n=1}^{\infty}\frac{m^2\pi^2}{a^2}V_{mn}sin\left(\frac{m\pi x}{a}\right)cos\left(\frac{n\pi y}{b}\right)sin\omega t\right\}$$

$$+\frac{4}{3h^2}E_{62}\left\{\sum_{m=1}^{\infty}\sum_{n=1}^{\infty}\frac{n^2\pi^2}{b^2}V_{mn}sin\left(\frac{m\pi x}{a}\right)cos\left(\frac{n\pi y}{b}\right)sin\omega t\right\}$$

$$+\frac{4}{3h^2}E_{66}\left\{\sum_{m=1}^{\infty}\sum_{n=1}^{\infty}\frac{mn\pi^2}{ab}V_{mn}cos\left(\frac{m\pi x}{a}\right)sin\left(\frac{n\pi y}{b}\right)sin\omega t\right\}$$

$$k_{43}=-A_{54}\left\{\sum_{m=1}^{\infty}\sum_{n=1}^{\infty}\frac{n\pi}{b}W_{mn}sin\left(\frac{m\pi x}{a}\right)sin\left(\frac{n\pi y}{b}\right)cos\omega t\right\}$$

$$- A_{55}\left\{\sum_{m=1}^{\infty}\sum_{n=1}^{\infty}\frac{m\pi}{a}W_{mn}cos\left(\frac{m\pi x}{a}\right)sin\left(\frac{n\pi y}{b}\right)sin\omega t\right\}$$

$$+ \frac{B_{11}}{R_1}\left\{\sum_{m=1}^{\infty}\sum_{n=1}^{\infty}\frac{m\pi}{a}W_{mn}cos\left(\frac{m\pi x}{a}\right)sin\left(\frac{n\pi y}{b}\right)sin\omega t\right\}$$

$$+ \frac{B_{12}}{R_2}\left\{\sum_{m=1}^{\infty}\sum_{n=1}^{\infty}\frac{m\pi}{a}W_{mn}cos\left(\frac{m\pi x}{a}\right)sin\left(\frac{n\pi y}{b}\right)sin\omega t\right\}$$

$$+ \frac{B_{61}}{R_1}\left\{\sum_{m=1}^{\infty}\sum_{n=1}^{\infty}\frac{n\pi}{b}W_{mn}sin\left(\frac{m\pi x}{a}\right)cos\left(\frac{n\pi y}{b}\right)sin\omega t\right\}$$

$$+ \frac{B_{62}}{R_2}\left\{\sum_{m=1}^{\infty}\sum_{n=1}^{\infty}\frac{n\pi}{b}W_{mn}sin\left(\frac{m\pi x}{a}\right)cos\left(\frac{n\pi y}{b}\right)sin\omega t\right\}$$

$$+ \frac{4}{h^2}D_{54}\left\{2\sum_{m=1}^{\infty}\sum_{n=1}^{\infty}\frac{n\pi}{b}W_{mn}sin\left(\frac{m\pi x}{a}\right)cos\left(\frac{n\pi y}{b}\right)sin\omega t\right\}$$

$$+ \frac{4}{h^2}D_{55}\left\{2\sum_{m=1}^{\infty}\sum_{n=1}^{\infty}\frac{m\pi}{a}W_{mn}cos\left(\frac{m\pi x}{a}\right)sin\left(\frac{n\pi y}{b}\right)sin\omega t\right\}$$

$$- \frac{4}{3h^2R_1}E_{11}\left\{\sum_{m=1}^{\infty}\sum_{n=1}^{\infty}\frac{m\pi}{a}W_{mn}cos\left(\frac{m\pi x}{a}\right)sin\left(\frac{n\pi y}{b}\right)sin\omega t\right\}$$

$$- \frac{4}{3h^2R_2}E_{12}\left\{\sum_{m=1}^{\infty}\sum_{n=1}^{\infty}\frac{m\pi}{a}W_{mn}cos\left(\frac{m\pi x}{a}\right)sin\left(\frac{n\pi y}{b}\right)sin\omega t\right\}$$

$$- \frac{4}{3h^2R_1}E_{61}\left\{\sum_{m=1}^{\infty}\sum_{n=1}^{\infty}\frac{n\pi}{b}W_{mn}sin\left(\frac{m\pi x}{a}\right)cos\left(\frac{n\pi y}{b}\right)sin\omega t\right\}$$

$$- \frac{4}{3h^2R_2}E_{62}\left\{\sum_{m=1}^{\infty}\sum_{n=1}^{\infty}\frac{n\pi}{b}W_{mn}sin\left(\frac{m\pi x}{a}\right)cos\left(\frac{n\pi y}{b}\right)sin\omega t\right\}$$

$$+ \frac{4}{3h^2}F_{11}\left\{\sum_{m=1}^{\infty}\sum_{n=1}^{\infty}\frac{m^3\pi^3}{a^3}W_{mn}cos\left(\frac{m\pi x}{a}\right)sin\left(\frac{n\pi y}{b}\right)sin\omega t\right\}$$

$$+ \frac{4}{3h^2}F_{12}\left\{\sum_{m=1}^{\infty}\sum_{n=1}^{\infty}\frac{mn^2\pi^3}{ab^2}W_{mn}cos\left(\frac{m\pi x}{a}\right)sin\left(\frac{n\pi y}{b}\right)sin\omega t\right\}$$

$$+\frac{4}{3h^2}F_{16}\left\{2\sum_{m=1}^{\infty}\sum_{n=1}^{\infty}\frac{m^2n\pi^3}{a^2b}W_{mn}sin\left(\frac{m\pi x}{a}\right)cos\left(\frac{n\pi y}{b}\right)sin\omega t\right\}$$

$$+\frac{4}{3h^2}F_{61}\left\{\sum_{m=1}^{\infty}\sum_{n=1}^{\infty}\frac{m^2n\pi^3}{a^2b}W_{mn}sin\left(\frac{m\pi x}{a}\right)cos\left(\frac{n\pi y}{b}\right)sin\omega t\right\}$$

$$+\frac{4}{3h^2}F_{62}\left\{\sum_{m=1}^{\infty}\sum_{n=1}^{\infty}\frac{n^3\pi^3}{b^3}W_{mn}sin\left(\frac{m\pi x}{a}\right)cos\left(\frac{n\pi y}{b}\right)sin\omega t\right\}$$

$$+\frac{4}{3h^2}F_{66}\left\{2\sum_{m=1}^{\infty}\sum_{n=1}^{\infty}\frac{mn^2\pi^3}{ab^2}W_{mn}cos\left(\frac{m\pi x}{a}\right)sin\left(\frac{n\pi y}{b}\right)sin\omega t\right\}$$

$$-\frac{16}{h^4}F_{54}\left\{\sum_{m=1}^{\infty}\sum_{n=1}^{\infty}\frac{n\pi}{b}W_{mn}sin\left(\frac{m\pi x}{a}\right)cos\left(\frac{n\pi y}{b}\right)sin\omega t\right\}$$

$$-\frac{16}{h^4}F_{55}\left\{\sum_{m=1}^{\infty}\sum_{n=1}^{\infty}\frac{m\pi}{a}W_{mn}cos\left(\frac{m\pi x}{a}\right)sin\left(\frac{n\pi y}{b}\right)sin\omega t\right\}$$

$$-\frac{16}{9h^4}H_{11}\left\{\sum_{m=1}^{\infty}\sum_{n=1}^{\infty}\frac{m^3\pi^3}{a^3}W_{mn}cos\left(\frac{m\pi x}{a}\right)sin\left(\frac{n\pi y}{b}\right)sin\omega t\right\}$$

$$-\frac{16}{9h^4}H_{12}\left\{\sum_{m=1}^{\infty}\sum_{n=1}^{\infty}\frac{mn^2\pi^3}{ab^2}W_{mn}cos\left(\frac{m\pi x}{a}\right)sin\left(\frac{n\pi y}{b}\right)sin\omega t\right\}$$

$$-\frac{16}{9h^4}H_{16}\left\{2\sum_{m=1}^{\infty}\sum_{n=1}^{\infty}\frac{m^2n\pi^3}{a^2b}W_{mn}sin\left(\frac{m\pi x}{a}\right)cos\left(\frac{n\pi y}{b}\right)sin\omega t\right\}$$

$$-\frac{16}{9h^4}H_{61}\left\{\sum_{m=1}^{\infty}\sum_{n=1}^{\infty}\frac{m^2n\pi^3}{a^2b}W_{mn}sin\left(\frac{m\pi x}{a}\right)cos\left(\frac{n\pi y}{b}\right)sin\omega t\right\}$$

$$-\frac{16}{9h^4}H_{62}\left\{\sum_{m=1}^{\infty}\sum_{n=1}^{\infty}\frac{n^3\pi^3}{b^3}W_{mn}sin\left(\frac{m\pi x}{a}\right)cos\left(\frac{n\pi y}{b}\right)sin\omega t\right\}$$

$$-\frac{16}{9h^4}H_{66}\left\{2\sum_{m=1}^{\infty}\sum_{n=1}^{\infty}\frac{mn^2\pi^3}{ab^2}W_{mn}cos\left(\frac{m\pi x}{a}\right)sin\left(\frac{n\pi y}{b}\right)sin\omega t\right\}$$

$$k_{44}=-A_{55}\left\{\sum_{m=1}^{\infty}\sum_{n=1}^{\infty}\psi_{mn}^{1}cos\left(\frac{m\pi x}{a}\right)sin\left(\frac{n\pi y}{b}\right)sin\omega t\right\}$$

$$- D_{11}\left\{\sum_{m=1}^{\infty}\sum_{n=1}^{\infty}\frac{m^2\pi^2}{a^2}\psi_{mn}^1 cos\left(\frac{m\pi x}{a}\right) sin\left(\frac{n\pi y}{b}\right) sin\omega t\right\}$$

$$- D_{16}\left\{\sum_{m=1}^{\infty}\sum_{n=1}^{\infty}\frac{mn\pi^2}{ab}\psi_{mn}^1 sin\left(\frac{m\pi x}{a}\right) cos\left(\frac{n\pi y}{b}\right) sin\omega t\right\}$$

$$- D_{61}\left\{\sum_{m=1}^{\infty}\sum_{n=1}^{\infty}\frac{mn\pi^2}{ab}\psi_{mn}^1 sin\left(\frac{m\pi x}{a}\right) cos\left(\frac{n\pi y}{b}\right) sin\omega t\right\}$$

$$- D_{66}\left\{\sum_{m=1}^{\infty}\sum_{n=1}^{\infty}\frac{n^2\pi^2}{b^2}\psi_{mn}^1 cos\left(\frac{m\pi x}{a}\right) sin\left(\frac{n\pi y}{b}\right) sin\omega t\right\}$$

$$+ \frac{4}{h^2}D_{55}\left\{2\sum_{m=1}^{\infty}\sum_{n=1}^{\infty}\psi_{mn}^1 cos\left(\frac{m\pi x}{a}\right) sin\left(\frac{n\pi y}{b}\right) sin\omega t\right\}$$

$$+ \frac{4}{3h^2}F_{11}\left\{2\sum_{m=1}^{\infty}\sum_{n=1}^{\infty}\frac{m^2\pi^2}{a^2}\psi_{mn}^1 cos\left(\frac{m\pi x}{a}\right) sin\left(\frac{n\pi y}{b}\right) sin\omega t\right\}$$

$$+ \frac{4}{3h^2}F_{16}\left\{2\sum_{m=1}^{\infty}\sum_{n=1}^{\infty}\frac{mn\pi^2}{ab}\psi_{mn}^1 sin\left(\frac{m\pi x}{a}\right) cos\left(\frac{n\pi y}{b}\right) sin\omega t\right\}$$

$$+ \frac{4}{3h^2}F_{61}\left\{2\sum_{m=1}^{\infty}\sum_{n=1}^{\infty}\frac{mn\pi^2}{ab}\psi_{mn}^1 sin\left(\frac{m\pi x}{a}\right) cos\left(\frac{n\pi y}{b}\right) sin\omega t\right\}$$

$$+ \frac{4}{3h^2}F_{66}\left\{2\sum_{m=1}^{\infty}\sum_{n=1}^{\infty}\frac{n^2\pi^2}{b^2}\psi_{mn}^1 cos\left(\frac{m\pi x}{a}\right) sin\left(\frac{n\pi y}{b}\right) sin\omega t\right\}$$

$$- \frac{16}{h^4}F_{55}\left\{\sum_{m=1}^{\infty}\sum_{n=1}^{\infty}\psi_{mn}^1 cos\left(\frac{m\pi x}{a}\right) sin\left(\frac{n\pi y}{b}\right) sin\omega t\right\}$$

$$- \frac{16}{9h^4}H_{11}\left\{\sum_{m=1}^{\infty}\sum_{n=1}^{\infty}\frac{m^2\pi^2}{a^2}\psi_{mn}^1 cos\left(\frac{m\pi x}{a}\right) sin\left(\frac{n\pi y}{b}\right) sin\omega t\right\}$$

$$- \frac{16}{9h^4}H_{16}\left\{\sum_{m=1}^{\infty}\sum_{n=1}^{\infty}\frac{mn\pi^2}{ab}\psi_{mn}^1 sin\left(\frac{m\pi x}{a}\right) cos\left(\frac{n\pi y}{b}\right) sin\omega t\right\}$$

$$- \frac{16}{9h^4}H_{61}\left\{\sum_{m=1}^{\infty}\sum_{n=1}^{\infty}\frac{mn\pi^2}{ab}\psi_{mn}^1 sin\left(\frac{m\pi x}{a}\right) cos\left(\frac{n\pi y}{b}\right) sin\omega t\right\}$$

$$- \frac{16}{9h^4} H_{66} \left\{ \sum_{m=1}^{\infty} \sum_{n=1}^{\infty} \frac{n^2\pi^2}{b^2} \psi_{mn}^1 cos\left(\frac{m\pi x}{a}\right) sin\left(\frac{n\pi y}{b}\right) sin\omega t \right\}$$

$$k_{45} = -A_{54} \left\{ \sum_{m=1}^{\infty} \sum_{n=1}^{\infty} \psi_{mn}^2 sin\left(\frac{m\pi x}{a}\right) cos\left(\frac{n\pi y}{b}\right) sin\omega t \right\}$$

$$- D_{12} \left\{ \sum_{m=1}^{\infty} \sum_{n=1}^{\infty} \frac{mn\pi^2}{ab} \psi_{mn}^2 cos\left(\frac{m\pi x}{a}\right) sin\left(\frac{n\pi y}{b}\right) sin\omega t \right\}$$

$$- D_{16} \left\{ \sum_{m=1}^{\infty} \sum_{n=1}^{\infty} \frac{m^2\pi^2}{a^2} \psi_{mn}^2 sin\left(\frac{m\pi x}{a}\right) cos\left(\frac{n\pi y}{b}\right) sin\omega t \right\}$$

$$- D_{62} \left\{ \sum_{m=1}^{\infty} \sum_{n=1}^{\infty} \frac{n^2\pi^2}{b^2} \psi_{mn}^2 sin\left(\frac{m\pi x}{a}\right) cos\left(\frac{n\pi y}{b}\right) sin\omega t \right\}$$

$$- D_{66} \left\{ \sum_{m=1}^{\infty} \sum_{n=1}^{\infty} \frac{mn\pi^2}{ab} \psi_{mn}^2 cos\left(\frac{m\pi x}{a}\right) sin\left(\frac{n\pi y}{b}\right) sin\omega t \right\}$$

$$+ \frac{4}{h^2} D_{54} \left\{ 2 \sum_{m=1}^{\infty} \sum_{n=1}^{\infty} \psi_{mn}^2 sin\left(\frac{m\pi x}{a}\right) cos\left(\frac{n\pi y}{b}\right) sin\omega t \right\}$$

$$+ \frac{4}{3h^2} F_{12} \left\{ 2 \sum_{m=1}^{\infty} \sum_{n=1}^{\infty} \frac{mn\pi^2}{ab} \psi_{mn}^2 cos\left(\frac{m\pi x}{a}\right) sin\left(\frac{n\pi y}{b}\right) sin\omega t \right\}$$

$$+ \frac{4}{3h^2} F_{16} \left\{ 2 \sum_{m=1}^{\infty} \sum_{n=1}^{\infty} \frac{m^2\pi^2}{a^2} \psi_{mn}^2 sin\left(\frac{m\pi x}{a}\right) cos\left(\frac{n\pi y}{b}\right) sin\omega t \right\}$$

$$+ \frac{4}{3h^2} F_{62} \left\{ 2 \sum_{m=1}^{\infty} \sum_{n=1}^{\infty} \frac{n^2\pi^2}{b^2} \psi_{mn}^2 sin\left(\frac{m\pi x}{a}\right) cos\left(\frac{n\pi y}{b}\right) sin\omega t \right\}$$

$$+ \frac{4}{3h^2} F_{66} \left\{ 2 \sum_{m=1}^{\infty} \sum_{n=1}^{\infty} \frac{mn\pi^2}{ab} \psi_{mn}^2 cos\left(\frac{m\pi x}{a}\right) sin\left(\frac{n\pi y}{b}\right) sin\omega t \right\}$$

$$- \frac{16}{h^4} F_{54} \left\{ \sum_{m=1}^{\infty} \sum_{n=1}^{\infty} \psi_{mn}^2 sin\left(\frac{m\pi x}{a}\right) cos\left(\frac{n\pi y}{b}\right) sin\omega t \right\}$$

$$- \frac{16}{9h^4} H_{12} \left\{ \sum_{m=1}^{\infty} \sum_{n=1}^{\infty} \frac{mn\pi^2}{ab} \psi_{mn}^2 cos\left(\frac{m\pi x}{a}\right) sin\left(\frac{n\pi y}{b}\right) sin\omega t \right\}$$

$$- \frac{16}{9h^4} H_{16} \left\{ \sum_{m=1}^{\infty} \sum_{n=1}^{\infty} \frac{m^2\pi^2}{a^2} \psi_{mn}^2 sin\left(\frac{m\pi x}{a}\right) cos\left(\frac{n\pi y}{b}\right) sin\omega t \right\}$$

$$- \frac{16}{9h^4} H_{62} \left\{ \sum_{m=1}^{\infty} \sum_{n=1}^{\infty} \frac{n^2\pi^2}{b^2} \psi_{mn}^2 sin\left(\frac{m\pi x}{a}\right) cos\left(\frac{n\pi y}{b}\right) sin\omega t \right\}$$

$$- \frac{16}{9h^4} H_{66} \left\{ \sum_{m=1}^{\infty} \sum_{n=1}^{\infty} \frac{mn\pi^2}{ab} \psi_{mn}^2 cos\left(\frac{m\pi x}{a}\right) sin\left(\frac{n\pi y}{b}\right) sin\omega t \right\}$$

$$k_{51} = -B_{21} \left\{ \sum_{m=1}^{\infty} \sum_{n=1}^{\infty} \frac{mn\pi^2}{ab} U_{mn} sin\left(\frac{m\pi x}{a}\right) cos\left(\frac{n\pi y}{b}\right) sin\omega t \right\}$$

$$- B_{26} \left\{ \sum_{m=1}^{\infty} \sum_{n=1}^{\infty} \frac{n^2\pi^2}{b^2} U_{mn} cos\left(\frac{m\pi x}{a}\right) sin\left(\frac{n\pi y}{b}\right) sin\omega t \right\}$$

$$- B_{61} \left\{ \sum_{m=1}^{\infty} \sum_{n=1}^{\infty} \frac{m^2\pi^2}{a^2} U_{mn} cos\left(\frac{m\pi x}{a}\right) sin\left(\frac{n\pi y}{b}\right) sin\omega t \right\}$$

$$- B_{66} \left\{ \sum_{m=1}^{\infty} \sum_{n=1}^{\infty} \frac{mn\pi^2}{ab} U_{mn} sin\left(\frac{m\pi x}{a}\right) cos\left(\frac{n\pi y}{b}\right) sin\omega t \right\}$$

$$+ \frac{4}{3h^2} E_{21} \left\{ \sum_{m=1}^{\infty} \sum_{n=1}^{\infty} \frac{mn\pi^2}{ab} U_{mn} sin\left(\frac{m\pi x}{a}\right) cos\left(\frac{n\pi y}{b}\right) sin\omega t \right\}$$

$$+ \frac{4}{3h^2} E_{26} \left\{ \sum_{m=1}^{\infty} \sum_{n=1}^{\infty} \frac{n^2\pi^2}{b^2} U_{mn} cos\left(\frac{m\pi x}{a}\right) sin\left(\frac{n\pi y}{b}\right) sin\omega t \right\}$$

$$+ \frac{4}{3h^2} E_{61} \left\{ \sum_{m=1}^{\infty} \sum_{n=1}^{\infty} \frac{m^2\pi^2}{a^2} U_{mn} cos\left(\frac{m\pi x}{a}\right) sin\left(\frac{n\pi y}{b}\right) sin\omega t \right\}$$

$$+ \frac{4}{3h^2} E_{66} \left\{ \sum_{m=1}^{\infty} \sum_{n=1}^{\infty} \frac{mn\pi^2}{ab} U_{mn} sin\left(\frac{m\pi x}{a}\right) cos\left(\frac{n\pi y}{b}\right) sin\omega t \right\}$$

$$k_{52} = -B_{22} \left\{ \sum_{m=1}^{\infty} \sum_{n=1}^{\infty} \frac{n^2\pi^2}{b^2} V_{mn} sin\left(\frac{m\pi x}{a}\right) cos\left(\frac{n\pi y}{b}\right) sin\omega t \right\}$$

$$- B_{26} \left\{ \sum_{m=1}^{\infty} \sum_{n=1}^{\infty} \frac{mn\pi^2}{ab} V_{mn} cos\left(\frac{m\pi x}{a}\right) sin\left(\frac{n\pi y}{b}\right) sin\omega t \right\}$$

$$- B_{62}\left\{\sum_{m=1}^{\infty}\sum_{n=1}^{\infty}\frac{mn\pi^2}{ab}V_{mn}cos\left(\frac{m\pi x}{a}\right)sin\left(\frac{n\pi y}{b}\right)sin\omega t\right\}$$

$$- B_{66}\left\{\sum_{m=1}^{\infty}\sum_{n=1}^{\infty}\frac{m^2\pi^2}{a^2}V_{mn}sin\left(\frac{m\pi x}{a}\right)cos\left(\frac{n\pi y}{b}\right)sin\omega t\right\}$$

$$+ \frac{4}{3h^2}E_{22}\left\{\sum_{m=1}^{\infty}\sum_{n=1}^{\infty}\frac{n^2\pi^2}{b^2}V_{mn}sin\left(\frac{m\pi x}{a}\right)cos\left(\frac{n\pi y}{b}\right)sin\omega t\right\}$$

$$+ \frac{4}{3h^2}E_{26}\left\{\sum_{m=1}^{\infty}\sum_{n=1}^{\infty}\frac{mn\pi^2}{ab}V_{mn}cos\left(\frac{m\pi x}{a}\right)sin\left(\frac{n\pi y}{b}\right)sin\omega t\right\}$$

$$+ \frac{4}{3h^2}E_{62}\left\{\sum_{m=1}^{\infty}\sum_{n=1}^{\infty}\frac{mn\pi^2}{ab}V_{mn}cos\left(\frac{m\pi x}{a}\right)sin\left(\frac{n\pi y}{b}\right)sin\omega t\right\}$$

$$+ \frac{4}{3h^2}E_{66}\left\{\sum_{m=1}^{\infty}\sum_{n=1}^{\infty}\frac{m^2\pi^2}{a^2}V_{mn}sin\left(\frac{m\pi x}{a}\right)cos\left(\frac{n\pi y}{b}\right)sin\omega t\right\}$$

$$k_{53} = -A_{45}\left\{\sum_{m=1}^{\infty}\sum_{n=1}^{\infty}\frac{m\pi}{a}W_{mn}cos\left(\frac{m\pi x}{a}\right)sin\left(\frac{n\pi y}{b}\right)sin\omega t\right\}$$

$$- A_{44}\left\{\sum_{m=1}^{\infty}\sum_{n=1}^{\infty}\frac{n\pi}{b}W_{mn}sin\left(\frac{m\pi x}{a}\right)cos\left(\frac{n\pi y}{b}\right)sin\omega t\right\}$$

$$+ \frac{B_{21}}{R_1}\left\{\sum_{m=1}^{\infty}\sum_{n=1}^{\infty}\frac{n\pi}{b}W_{mn}sin\left(\frac{m\pi x}{a}\right)cos\left(\frac{n\pi y}{b}\right)sin\omega t\right\}$$

$$+ \frac{B_{22}}{R_2}\left\{\sum_{m=1}^{\infty}\sum_{n=1}^{\infty}\frac{n\pi}{b}W_{mn}sin\left(\frac{m\pi x}{a}\right)cos\left(\frac{n\pi y}{b}\right)sin\omega t\right\}$$

$$+ \frac{B_{61}}{R_1}\left\{\sum_{m=1}^{\infty}\sum_{n=1}^{\infty}\frac{m\pi}{a}W_{mn}cos\left(\frac{m\pi x}{a}\right)sin\left(\frac{n\pi y}{b}\right)sin\omega t\right\}$$

$$+ \frac{B_{62}}{R_2}\left\{\sum_{m=1}^{\infty}\sum_{n=1}^{\infty}\frac{m\pi}{a}W_{mn}cos\left(\frac{m\pi x}{a}\right)sin\left(\frac{n\pi y}{b}\right)sin\omega t\right\}$$

$$+ \frac{4}{h^2}D_{45}\left\{2\sum_{m=1}^{\infty}\sum_{n=1}^{\infty}\frac{m\pi}{a}W_{mn}cos\left(\frac{m\pi x}{a}\right)sin\left(\frac{n\pi y}{b}\right)sin\omega t\right\}$$

$$+\frac{4}{h^2}D_{44}\left\{2\sum_{m=1}^{\infty}\sum_{n=1}^{\infty}\frac{n\pi}{b}W_{mn}sin\left(\frac{m\pi x}{a}\right)cos\left(\frac{n\pi y}{b}\right)sin\omega t\right\}$$

$$-\frac{4}{3h^2R_1}E_{21}\left\{\sum_{m=1}^{\infty}\sum_{n=1}^{\infty}\frac{n\pi}{b}W_{mn}sin\left(\frac{m\pi x}{a}\right)cos\left(\frac{n\pi y}{b}\right)sin\omega t\right\}$$

$$-\frac{4}{3h^2R_2}E_{22}\left\{\sum_{m=1}^{\infty}\sum_{n=1}^{\infty}\frac{n\pi}{b}W_{mn}sin\left(\frac{m\pi x}{a}\right)cos\left(\frac{n\pi y}{b}\right)sin\omega t\right\}$$

$$-\frac{4}{3h^2R_1}E_{61}\left\{\sum_{m=1}^{\infty}\sum_{n=1}^{\infty}\frac{m\pi}{a}W_{mn}cos\left(\frac{m\pi x}{a}\right)sin\left(\frac{n\pi y}{b}\right)sin\omega t\right\}$$

$$-\frac{4}{3h^2R_2}E_{62}\left\{\sum_{m=1}^{\infty}\sum_{n=1}^{\infty}\frac{m\pi}{a}W_{mn}cos\left(\frac{m\pi x}{a}\right)sin\left(\frac{n\pi y}{b}\right)sin\omega t\right\}$$

$$+\frac{4}{3h^2}F_{21}\left\{\sum_{m=1}^{\infty}\sum_{n=1}^{\infty}\frac{m^2n\pi^3}{a^2b}W_{mn}sin\left(\frac{m\pi x}{a}\right)cos\left(\frac{n\pi y}{b}\right)sin\omega t\right\}$$

$$+\frac{4}{3h^2}F_{22}\left\{\sum_{m=1}^{\infty}\sum_{n=1}^{\infty}\frac{n^3\pi^3}{b^3}W_{mn}sin\left(\frac{m\pi x}{a}\right)cos\left(\frac{n\pi y}{b}\right)sin\omega t\right\}$$

$$+\frac{4}{3h^2}F_{26}\left\{2\sum_{m=1}^{\infty}\sum_{n=1}^{\infty}\frac{mn^2\pi^3}{ab^2}W_{mn}cos\left(\frac{m\pi x}{a}\right)sin\left(\frac{n\pi y}{b}\right)sin\omega t\right\}$$

$$+\frac{4}{3h^2}F_{61}\left\{\sum_{m=1}^{\infty}\sum_{n=1}^{\infty}\frac{m^3\pi^3}{a^3}W_{mn}cos\left(\frac{m\pi x}{a}\right)sin\left(\frac{n\pi y}{b}\right)sin\omega t\right\}$$

$$+\frac{4}{3h^2}F_{62}\left\{\sum_{m=1}^{\infty}\sum_{n=1}^{\infty}\frac{mn^2\pi^3}{ab^2}W_{mn}cos\left(\frac{m\pi x}{a}\right)sin\left(\frac{n\pi y}{b}\right)sin\omega t\right\}$$

$$+\frac{4}{3h^2}F_{66}\left\{2\sum_{m=1}^{\infty}\sum_{n=1}^{\infty}\frac{m^2n\pi^3}{a^2b}W_{mn}sin\left(\frac{m\pi x}{a}\right)cos\left(\frac{n\pi y}{b}\right)sin\omega t\right\}$$

$$-\frac{16}{h^4}F_{45}\left\{\sum_{m=1}^{\infty}\sum_{n=1}^{\infty}\frac{m\pi}{a}W_{mn}cos\left(\frac{m\pi x}{a}\right)sin\left(\frac{n\pi y}{b}\right)sin\omega t\right\}$$

$$-\frac{16}{h^4}F_{44}\left\{\sum_{m=1}^{\infty}\sum_{n=1}^{\infty}\frac{n\pi}{b}W_{mn}sin\left(\frac{m\pi x}{a}\right)cos\left(\frac{n\pi y}{b}\right)sin\omega t\right\}$$

$$-\frac{16}{9h^4}H_{21}\left\{\sum_{m=1}^{\infty}\sum_{n=1}^{\infty}\frac{m^2n\pi^3}{a^2b}W_{mn}sin\left(\frac{m\pi x}{a}\right)cos\left(\frac{n\pi y}{b}\right)sin\omega t\right\}$$

$$-\frac{16}{9h^4}H_{22}\left\{\sum_{m=1}^{\infty}\sum_{n=1}^{\infty}\frac{n^3\pi^3}{b^3}W_{mn}sin\left(\frac{m\pi x}{a}\right)cos\left(\frac{n\pi y}{b}\right)sin\omega t\right\}$$

$$-\frac{16}{9h^4}H_{26}\left\{2\sum_{m=1}^{\infty}\sum_{n=1}^{\infty}\frac{mn^2\pi^3}{ab^2}W_{mn}cos\left(\frac{m\pi x}{a}\right)sin\left(\frac{n\pi y}{b}\right)sin\omega t\right\}$$

$$-\frac{16}{9h^4}H_{61}\left\{\sum_{m=1}^{\infty}\sum_{n=1}^{\infty}\frac{m^3\pi^3}{a^3}W_{mn}cos\left(\frac{m\pi x}{a}\right)sin\left(\frac{n\pi y}{b}\right)sin\omega t\right\}$$

$$-\frac{16}{9h^4}H_{62}\left\{\sum_{m=1}^{\infty}\sum_{n=1}^{\infty}\frac{mn^2\pi^3}{ab^2}W_{mn}cos\left(\frac{m\pi x}{a}\right)sin\left(\frac{n\pi y}{b}\right)sin\omega t\right\}$$

$$-\frac{16}{9h^4}H_{66}\left\{2\sum_{m=1}^{\infty}\sum_{n=1}^{\infty}\frac{m^2n\pi^3}{a^2b}W_{mn}sin\left(\frac{m\pi x}{a}\right)cos\left(\frac{n\pi y}{b}\right)sin\omega t\right\}$$

$$k_{54}=-A_{45}\left\{\sum_{m=1}^{\infty}\sum_{n=1}^{\infty}\psi^1_{mn}cos\left(\frac{m\pi x}{a}\right)sin\left(\frac{n\pi y}{b}\right)sin\omega t\right\}$$

$$-D_{21}\left\{\sum_{m=1}^{\infty}\sum_{n=1}^{\infty}\frac{mn\pi^2}{ab}\psi^1_{mn}sin\left(\frac{m\pi x}{a}\right)cos\left(\frac{n\pi y}{b}\right)sin\omega t\right\}$$

$$-D_{26}\left\{\sum_{m=1}^{\infty}\sum_{n=1}^{\infty}\frac{n^2\pi^2}{b^2}\psi^1_{mn}cos\left(\frac{m\pi x}{a}\right)sin\left(\frac{n\pi y}{b}\right)sin\omega t\right\}$$

$$-D_{61}\left\{\sum_{m=1}^{\infty}\sum_{n=1}^{\infty}\frac{m^2\pi^2}{a^2}\psi^1_{mn}cos\left(\frac{m\pi x}{a}\right)sin\left(\frac{n\pi y}{b}\right)sin\omega t\right\}$$

$$-D_{66}\left\{\sum_{m=1}^{\infty}\sum_{n=1}^{\infty}\frac{mn\pi^2}{ab}\psi^1_{mn}sin\left(\frac{m\pi x}{a}\right)cos\left(\frac{n\pi y}{b}\right)sin\omega t\right\}$$

$$+\frac{4}{h^2}D_{45}\left\{2\sum_{m=1}^{\infty}\sum_{n=1}^{\infty}\psi^1_{mn}cos\left(\frac{m\pi x}{a}\right)sin\left(\frac{n\pi y}{b}\right)sin\omega t\right\}$$

$$+\frac{4}{3h^2}F_{21}\left\{2\sum_{m=1}^{\infty}\sum_{n=1}^{\infty}\frac{mn\pi^2}{ab}\psi^1_{mn}sin\left(\frac{m\pi x}{a}\right)cos\left(\frac{n\pi y}{b}\right)sin\omega t\right\}$$

$$+\frac{4}{3h^2}F_{26}\left\{2\sum_{m=1}^{\infty}\sum_{n=1}^{\infty}\frac{n^2\pi^2}{b^2}\psi_{mn}^1 cos\left(\frac{m\pi x}{a}\right)sin\left(\frac{n\pi y}{b}\right)sin\omega t\right\}$$

$$+\frac{4}{3h^2}F_{61}\left\{2\sum_{m=1}^{\infty}\sum_{n=1}^{\infty}\frac{m^2\pi^2}{a^2}\psi_{mn}^1 cos\left(\frac{m\pi x}{a}\right)sin\left(\frac{n\pi y}{b}\right)sin\omega t\right\}$$

$$+\frac{4}{3h^2}F_{66}\left\{2\sum_{m=1}^{\infty}\sum_{n=1}^{\infty}\frac{mn\pi^2}{ab}\psi_{mn}^1 sin\left(\frac{m\pi x}{a}\right)cos\left(\frac{n\pi y}{b}\right)sin\omega t\right\}$$

$$-\frac{16}{h^4}F_{45}\left\{\sum_{m=1}^{\infty}\sum_{n=1}^{\infty}\psi_{mn}^1 cos\left(\frac{m\pi x}{a}\right)sin\left(\frac{n\pi y}{b}\right)sin\omega t\right\}$$

$$-\frac{16}{9h^4}H_{21}\left\{\sum_{m=1}^{\infty}\sum_{n=1}^{\infty}\frac{mn\pi^2}{ab}\psi_{mn}^1 sin\left(\frac{m\pi x}{a}\right)cos\left(\frac{n\pi y}{b}\right)sin\omega t\right\}$$

$$-\frac{16}{9h^4}H_{26}\left\{\sum_{m=1}^{\infty}\sum_{n=1}^{\infty}\frac{n^2\pi^2}{b^2}\psi_{mn}^1 cos\left(\frac{m\pi x}{a}\right)sin\left(\frac{n\pi y}{b}\right)sin\omega t\right\}$$

$$-\frac{16}{9h^4}H_{61}\left\{\sum_{m=1}^{\infty}\sum_{n=1}^{\infty}\frac{m^2\pi^2}{a^2}\psi_{mn}^1 cos\left(\frac{m\pi x}{a}\right)sin\left(\frac{n\pi y}{b}\right)sin\omega t\right\}$$

$$-\frac{16}{9h^4}H_{66}\left\{\sum_{m=1}^{\infty}\sum_{n=1}^{\infty}\frac{mn\pi^2}{ab}\psi_{mn}^1 sin\left(\frac{m\pi x}{a}\right)cos\left(\frac{n\pi y}{b}\right)sin\omega t\right\}$$

$$k_{55}=-A_{44}\left\{\sum_{m=1}^{\infty}\sum_{n=1}^{\infty}\psi_{mn}^2 sin\left(\frac{m\pi x}{a}\right)cos\left(\frac{n\pi y}{b}\right)sin\omega t\right\}$$

$$-D_{22}\left\{\sum_{m=1}^{\infty}\sum_{n=1}^{\infty}\frac{n^2\pi^2}{b^2}\psi_{mn}^2 sin\left(\frac{m\pi x}{a}\right)cos\left(\frac{n\pi y}{b}\right)sin\omega t\right\}$$

$$-D_{26}\left\{\sum_{m=1}^{\infty}\sum_{n=1}^{\infty}\frac{mn\pi^2}{ab}\psi_{mn}^2 cos\left(\frac{m\pi x}{a}\right)sin\left(\frac{n\pi y}{b}\right)sin\omega t\right\}$$

$$-D_{62}\left\{\sum_{m=1}^{\infty}\sum_{n=1}^{\infty}\frac{mn\pi^2}{ab}\psi_{mn}^2 cos\left(\frac{m\pi x}{a}\right)sin\left(\frac{n\pi y}{b}\right)sin\omega t\right\}$$

$$-D_{66}\left\{\sum_{m=1}^{\infty}\sum_{n=1}^{\infty}\frac{m^2\pi^2}{a^2}\psi_{mn}^2 sin\left(\frac{m\pi x}{a}\right)cos\left(\frac{n\pi y}{b}\right)sin\omega t\right\}$$

$$+\frac{4}{h^2}D_{44}\left\{2\sum_{m=1}^{\infty}\sum_{n=1}^{\infty}\psi_{mn}^2 sin\left(\frac{m\pi x}{a}\right)cos\left(\frac{n\pi y}{b}\right)sin\omega t\right\}$$

$$+\frac{4}{3h^2}F_{22}\left\{2\sum_{m=1}^{\infty}\sum_{n=1}^{\infty}\frac{n^2\pi^2}{b^2}\psi_{mn}^2 sin\left(\frac{m\pi x}{a}\right)cos\left(\frac{n\pi y}{b}\right)sin\omega t\right\}$$

$$+\frac{4}{3h^2}F_{26}\left\{2\sum_{m=1}^{\infty}\sum_{n=1}^{\infty}\frac{mn\pi^2}{ab}\psi_{mn}^2 cos\left(\frac{m\pi x}{a}\right)sin\left(\frac{n\pi y}{b}\right)sin\omega t\right\}$$

$$+\frac{4}{3h^2}F_{62}\left\{2\sum_{m=1}^{\infty}\sum_{n=1}^{\infty}\frac{mn\pi^2}{ab}\psi_{mn}^2 cos\left(\frac{m\pi x}{a}\right)sin\left(\frac{n\pi y}{b}\right)sin\omega t\right\}$$

$$+\frac{4}{3h^2}F_{66}\left\{2\sum_{m=1}^{\infty}\sum_{n=1}^{\infty}\frac{m^2\pi^2}{a^2}\psi_{mn}^2 sin\left(\frac{m\pi x}{a}\right)cos\left(\frac{n\pi y}{b}\right)sin\omega t\right\}$$

$$-\frac{16}{h^4}F_{44}\left\{\sum_{m=1}^{\infty}\sum_{n=1}^{\infty}\psi_{mn}^2 sin\left(\frac{m\pi x}{a}\right)cos\left(\frac{n\pi y}{b}\right)sin\omega t\right\}$$

$$-\frac{16}{9h^4}H_{22}\left\{\sum_{m=1}^{\infty}\sum_{n=1}^{\infty}\frac{n^2\pi^2}{b^2}\psi_{mn}^2 sin\left(\frac{m\pi x}{a}\right)cos\left(\frac{n\pi y}{b}\right)sin\omega t\right\}$$

$$-\frac{16}{9h^4}H_{26}\left\{\sum_{m=1}^{\infty}\sum_{n=1}^{\infty}\frac{mn\pi^2}{ab}\psi_{mn}^2 cos\left(\frac{m\pi x}{a}\right)sin\left(\frac{n\pi y}{b}\right)sin\omega t\right\}$$

$$-\frac{16}{9h^4}H_{62}\left\{\sum_{m=1}^{\infty}\sum_{n=1}^{\infty}\frac{mn\pi^2}{ab}\psi_{mn}^2 cos\left(\frac{m\pi x}{a}\right)sin\left(\frac{n\pi y}{b}\right)sin\omega t\right\}$$

$$-\frac{16}{9h^4}H_{66}\left\{\sum_{m=1}^{\infty}\sum_{n=1}^{\infty}\frac{m^2\pi^2}{a^2}\psi_{mn}^2 sin\left(\frac{m\pi x}{a}\right)cos\left(\frac{n\pi y}{b}\right)sin\omega t\right\}$$

A.2 Mass Matrix Coefficent

$$M_{11}=-\overline{I_1}\left\{\sum_{m=1}^{\infty}\sum_{n=1}^{\infty}\omega^2 U_{mn}cos\left(\frac{m\pi x}{a}\right)sin\left(\frac{n\pi y}{b}\right)sin\omega t\right\}$$

$$M_{12}=0$$

$$M_{13} = +\overline{I_3}\left\{\sum_{m=1}^{\infty}\sum_{n=1}^{\infty}\omega^2\frac{m\pi}{a}W_{mn}cos\left(\frac{m\pi x}{a}\right)sin\left(\frac{n\pi y}{b}\right)sin\omega t\right\}$$

$$M_{14} = -\overline{I_2}\left\{\sum_{m=1}^{\infty}\sum_{n=1}^{\infty}\omega^2\psi^1_{mn}cos\left(\frac{m\pi x}{a}\right)sin\left(\frac{n\pi y}{b}\right)sin\omega t\right\}$$

$$M_{15} = 0$$

$$M_{21} = 0$$

$$M_{22} = -\overline{I_1}'\left\{\sum_{m=1}^{\infty}\sum_{n=1}^{\infty}\omega^2V_{mn}sin\left(\frac{m\pi x}{a}\right)cos\left(\frac{n\pi y}{b}\right)sin\omega t\right\}$$

$$M_{23} = +\overline{I_3}'\left\{\sum_{m=1}^{\infty}\sum_{n=1}^{\infty}\omega^2\frac{n\pi}{b}W_{mn}sin\left(\frac{m\pi x}{a}\right)cos\left(\frac{n\pi y}{b}\right)sin\omega t\right\}$$

$$M_{24} = 0$$

$$M_{25} = -\overline{I_2}'\left\{\sum_{m=1}^{\infty}\sum_{n=1}^{\infty}\omega^2\psi^2_{mn}sin\left(\frac{m\pi x}{a}\right)cos\left(\frac{n\pi y}{b}\right)sin\omega t\right\}$$

$$M_{31} = +\overline{I_3}\left\{\sum_{m=1}^{\infty}\sum_{n=1}^{\infty}\omega^2U_{mn}\frac{m\pi}{a}sin\left(\frac{m\pi x}{a}\right)sin\left(\frac{n\pi y}{b}\right)sin\omega t\right\}$$

$$M_{32} = +\overline{I_3}'\left\{\sum_{m=1}^{\infty}\sum_{n=1}^{\infty}\omega^2V_{mn}\frac{n\pi}{b}sin\left(\frac{m\pi x}{a}\right)sin\left(\frac{n\pi y}{b}\right)sin\omega t\right\}$$

$$M_{33} = -I_1\left\{\sum_{m=1}^{\infty}\sum_{n=1}^{\infty}\omega^2W_{mn}sin\left(\frac{m\pi x}{a}\right)sin\left(\frac{n\pi y}{b}\right)sin\omega t\right\}$$

$$-\frac{16I_7}{9h^4}\left\{\sum_{m=1}^{\infty}\sum_{n=1}^{\infty}\omega^2\frac{m^2\pi^2}{a^2}W_{mn}sin\left(\frac{m\pi x}{a}\right)sin\left(\frac{n\pi y}{b}\right)sin\omega t\right\}$$

$$-\frac{16I_7}{9h^4}\left\{\sum_{m=1}^{\infty}\sum_{n=1}^{\infty}\omega^2\frac{n^2\pi^2}{b^2}W_{mn}sin\left(\frac{m\pi x}{a}\right)sin\left(\frac{n\pi y}{b}\right)sin\omega t\right\}$$

$$M_{34}=+\overline{I_5}\left\{\sum_{m=1}^{\infty}\sum_{n=1}^{\infty}\omega^2\psi^1_{mn}\frac{m\pi}{a}sin\left(\frac{m\pi x}{a}\right)sin\left(\frac{n\pi y}{b}\right)sin\omega t\right\}$$

$$M_{35}=+\overline{I_5}'\left\{\sum_{m=1}^{\infty}\sum_{n=1}^{\infty}\omega^2\psi^2_{mn}\frac{n\pi}{b}sin\left(\frac{m\pi x}{a}\right)sin\left(\frac{n\pi y}{b}\right)sin\omega t\right\}$$

$$M_{41}=-\overline{I_2}\left\{\sum_{m=1}^{\infty}\sum_{n=1}^{\infty}\omega^2U_{mn}cos\left(\frac{m\pi x}{a}\right)sin\left(\frac{n\pi y}{b}\right)sin\omega t\right\}$$

$$M_{42}=0$$

$$M_{43}=\overline{I_5}\left\{\sum_{m=1}^{\infty}\sum_{n=1}^{\infty}\omega^2\frac{m\pi}{a}W_{mn}cos\left(\frac{m\pi x}{a}\right)sin\left(\frac{n\pi y}{b}\right)sin\omega t\right\}$$

$$M_{44}=-\overline{I_4}\left\{\sum_{m=1}^{\infty}\sum_{n=1}^{\infty}\omega^2\psi^1_{mn}cos\left(\frac{m\pi x}{a}\right)sin\left(\frac{n\pi y}{b}\right)sin\omega t\right\}$$

$$M_{45}=0$$

$$M_{51}=0$$

$$M_{52}=-\overline{I_2}'\left\{\sum_{m=1}^{\infty}\sum_{n=1}^{\infty}\omega^2V_{mn}sin\left(\frac{m\pi x}{a}\right)cos\left(\frac{n\pi y}{b}\right)sin\omega t\right\}$$

$$M_{53}=\overline{I_5}'\left\{\sum_{m=1}^{\infty}\sum_{n=1}^{\infty}\omega^2\frac{n\pi}{b}W_{mn}sin\left(\frac{m\pi x}{a}\right)cos\left(\frac{n\pi y}{b}\right)sin\omega t\right\}$$

$$M_{54}=0$$

$$M_{55}=-\overline{I_4}'\left\{\sum_{m=1}^{\infty}\sum_{n=1}^{\infty}\omega^2\psi^2_{mn}sin\left(\frac{m\pi x}{a}\right)cos\left(\frac{n\pi y}{b}\right)sin\omega t\right\}$$

Appendix B

B.1 Coefficent of characterstic Equation

$$B_1 = p_{11}+p_{22}+p_{33}+p_{44}+p_{55}$$

$$B_2 = -p_{11}p_{22}-p_{11}p_{33}-p_{11}p_{44}-p_{11}p_{55}-p_{22}p_{33}-p_{22}p_{44}-p_{22}p_{55}-p_{33}p_{44}-p_{33}p_{55}-p_{44}p_{55}$$
$$+p_{45}p_{54}+p_{34}p_{43}+p_{35}p_{53}+p_{23}p_{32}+p_{24}p_{42}+p_{25}p_{52}+p_{12}p_{21}+p_{13}p_{31}+p_{41}p_{14}+p_{15}p_{51}$$

$$B_3 = p_{11}p_{22}p_{33}+p_{11}p_{22}p_{44}+p_{11}p_{22}p_{55}+p_{11}p_{33}p_{44}+p_{11}p_{33}p_{55}+p_{11}p_{55}p_{44}-p_{11}p_{45}p_{54}-p_{11}p_{34}p_{43}$$
$$-p_{11}p_{53}p_{35}+p_{22}p_{33}p_{44}+p_{22}p_{55}p_{33}+p_{22}p_{44}p_{55}-p_{45}p_{22}p_{54}-p_{22}p_{34}p_{43}-p_{22}p_{35}p_{53}+p_{33}p_{44}p_{55}$$
$$-p_{33}p_{45}p_{54}-p_{34}p_{43}p_{55}+p_{34}p_{53}p_{45}+p_{35}p_{43}p_{54}-p_{35}p_{53}p_{44}-p_{23}p_{32}p_{11}-p_{32}p_{23}p_{44}-p_{23}p_{32}p_{53}$$
$$+p_{23}p_{34}p_{42}+p_{23}p_{35}p_{52}-p_{24}p_{42}p_{11}+p_{24}p_{32}p_{43}-p_{24}p_{33}p_{42}-p_{24}p_{42}p_{55}+p_{45}p_{52}p_{24}-p_{11}p_{25}p_{52}$$
$$+p_{25}p_{53}p_{32}-p_{25}p_{33}p_{52}+p_{42}p_{54}p_{25}-p_{25}p_{52}p_{44}-p_{12}p_{21}p_{33}-p_{12}p_{21}p_{44}-p_{12}p_{21}p_{55}+p_{12}p_{24}p_{41}$$
$$+p_{12}p_{25}p_{51}+p_{13}p_{21}p_{32}-p_{13}p_{22}p_{31}-p_{13}p_{31}p_{44}-p_{13}p_{31}p_{55}+p_{13}p_{34}p_{41}+p_{13}p_{35}p_{51}-p_{14}p_{21}p_{42}$$
$$-p_{14}p_{22}p_{41}+p_{14}p_{31}p_{43}-p_{14}p_{33}p_{41}-p_{14}p_{41}p_{55}+p_{14}p_{45}p_{51}+p_{15}p_{21}p_{52}-p_{15}p_{51}p_{22}+p_{15}p_{31}p_{52}$$
$$p_{15}p_{51}p_{33}+p_{41}p_{15}p_{54}-p_{15}p_{44}p_{51}$$

$$B_4 = -p_{11}p_{22}p_{33}p_{44}-p_{11}p_{22}p_{33}p_{55}-p_{11}p_{22}p_{55}p_{44}+p_{11}p_{22}p_{45}p_{54}+p_{11}p_{22}p_{34}p_{43}+p_{11}p_{22}p_{53}p_{35}$$
$$-p_{11}p_{33}p_{44}p_{55}+p_{11}p_{33}p_{45}p_{54}+p_{11}p_{55}p_{34}p_{43}-p_{11}p_{34}p_{53}p_{45}-p_{11}p_{35}p_{43}p_{54}+p_{11}p_{35}p_{53}p_{44}$$
$$-p_{22}p_{33}p_{44}p_{55}+p_{22}p_{33}p_{45}p_{54}+p_{22}p_{55}p_{34}p_{43}-p_{22}p_{34}p_{53}p_{45}-p_{22}p_{35}p_{43}p_{54}+p_{22}p_{35}p_{53}p_{44}$$
$$+p_{23}p_{11}p_{32}p_{44}+p_{23}p_{11}p_{32}p_{55}-p_{23}p_{11}p_{34}p_{42}-p_{23}p_{11}p_{35}p_{52}+p_{23}p_{32}p_{44}p_{55}-p_{23}p_{45}p_{54}p_{32}$$
$$-p_{35}p_{52}p_{44}p_{23}-p_{24}p_{11}p_{32}p_{43}+p_{24}p_{11}p_{33}p_{42}+p_{24}p_{11}p_{42}p_{55}-p_{24}p_{11}p_{45}p_{52}-p_{24}p_{32}p_{43}p_{55}$$
$$+p_{24}p_{32}p_{45}p_{53}+p_{24}p_{33}p_{42}p_{55}-p_{24}p_{33}p_{45}p_{52}-p_{24}p_{35}p_{42}p_{53}+p_{24}p_{35}p_{43}p_{52}-p_{11}p_{25}p_{53}p_{32}$$
$$+p_{11}p_{25}p_{33}p_{52}-p_{11}p_{25}p_{42}p_{54}+p_{11}p_{25}p_{52}p_{44}+p_{25}p_{32}p_{43}p_{54}-p_{25}p_{32}p_{44}p_{53}-p_{25}p_{33}p_{42}p_{54}$$
$$+p_{25}p_{33}p_{52}p_{44}+p_{25}p_{34}p_{42}p_{53}-p_{25}p_{34}p_{43}p_{52}+p_{12}p_{21}p_{33}p_{44}+p_{12}p_{21}p_{33}p_{55}+p_{12}p_{21}p_{44}p_{55}$$
$$-p_{12}p_{21}p_{45}p_{54}-p_{12}p_{21}p_{34}p_{43}-p_{12}p_{21}p_{35}p_{53}-p_{12}p_{23}p_{31}p_{43}+p_{12}p_{23}p_{34}p_{41}+p_{12}p_{24}p_{31}p_{43}$$
$$-p_{12}p_{24}p_{33}p_{41}-p_{12}p_{24}p_{41}p_{55}+p_{12}p_{24}p_{51}p_{45}+p_{12}p_{25}p_{53}p_{31}-p_{12}p_{25}p_{33}p_{51}+p_{12}p_{25}p_{41}p_{54}$$
$$-p_{12}p_{25}p_{51}p_{44}-p_{13}p_{21}p_{32}p_{44}-p_{13}p_{21}p_{32}p_{55}+p_{13}p_{21}p_{34}p_{42}-p_{13}p_{21}p_{35}p_{52}+p_{13}p_{22}p_{31}p_{44}$$
$$+p_{13}p_{22}p_{31}p_{55}-p_{13}p_{22}p_{34}p_{41}-p_{13}p_{22}p_{35}p_{51}+p_{13}p_{31}p_{44}p_{55}-p_{13}p_{31}p_{51}p_{45}-p_{13}p_{34}p_{41}p_{55}$$
$$+p_{13}p_{34}p_{45}p_{51}+p_{13}p_{35}p_{41}p_{54}-p_{13}p_{35}p_{51}p_{44}-p_{13}p_{24}p_{31}p_{42}+p_{13}p_{24}p_{32}p_{41}-p_{13}p_{25}p_{31}p_{52}$$
$$+p_{13}p_{25}p_{32}p_{51}+p_{14}p_{21}p_{32}p_{43}-p_{14}p_{21}p_{33}p_{42}-p_{14}p_{21}p_{42}p_{55}+p_{14}p_{21}p_{52}p_{45}-p_{14}p_{22}p_{31}p_{43}$$
$$+p_{14}p_{22}p_{33}p_{41}+p_{14}p_{22}p_{41}p_{55}-p_{14}p_{22}p_{45}p_{51}-p_{14}p_{31}p_{43}p_{55}+p_{14}p_{45}p_{53}p_{31}+p_{14}p_{33}p_{41}p_{55}$$
$$-p_{14}p_{33}p_{45}p_{51}-p_{35}p_{41}p_{14}p_{53}+p_{14}p_{51}p_{35}p_{43}+p_{14}p_{23}p_{31}p_{42}-p_{14}p_{23}p_{32}p_{41}-p_{14}p_{25}p_{41}p_{52}$$
$$+p_{14}p_{25}p_{42}p_{51}+p_{15}p_{21}p_{32}p_{53}+p_{15}p_{21}p_{33}p_{22}+p_{15}p_{21}p_{42}p_{54}-p_{15}p_{21}p_{52}p_{44}-p_{15}p_{22}p_{31}p_{52}$$

$$
\begin{aligned}
&+p_{51}p_{22}p_{33}p_{15}-p_{15}p_{22}p_{41}p_{54}+p_{15}p_{22}p_{44}p_{51}+p_{15}p_{31}p_{43}p_{54}-p_{15}p_{31}p_{52}p_{44}-p_{15}p_{33}p_{41}p_{54}\\
&+p_{15}p_{33}p_{44}p_{51}+p_{15}p_{34}p_{41}p_{52}-p_{15}p_{34}p_{43}p_{51}+p_{15}p_{23}p_{31}p_{52}-p_{15}p_{23}p_{32}p_{51}+p_{15}p_{24}p_{41}p_{52}\\
&-p_{15}p_{24}p_{42}p_{51}-p_{23}p_{34}p_{42}p_{55}+p_{23}p_{34}p_{45}p_{52}+p_{35}p_{42}p_{54}p_{23}
\end{aligned}
$$

$$
\begin{aligned}
B_5 = {} & p_{11}p_{22}p_{33}p_{44}p_{55}-p_{11}p_{22}p_{33}p_{45}p_{54}-p_{11}p_{22}p_{34}p_{43}p_{55}+p_{11}p_{22}p_{34}p_{53}p_{45}+p_{11}p_{22}p_{35}p_{43}p_{54}\\
&-p_{11}p_{22}p_{35}p_{53}p_{44}-p_{23}p_{11}p_{32}p_{44}p_{55}+p_{45}p_{54}p_{32}p_{23}p_{11}+p_{23}p_{11}p_{34}p_{42}p_{55}-p_{23}p_{11}p_{34}p_{45}p_{52}\\
&-p_{23}p_{11}p_{35}p_{42}p_{54}+p_{23}p_{11}p_{35}p_{52}p_{44}+p_{24}p_{11}p_{32}p_{43}p_{55}-p_{24}p_{11}p_{32}p_{45}p_{53}-p_{24}p_{11}p_{33}p_{42}p_{55}\\
&+p_{24}p_{11}p_{33}p_{45}p_{52}+p_{24}p_{11}p_{35}p_{42}p_{53}-p_{24}p_{11}p_{35}p_{43}p_{52}-p_{11}p_{25}p_{32}p_{43}p_{54}+p_{11}p_{25}p_{32}p_{44}p_{53}\\
&+p_{33}p_{42}p_{54}p_{11}p_{25}-p_{11}p_{25}p_{33}p_{52}p_{44}-p_{11}p_{25}p_{34}p_{42}p_{53}+p_{11}p_{25}p_{34}p_{43}p_{52}-p_{12}p_{21}p_{33}p_{44}p_{55}\\
&+p_{12}p_{21}p_{33}p_{45}p_{54}+p_{12}p_{21}p_{34}p_{43}p_{55}-p_{12}p_{21}p_{34}p_{45}p_{53}-p_{12}p_{21}p_{35}p_{43}p_{54}+p_{12}p_{21}p_{35}p_{53}p_{44}\\
&+p_{12}p_{23}p_{31}p_{43}p_{55}-p_{12}p_{23}p_{31}p_{45}p_{53}-p_{12}p_{23}p_{34}p_{41}p_{55}+p_{12}p_{23}p_{34}p_{51}p_{45}+p_{12}p_{23}p_{35}p_{41}p_{53}\\
&-p_{12}p_{23}p_{35}p_{43}p_{51}-p_{12}p_{24}p_{31}p_{43}p_{55}+p_{12}p_{24}p_{31}p_{53}p_{45}+p_{12}p_{24}p_{33}p_{41}p_{55}-p_{12}p_{24}p_{33}p_{51}p_{45}\\
&-p_{12}p_{24}p_{35}p_{41}p_{53}+p_{12}p_{24}p_{35}p_{51}p_{43}+p_{12}p_{25}p_{31}p_{43}p_{54}-p_{12}p_{25}p_{31}p_{44}p_{53}-p_{12}p_{25}p_{33}p_{41}p_{54}\\
&-p_{12}p_{25}p_{33}p_{51}p_{44}+p_{12}p_{25}p_{34}p_{41}p_{53}-p_{12}p_{25}p_{34}p_{43}p_{51}+p_{13}p_{21}p_{32}p_{44}p_{55}-p_{13}p_{21}p_{32}p_{45}p_{54}\\
&-p_{13}p_{21}p_{34}p_{42}p_{55}+p_{13}p_{21}p_{34}p_{52}p_{45}-p_{13}p_{21}p_{35}p_{42}p_{54}+p_{13}p_{21}p_{35}p_{52}p_{44}-p_{13}p_{22}p_{31}p_{44}p_{55}\\
&+p_{13}p_{22}p_{51}p_{45}p_{31}+p_{13}p_{22}p_{34}p_{41}p_{55}-p_{13}p_{22}p_{34}p_{45}p_{51}-p_{13}p_{22}p_{35}p_{41}p_{54}+p_{13}p_{22}p_{35}p_{51}p_{44}\\
&+p_{13}p_{24}p_{31}p_{42}p_{55}-p_{13}p_{24}p_{31}p_{52}p_{45}-p_{13}p_{24}p_{32}p_{41}p_{55}+p_{13}p_{24}p_{32}p_{45}p_{51}-p_{13}p_{24}p_{35}p_{41}p_{52}\\
&+p_{13}p_{24}p_{42}p_{51}p_{35}-p_{13}p_{25}p_{31}p_{42}p_{54}+p_{13}p_{25}p_{31}p_{44}p_{52}+p_{13}p_{25}p_{32}p_{41}p_{54}-p_{13}p_{25}p_{32}p_{44}p_{51}\\
&-p_{13}p_{25}p_{34}p_{41}p_{52}+p_{13}p_{25}p_{42}p_{51}p_{34}-p_{14}p_{21}p_{32}p_{43}p_{55}+p_{14}p_{21}p_{32}p_{45}p_{53}+p_{14}p_{21}p_{33}p_{42}p_{55}\\
&-p_{14}p_{21}p_{33}p_{52}p_{45}-p_{14}p_{21}p_{35}p_{42}p_{53}+p_{14}p_{21}p_{35}p_{52}p_{43}+p_{14}p_{22}p_{31}p_{43}p_{55}-p_{14}p_{22}p_{45}p_{53}p_{31}\\
&-p_{14}p_{22}p_{33}p_{41}p_{55}+p_{14}p_{22}p_{33}p_{45}p_{51}+p_{14}p_{22}p_{35}p_{41}p_{53}-p_{14}p_{22}p_{51}p_{35}p_{43}-p_{14}p_{23}p_{31}p_{42}p_{55}\\
&+p_{14}p_{23}p_{31}p_{52}p_{45}+p_{41}p_{23}p_{32}p_{41}p_{55}-p_{14}p_{23}p_{32}p_{51}p_{45}-p_{14}p_{23}p_{35}p_{41}p_{52}+p_{14}p_{23}p_{35}p_{42}p_{51}\\
&+p_{14}p_{25}p_{31}p_{42}p_{53}-p_{14}p_{25}p_{31}p_{52}p_{43}-p_{14}p_{25}p_{32}p_{41}p_{53}+p_{14}p_{25}p_{32}p_{43}p_{51}+p_{14}p_{25}p_{33}p_{41}p_{52}\\
&-p_{14}p_{25}p_{33}p_{42}p_{51}+p_{15}p_{21}p_{32}p_{43}p_{54}-p_{15}p_{21}p_{32}p_{53}p_{44}-p_{15}p_{21}p_{33}p_{42}p_{54}+p_{15}p_{21}p_{33}p_{52}p_{44}\\
&+p_{15}p_{21}p_{34}p_{42}p_{53}-p_{15}p_{21}p_{34}p_{43}p_{52}-p_{15}p_{22}p_{31}p_{43}p_{54}+p_{15}p_{22}p_{31}p_{52}p_{44}+p_{15}p_{22}p_{33}p_{41}p_{54}\\
&-p_{15}p_{22}p_{33}p_{44}p_{51}-p_{34}p_{41}p_{52}p_{15}p_{22}+p_{15}p_{22}p_{34}p_{43}p_{51}+p_{15}p_{23}p_{31}p_{42}p_{54}-p_{15}p_{23}p_{31}p_{52}p_{44}\\
&-p_{15}p_{23}p_{32}p_{41}p_{54}+p_{15}p_{23}p_{51}p_{44}p_{32}+p_{15}p_{23}p_{34}p_{41}p_{52}-p_{15}p_{23}p_{34}p_{42}p_{51}-p_{15}p_{24}p_{31}p_{42}p_{53}\\
&+p_{15}p_{24}p_{31}p_{52}p_{43}+p_{15}p_{24}p_{32}p_{41}p_{53}-p_{15}p_{24}p_{32}p_{43}p_{51}-p_{15}p_{24}p_{33}p_{41}p_{52}+p_{15}p_{24}p_{33}p_{42}p_{51}
\end{aligned}
$$